

SEMMELWEIS EGYETEM
DOKTORI ISKOLA

Ph.D. értekezések

3036.

BOHUSNÉ BARTA BETTINA ARANKA

Gasztroenterológia
című program

Programvezető: Dr. Molnár Béla, kutatóprofesszor

Témavezető: Dr. Sipos Ferenc, egyetemi adjunktus

Konzulens: Dr. Múzes Györgyi, egyetemi docens

**THE INTERPLAY OF TLR9-MEDIATED AUTOPHAGY
RESPONSE AND GROWTH FACTOR SIGNALING
INHIBITION IN COLON ADENOCARCINOMA CELLS:
CELL-FREE DNA EXPERIMENTS**

PhD thesis

Bettina Aranka Bohusné Barta

Semmelweis University Doctoral School
Károly Rácz Conservative Medicine Division



Supervisor: Ferenc Sipos MD, Ph.D

Consultant: Györgyi Múzes MD, C.Sc, med. habil.

Official reviewers: Pál Miheller MD, Ph.D, med. habil.

Gábor Rubovszky MD, Ph.D

Head of the Comprehensive Exam Committee: Zoltán Prohászka MD, D.Sc

Members of the Comprehensive Exam Committee: Miklós Máté MD, Ph.D

Gábor Firneisz MD, Ph.D

Budapest

2024

TABLE OF CONTENTS

LIST OF ABBREVIATIONS	5
1. INTRODUCTION	8
1.1 <i>The origin and characteristics of cfDNA</i>	8
1.2 <i>Recognition and immunomodulatory role of cfDNA</i>	11
1.2.1 <i>Description and features of TLRs and TLR9 signaling</i>	15
1.2.1.1 <i>Types of CpG-ODNs</i>	18
1.2.2 <i>TLR9 in inflammation and malignancy</i>	19
1.3 <i>Characteristics and process of autophagy</i>	22
1.3.1 <i>Autophagy and TLR9 signaling in cancer</i>	26
1.3.1.1 <i>The role of TLRs in the regulation of autophagy</i>	26
1.3.1.2 <i>The role of autophagy in the regulation of TLRs</i>	27
1.3.1.3 <i>The role of TLRs and autophagy in cancer</i>	28
1.4 <i>cfDNA in tumors</i>	29
1.5 <i>HGFR: functions, relationship with autophagy and cancer</i>	33
1.6 <i>IGF1R: functions, relationship with autophagy and cancer</i>	35
2. OBJECTIVES	40
3. MATERIALS AND METHODS	41
3.1 <i>Selection and maintenance of HT29 cell culture; self-DNA isolation</i>	41
3.2 <i>Fragmentation and hypermethylation of self-DNA</i>	42
3.3 <i>HT29 cell treatments</i>	42
3.4 <i>Inhibition of TLR9, HGFR, and IGF1R signaling and autophagy</i>	43
3.5 <i>Cell viability and proliferation measurements</i>	44
3.6 <i>Total mRNA isolation and NanoString analysis</i>	44
3.7 <i>Taqman real-time PCR analysis</i>	45
3.8 <i>Immunocytochemistry for HGFR, IGF1R, CD133, TLR9 and autophagy</i>	46
3.9 <i>WES Simple and assessment of autophagic flux</i>	46
3.10 <i>Cell counting and interpretation of immunoreactions</i>	47
3.11 <i>Transmission electron microscopy for evaluation of autophagy</i>	47
3.12 <i>Semithin sections</i>	47
3.13 <i>Statistical analysis</i>	48

4. RESULTS	49
4.1 <i>Cell viability and proliferation measurements (HGFR studies)</i>	49
4.2 <i>Cell viability and proliferation measurements (IGF1R studies)</i>	51
4.3 <i>NanoString and Taqman gene expression analyses (HGFR studies)</i>	53
4.4 <i>NanoString and Taqman gene expression analyses (IGF1R studies)</i>	56
4.5 <i>Immunocytochemistry and WES Simple (HGFR studies)</i>	58
4.6 <i>Immunocytochemistry and WES Simple (IGF1R studies)</i>	61
4.7 <i>Transmission electron microscopy (HGFR studies)</i>	64
4.8 <i>Transmission electron microscopy (IGF1R studies)</i>	66
4.9 <i>Semithin sections (HGFR studies)</i>	68
4.10 <i>Semithin sections (IGF1R studies)</i>	69
5. DISCUSSION	70
5.1 <i>The interconnection of TLR9-mediated autophagy response and HGFR signaling</i>	70
5.2 <i>The interconnection of TLR9-mediated autophagy response and IGF1R signaling</i>	75
6. CONCLUSIONS	80
7. SUMMARY	82
8. REFERENCES	83
9. BIBLIOGRAPHY OF THE CANDIDATE’S PUBLICATIONS	122
10. ACKNOWLEDGEMENTS	124
11. SUPPLEMENTS	125

LIST OF ABBREVIATIONS

Ago2: argonaute 2 protein	cGAS-STING: cyclic GMP-AMP synthase- signaling effector stimulator of interferon genes
AIM2: absent in melanoma-2 receptor	c-Met: C mesenchymal epithelial transition factor /HGFR/
AKBA: chemopreventive characteristics of 3- acetyl-11-keto- β -boswellic acid	CpG: cytosolic cytosine-phosphate-guanine
AKT: Ak strain transforming	CpG-ODN: CpG-oligodeoxynucleotide
ALR: AIM2-like receptor	CREB: cAMP-response element binding protein
AMPK: AMP-activated protein kinase	CRC: colorectal cancer
ANOVA: analysis of variance	DAMP: danger-associated molecular pattern
AP: activator protein	DC: dendritic cell
APC: antigen-presenting cell	DISU: 4,4'-Diisothiocyanatostilbene-2,2'- disulfonic acid
ASC: apoptosis-associated speck-like protein including a C-terminal caspase recruitment domain	DMSO: dimethyl sulfoxide
ATG: autophagy-related gene	dsDNA: double-stranded DNA
ATG16L1: autophagy related 16 like 1	EDTA: ethylenediaminetetraacetic acid
ATP: adenosine-triphosphate	EGFR: epidermal growth factor receptor
Av: autophagic vacuole	EMT: epithelial–mesenchymal transition
BA145: powerful natural analog of AKBA	ER: endoplasmic reticulum
Bad: Bcl-2-associated agonist of cell death	ERK: extracellular signal-regulated kinase
BAFFR: B cell activating factor (BAFF) receptor	ELK: erythroblast transformation specific (ETS) domain-containing protein
Bax: Bcl-2 associated X	ET: extracellular trap
Bcl-2: B-cell lymphoma 2	FAK: focal adhesion kinase
BECN1: Beclin-1	FBS: fetal bovine serum
Caco-2: colon adenocarcinoma cell line	Gab1: GRB2 associated binding protein 1
CASP1: procaspase 1 enzyme	GAPDH: glyceraldehyde-3-phosphate dehydrogenase
CCDC25: coiled-coil domain containing protein-25	g/f/mDNA: genomic/ fragmented/ hypermethylated self-DNA
CD: cluster of differentiation	GO: graphene oxide
CD95L: CD95 (Fas) ligand	Grb2: growth factor receptor-bound protein 2
CD133: cluster of differentiation 133 /prominin 1, PROM1/	GSDMD: linker region of gasdermin D
cfDNA: cell-free deoxynucleic acids	HBB: hemoglobin subunit beta
cGAS: cyclic guanosine monophosphate- adenosine monophosphate synthase	HCC: hepatic cell carcinoma
	HDL: high-density lipoprotein

HER: human epidermal growth factor receptor

HGF: hepatocyte growth factor

HGFR: hepatocyte growth factor receptor
/c-Met/

HIN: hematopoietic interferon-inducible nuclear

HMGB: DAMP protein high-mobility group B

HMGB1: high mobility group box 1

IGF1: insulin-like growth factor 1

IGF1R: insulin-like growth factor 1 receptor

IgM: immunoglobulin-M

IKB α/β : kinase complex (IKK)

I κ B: kinase (IKK) complex that consists of two kinases (IKK α and IKK β)

IKK: I κ B kinase

IL: interleukin

IL-1r: interleukin-1 receptor

IFN: interferon

IRAK: interleukin receptor-associated kinase

IRF: interferon regulatory factor

IRS: insulin receptor substrates

JAK/STAT: Janus kinase/signal transducer and activator of transcription

JNK: C-jun N-terminal kinase

K⁺: potassium ion

KRAS: Kirsten rat sarcoma virus

LAP: LC3-associated phagocytosis

LC3: microtubule-associated protein light chain 3

LRO: lysosome-related organelle

MAP1LC3: microtubule-associated protein 1 light chain 3

MALDI-TOF: matrix-assisted laser desorption-ionization time-of-flight mass spectrometry

MAPK: mitogen activated phosphokinase/protein kinase

MEK: mitogen-activated extracellular signal-regulated kinase

MHC I/II: major histocompatibility complex class I/II

mRNA: messenger RNA

mTOR: mammalian target of rapamycin

mTORC: mTOR complex

MUC-1: transmembrane glycoprotein mucin 1

MVB: multivesicular body

MyD88: myeloid differentiation primary response gene 88

NEAT1: nuclear paraspeckle assembly transcript 1

NEMO: nuclear factor-kappa B essential modulator

NET: neutrophil extracellular trap

NIK: nuclear factor-kappa B-inducing kinases

NIPT: non-invasive prenatal testing

NF- κ B: nuclear factor kappa-B

NK: natural killer

NOD-SCID: nonobese diabetic-severe combined immunodeficiency

ODN: synthetic CpG-oligodeoxyribonucleotide

P: phosphor

PAMP: pathogen-associated molecular pattern

PBS: phosphate buffered saline

PCR: polymerase chain reaction

pDC: plasmacytoid dendritic cell

PD-L1: programmed death ligand 1

PI3K: phosphoinositide 3-kinase

PKC: protein kinase C

PM: plasma membrane

poly(I:C): polyinosinic:polycytidylic acid

PPP: picropodophyllin

PRR: pattern-recognition receptor

PYD: pyrin domain

RAC1: Ras-related C3 botulinum toxin substrate 1

RAF: rapidly accelerated fibrosarcoma

Ras: GTPase protein

RAS: rat sarcoma virus

RANK: receptor activator of nuclear factor-
 kappa B
 RELB: RelB gene product transcription factor
 RhD: rhesus D (blood type antigen/Rh+ or Rh-)
 RNA: ribonucleic acid
 RTK: receptor tyrosine kinase
 RT-PCR: reverse transcription-polymerase chain
 reaction
 ROS: reactive oxygen species
 S100: small acidic protein 100
 SAA: serum amyloid A
 Shc: adaptor protein
 SIRT1: sirtuin 1
 SOS: sinusoidal obstruction syndrome
 SOX2: SRY-related HMG-box transcription
 factor 2
 SphK1: sphingosine kinase 1
 SQSTM1: sequestosome 1 /p62/
 Src: SRC proto-oncogene, non-RTK
 ssRNA: single stranded RNA
 STAT: signal transducer and activator of
 transcription
 STING: cGAS-stimulator of interferon genes
 TAK1: transforming growth factor beta-
 activated kinase 1
 TBK1: tank-binding kinase 1
 TCR: T cell receptor
 TEM: transmission electron microscope
 Th1: type 1 T-helper
 TIRAP: Toll-interleukin 1 receptor domain-
 containing adapter protein
 TLR: Toll-like receptor
 TNF α : tumor necrosis factor alpha
 TP53: tumor protein p53
 TRAF: tumor necrosis factor receptor-
 associated factor
 TRAM: Toll-like receptor 4 adaptor protein
 Treg: regulatory T cell
 TRIF: Toll-interleukin-1 receptor-domain-
 containing adapter-inducing interferon
 TRX: three prime repair exonuclease 1
 Tukey HSD test: Tukey's honestly significant
 difference test
 ULK: Unc-51-like autophagy-activating kinases
 UNC93B1: Unc-93 homolog B1 transmembrane
 protein
 UVRAG: Beclin1-UV-irradiation resistance-
 associated gene
 VEGFR: vascular endothelial growth factor
 receptor
 VSV: vesicular stomatitis virus
 WES: capillary Western blot

1. INTRODUCTION

Mandel and Métais [1] are credited with the discovery of cell-free deoxy nucleic acids (cfDNA) in the plasma of cancer patients in 1948. Subsequent research identified a correlation between the concentration of cfDNA and the development of systemic lupus erythematosus [2]. The use of cfDNA for tumor diagnostics began in 1977, but the limitations of the available technology determine its effectiveness [3]. In 1997, real-time polymerase chain reaction was introduced, which enabled the detection of RhD (blood type antigen) and fetal sex in maternal plasma [4]. In 2011, the introduction of massive parallel sequencing marked a significant advancement in non-invasive fetal genetic disease detection [5]. Today, approximately fifty percent of prenatal genetic examinations employ non-invasive prenatal testing (NIPT) [6]. Recent changes, like the rise in the number of liquid biopsies and the need for more screening, disease activity monitoring, and therapeutic response assessment, have made it easier for cfDNA research to get going again. Examination of the 5' end of the extracellular DNA revealed that it is not a junk molecule, which makes it unique [7]. However, research into the immunological properties of cfDNA, such as its possible immunomodulatory or therapeutic benefits, is still in its early stages. Nevertheless, studies are mainly focused on the function of cfDNA as a biomarker.

The objective of my PhD work was to provide an insight into the extremely complex immunobiological effects of cfDNA in colon adenocarcinoma cells.

1.1 The origin and characteristics of cfDNA

cfDNA is often present in different human body fluids, and although certain parts of its molecular source have been determined, there is an increasing corpus of research focused on investigating the unidentified factors that contribute to its development [8,9]. Various hypothetical internal sources and their corresponding processes have been proposed, excluding external sources of cfDNA. Regarding the source of cfDNA, it is feasible to distinguish between cancerous cells (such as tumor cells found locally and circulating, micrometastases, and cells within the tumor microenvironment) and non-cancerous cells (including muscle cells, epithelial cells, ovum cells, bone cells, myeloid cells, and lymphoid cells) [10].

The mechanisms responsible for the release of cfDNA display significant variability. cfDNA is released by a number of processes, such as apoptosis, necrosis, pyroptosis, mitotic catastrophe, autophagy, phagocytosis, oncosis, NETosis, and DNA excision repair damage [11,12]. Alternatively, active release can also happen via macromolecular structures, including DNA-protein complexes, extracellular traps, micronucleation caused by genomic instability, extrachromosomal circular DNA, or microvesicles called exosomes [13-15]. These processes are illustrated in the **Figure 1**.

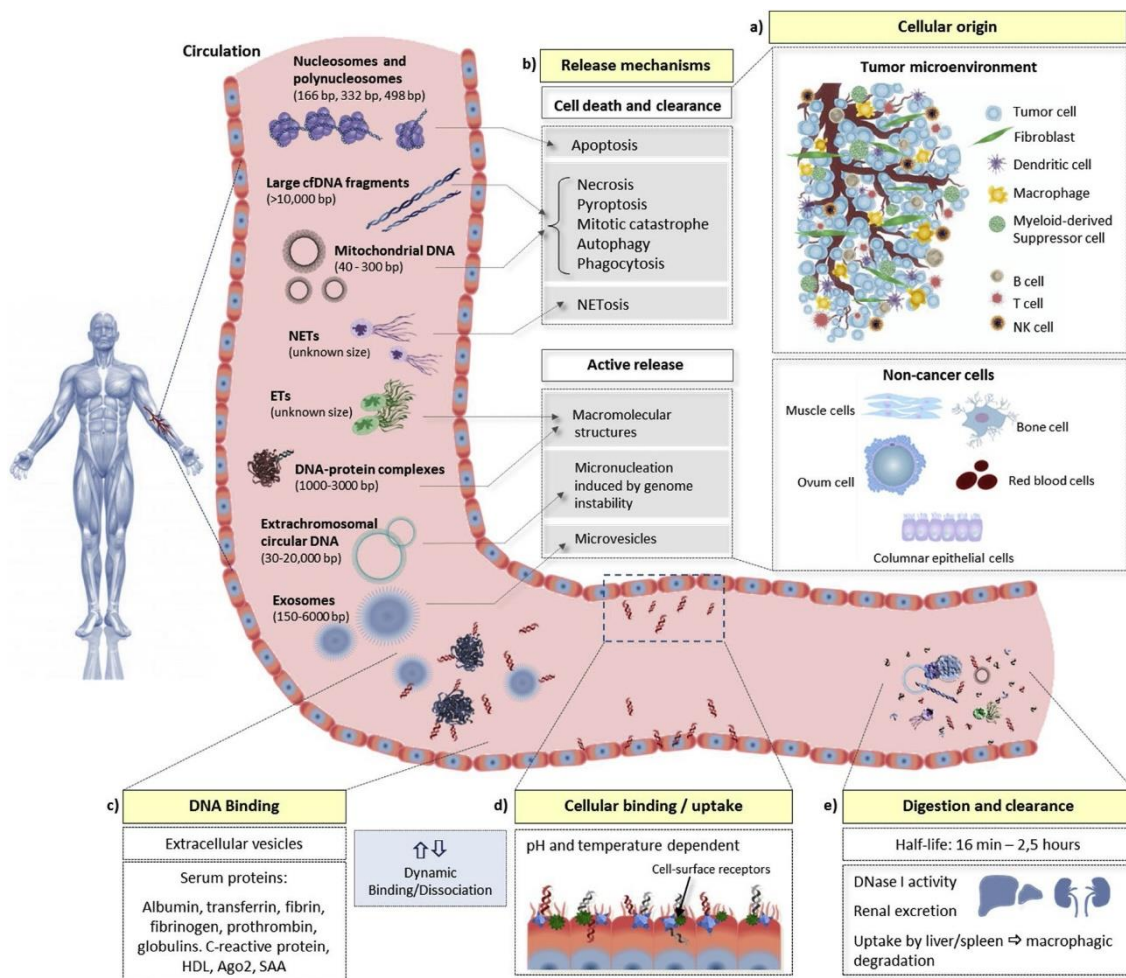


FIGURE 1 | The origin and characteristics of cfDNA [10].

a) Cell-free DNA (cfDNA) derives from various sources. DNA can be extracted from these cells by several mechanisms. b) The extracellular concentration of cfDNA is hence extremely contingent upon the velocity of its release from cells. Nevertheless, upon entering circulation, cfDNA levels are additionally affected by its. c) Dynamic interactions with extracellular vesicles and various serum proteins, d) Rates of binding, dissociation, and cellular internalization. e) Rates of degradation or clearance, encompassing the activity of DNase I, renal excretion into urine and absorption by the liver and spleen.

Ago2: argonaute 2 protein; ETs: extracellular traps; HDL: high-density lipoprotein; NETs: neutrophil extracellular traps; NK cell: natural killer cell; SAA: serum amyloid A

Due to the absence of universally acknowledged methods, circulating human cfDNA quantification is still uncertain, and the data is inconsistent. Different factors, such as the matrix (plasma, serum, urine, cerebral fluid, etc.), the sample collection method (CellSave tubes or tubes with EDTA), the centrifugation variables (speed, temperature, duration), the isolation kits, and the storage conditions for cfDNA, can all change the results of a measurement [16]. Healthy people have lower cfDNA levels than diseased individuals. Recent research found that human plasma cfDNA content can exceed 500 ng/ μ L [17-20]. Advanced tumors [18-20], autoimmune [21-25], inflammatory [26], traumatic [27,28], post-transplantation [29], or viral diseases [30,31] exhibit higher levels. Additionally, significant physical exercise, such as half marathons, ultramarathons, and TRX workouts [32,33], and pregnancy [34], might raise cfDNA levels. As early as the first trimester, maternal blood contains 10–15% fetal cfDNA, mostly from placental trophoblast cells [35,36].

The concentration of cfDNA may rise not only due to the indicated circumstances but also as a result of an increased release. Inadequate clearance mechanisms may significantly contribute to the elevated levels of circulating cfDNA. Extracellular nuclease analogues, namely DNase I and DNase I-like III (DNase I L3), effectively perform the process of breaking down both unbound and protein-bound DNA [37]. Deviations in DNase I activity, such as decreased serum DNase I activity, elevated levels of DNase I inhibitors, and new mutations in the enzyme, could potentially impact the ability of the enzyme to identify and break down DNA [38-40]. Furthermore, several factors, such as DNA-interacting molecules [41], anti-DNase antibodies [42,43], and deficiencies in DNase I activating cofactors (such as complement component C1q [44], TREX1 Dnase [45], serum amyloid P component [46], IgM [47], C-reactive protein [48], and mannan-binding lectin), can also affect the function of the enzyme [49].

1.2 Recognition and immunomodulatory role of cfDNA

cfDNA has been shown in experiments to have immunomodulatory capabilities in addition to its role as a biomarker and diagnostic tool. It has the ability to influence the onset, progression, or reduction of inflammation. Maintaining self-tolerance necessitates the presence of self-DNA in both the nucleus and the mitochondria. However, under stressful circumstances, self-DNA can enter the cytosol due to nuclear or mitochondrial damage. The absence of infection appears to activate the inflammatory response, which is most likely started by the production of internal warning signals known as danger-associated molecular patterns (DAMPs). These DAMPs later trigger immune responses through pattern-recognition receptors (PRRs). cfDNA has the capacity to serve as a DAMP [50,51].

Several DNA-sensing receptors can detect cfDNA. These include cGAS, TLR9, and AIM2 receptors [52].

The cGAS recognizes cytosolic DNA molecules, activating IRF3 and synthesizing IFN- β or type 1 IFNs [53]. Due to their higher binding ability, cGAS detects extracellular nucleosomes better than double-stranded DNA (dsDNA) [53]. When cytosolic DNA is identified, cGAS activates *STING* [54,55]. The recognition length of dsDNA is 36 base pairs or more by the cGAS enzyme. Detecting this event activates cGAS-*STING*-mediated effectors, leading to the production of type 1 IFNs and other cytokines that rely on NF- κ B, regardless of DNA sequence [50,56,57]. *STING* activates NF- κ B, MAPK, and STAT6, resulting in autophagosome formation. To accomplish this, *STING* forms *LC3* and *Atg9a* punctas. The process starts when *STING* finds cytosolic DNA [58-61]. In response to cytosolic dsDNA, *BECN1* interacts with cGAS to limit cyclic GMP-AMP production. Disrupting cGAS-dsDNA interactions accomplishes this inhibition. *BECN1* releases Rubicon, an autophagy suppressor, when cGAS interacts with it. Class III *PI3K* release induces autophagy. Thus, autophagy eliminates cytosolic dsDNA [62]. Autophagy eliminates cfDNA effectively and reduces inflammation. When autophagy is impaired, several cytosolic PRRs identify cfDNA and induce inflammation [62], as shown in **Figure 2**.

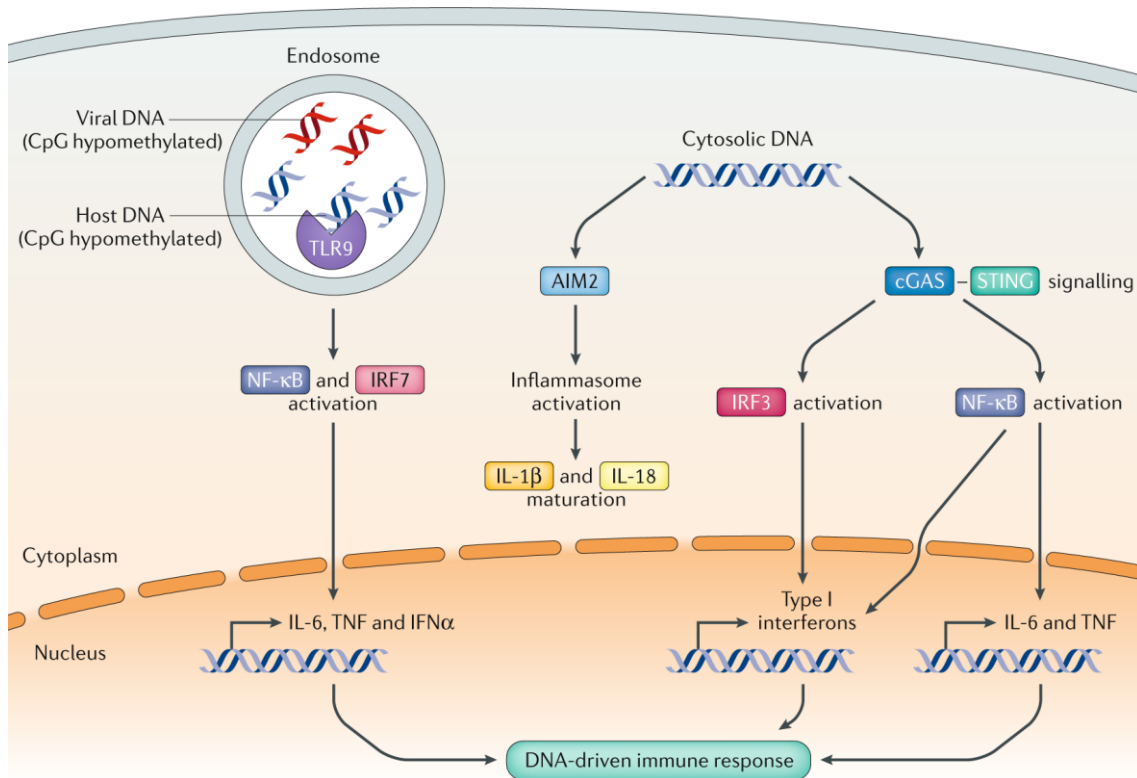


FIGURE 2 | DNA-sensing receptors [63].

The identification of pathogens by nucleic acid sensors is a fundamental aspect of innate immunity. RNA-sensing and DNA-sensing receptors detect foreign nucleic acids in subcellular compartments and, once identified, activate immunological signaling pathways to protect the host. The ability of native DNA to activate cGAS has been implicated as a crucial mechanism in triggering inflammation, and the cGAS-STING pathway has been implicated in the development of human inflammatory disorders and cancer.

AIM2: absent in melanoma-2 receptors; cGAS-STING: cyclic GMP-AMP synthase-signaling effector stimulator of interferon genes; CpG: cytosolic cytosine-phosphate-guanine; IFNα: interferon alpha; IL-1β/6/18: interleukin 1β/6/18; IRF3/7: interferon regulatory factor 3/7; NF-κB: nuclear factor kappa-B
TLR9: Toll-like receptor 9; TNF: tumor necrosis factor

TLR9 is detectable in the endoplasmic reticulum (ER) under normal physiological circumstances. However, when cytosolic CpG-DNAs or self-DNAs enter the endosome or endolysosome, TLR9 migrates to these cellular compartments and identifies them as significant DAMPs [64,65]. TLR9 activation initiates a signaling cascade that relies on *MyD88*. This pathway triggers the activation of IRF3, leading to the production of type 1 IFNs. Furthermore, it triggers the activation of *NF-κB*, which subsequently stimulates the synthesis of pro-inflammatory cytokines. These pathways contribute to the development of inflammation and inflammatory diseases [66]. The TIR domain of *MyD88* triggers the activation of IRAK-4 and IRAK-1, which are interleukin-1 receptor-associated kinases [67,68]. The protein IRAK-4 aids in *TRAF6* recruitment to induce TAK1 activation [69]. The TAK1 enzyme promotes the addition of K63-linked ubiquitin molecules to NEMO,

which in turn enables the phosphorylation of the IKK complex. This mechanism is essential in the signaling pathways of NF- κ B, IRF3, and MAPK [70]. TLR9 possesses the capacity to differentiate between two unique classifications of DNA, specifically DNA derived from pathogens and DNA produced from oneself. The study revealed that the interaction and stimulation of TLR9 by synthetic CpG-ODNs and cfDNAs are affected by parameters such as their nucleotide sequence, length, and ability to form dimers [71-73]. Intracellular compartmentalization of TLR9 is a process that helps distinguish between self-DNA and non-self-DNA, which comes from external sources. Binding leads to an increase in dimerization and subsequent activation [74].

Platelets have been shown to feature PRRs that can be triggered when they interact with DAMPs [75]. Both murine and human platelets express TLR9 [76,77], which is important since platelets play a crucial role in integrating innate and adaptive immune responses as well as their fundamental function in hemostasis [75]. Platelet activation triggers the production of P-selectin by platelets, which enables them to stick to many cell types, including granulocytes. As a result, this contact stimulates granulocyte activation, which then migrates to tissue damage sites. cfDNA activates platelets, which results in the formation of neutrophil extracellular traps (NETs) [75].

ALR protein becomes activated when it identifies and attaches to self-DNA molecules that enter the cytosol due to cellular injury or exosomes [78]. AIM2 is efficiently activated when it detects self-DNA, which is 80-300 base pairs long [79,80]. AIM2's HIN domain can find cytosolic DNA because it is expressed in hematopoietic cells, can be activated by interferon, and is located in the nucleus. To enhance inflammasome complex formation, AIM2's PYD interacts with ASC's PYD. This complex converts pro-CASP1 into CASP1 [79-81]. CASP1 fragments and releases pro-inflammatory cytokines IL-1 and IL-18 from their precursors [81]. CASP1 breaks GSDMD's linker region, releasing IL-1 and IL-18 from cells. The flow of K⁺ out of the GSDMD pore stops cGAS activity and the production of type 1 IFN through the *STING* pathway. The outflow of K⁺ also initiates pyroptosis [82-84]. cGAS-*STING* promotes type 1 IFN production, which AIM2-generated GSDMD inhibits [78]. Another finding is that the AIM2-ASC inflammasome inhibits *STING-TBK1*, which activates IRF3 and releases type 1 IFNs. AIM2 is quiescent without particular cytosolic DNA [85]. **Figure 3** illustrates these mechanisms.

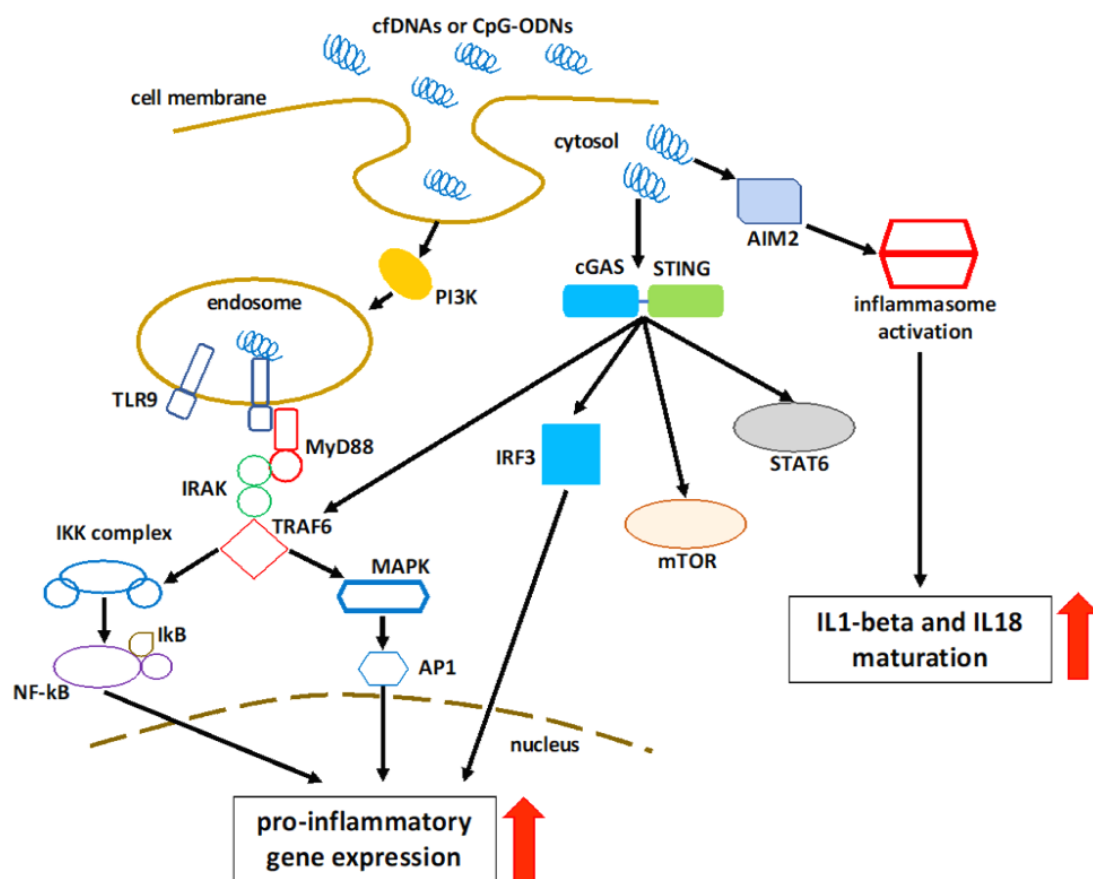


FIGURE 3 | Schematic representation of the cfDNA detection process and the subsequent activation of pathways [86].

The role of Class III PI3K in the internalization of cfDNA and CpG-ODNs into endosomal vesicles that contain TLR9 is apparent. The intracellular activation signal is sent by the interaction between cfDNA and TLR9. The MyD88 protein is specifically attracted to the Toll-interleukin-1 receptor domain of TLR9, resulting in the subsequent activation of the IRAK-TRAF6 complex. This mechanism triggers the activation of both the mitogen-activated protein kinase (MAPK) and inhibitor of IKK (I κ B kinase) complexes, leading to an increase in transcription factors such as NF- κ B and activator protein 1 (AP1). The activation of a *STING*-dependent immune response is initiated by the detection of DNA in the cytoplasm, which occurs through the cGAS-mediated pathway. The *cGAS-STING* pathway may activate several signaling molecules, such as IRFs, mTOR, STAT6, and MAPK, through both direct and indirect pathways. The AIM2 protein in the cytosol has a strong attraction to double-stranded DNA, resulting in the creation of a molecular complex called the AIM2 inflammasome. Consequently, the activation of caspase 1 occurs, which leads to the production of pro-inflammatory cytokines IL1-beta and IL18, finally causing pyroptosis.

AIM2: absent in melanoma-2 receptor; AP1: activator protein 1; cfDNA: cell-free deoxynucleic acids; cGAS-STING: cyclic GMP-AMP synthase-signaling effector stimulator of interferon genes; CpG-ODN: CpG-oligodeoxynucleotide; IL1-beta/18: interleukin 1-beta/18; I κ B: kinase (IKK) complex that consists of two kinases (IKK α and IKK β); IRAK: interleukin receptor-associated kinase; IRF3: interferon regulatory factor 3; MAPK: mitogen activated phosphokinase/protein kinase; mTOR: mammalian target of rapamycin; MyD88: myeloid differentiation primary response gene 88; NF- κ B: nuclear factor kappa-B; PI3K: phosphoinositide 3-kinase; STAT6: signal transducer and activator of transcription 6; TLR9: Toll-like receptor 9; TRAF6: tumor necrosis factor receptor-associated factor 6

1.2.1 Description and features of TLRs and TLR9 signaling

TLRs are type 1 transmembrane glycoproteins that have Toll/interleukin-1 receptor signaling domains and extracellular leucine repeats. The first receptor discovered was TLR4, and a total of 10 human TLRs and 13 mouse TLRs have been reported [87]. Innate and adaptive immune cells, including monocytes, macrophages, lymphocytes, mast cells, and dendritic cells, typically harbor TLRs. However, transformed epithelial cells can express TLR4, TLR5, and TLR9 [88]. Bacterial DNA fragments activate apical epithelial TLR9 to maintain colonic homeostasis [89].

TLRs recognize DNA, RNA, and microbial cell wall components. TLR1, TLR2, TLR4, TLR5, and TLR6 reside on the cell membrane, while TLR3, TLR7, TLR8, and TLR9 are primarily within [63,90-92]. TLR receptors are drawn to patterns seen in bacteria, fungi, protozoa, and viruses [93,94]. Lipids and lipopeptides (TLR1, -2, -4, -6), bacterial flagellin (TLR5), and nucleic acid fragments activate TLRs. TLR3 attracts viral dsRNA, while TLR7 and TLR8 can detect ssRNA. TLR7 can also identify immunoglobulin-self-RNA complexes in autoimmune diseases. Imiquimod binds to TLR7. Bacterial, viral, immunoglobulin-DNA complexes, and synthetic ODNs with unmethylated CpG sequences activate TLR9 [93,94].

TLRs signal innate and adaptive immune responses. Dysregulated adaptive and innate immune activation, amplified by immune evasion of tumor cells, leads to cytotoxic consequences. This can eliminate unhealthy cells or slow cancer growth. TLRs detect microbial PAMPs. They can engage endogenous ligands, such as DAMPs [95]. By stimulating pDCs and macrophages, bacterial DNA and synthetic ODNs activate the innate and adaptive immune systems [96].

TLR9 activation causes pDCs to produce IFN- α . After IFN- α regulates their synthesis, B cells secrete pro-inflammatory (IL-6 and TNF α) and anti-inflammatory (IL-10) cytokines. MHC II surface antigens are also produced upon activation [96,97].

TLR9 activation is a complex and multi-step process. The uptake process is the least understood of the steps and varies depending on the fragment composition of the DNA. Many cell types can efficiently uptake single-stranded DNA. Since endosomes contain TLR9, cationic lipids can boost the uptake of double-stranded DNA [96,97]. Non-specific endocytosis helps transport fluorescein-isothiocyanate-labeled CpG DNA to the intracellular compartment, according to the study. Since DNA sequences without CpG

dinucleotides activate TLR9, the transport mechanism is unspecific. Non-CpG sequences can also limit immune activation in competition [97]. Entering the intracellular compartment causes endosomal acidic maturation. pH-raising drugs like chloroquine and bafilomycin A1 can slow this action. The production of pro- and anti-inflammatory cytokines increases B-cell proliferation [97].

The signal molecules, including MyD88, TRAF6, IRAK-1, and -4, as well as the p50/p65 heterodimer of NF- κ B, lack specificity but are also involved in the signaling of other TLRs. The secretion of IFNs can also take place via a pathway associated with MAPK, which is now being thoroughly studied [98]. **Figure 4** summarises these processes.

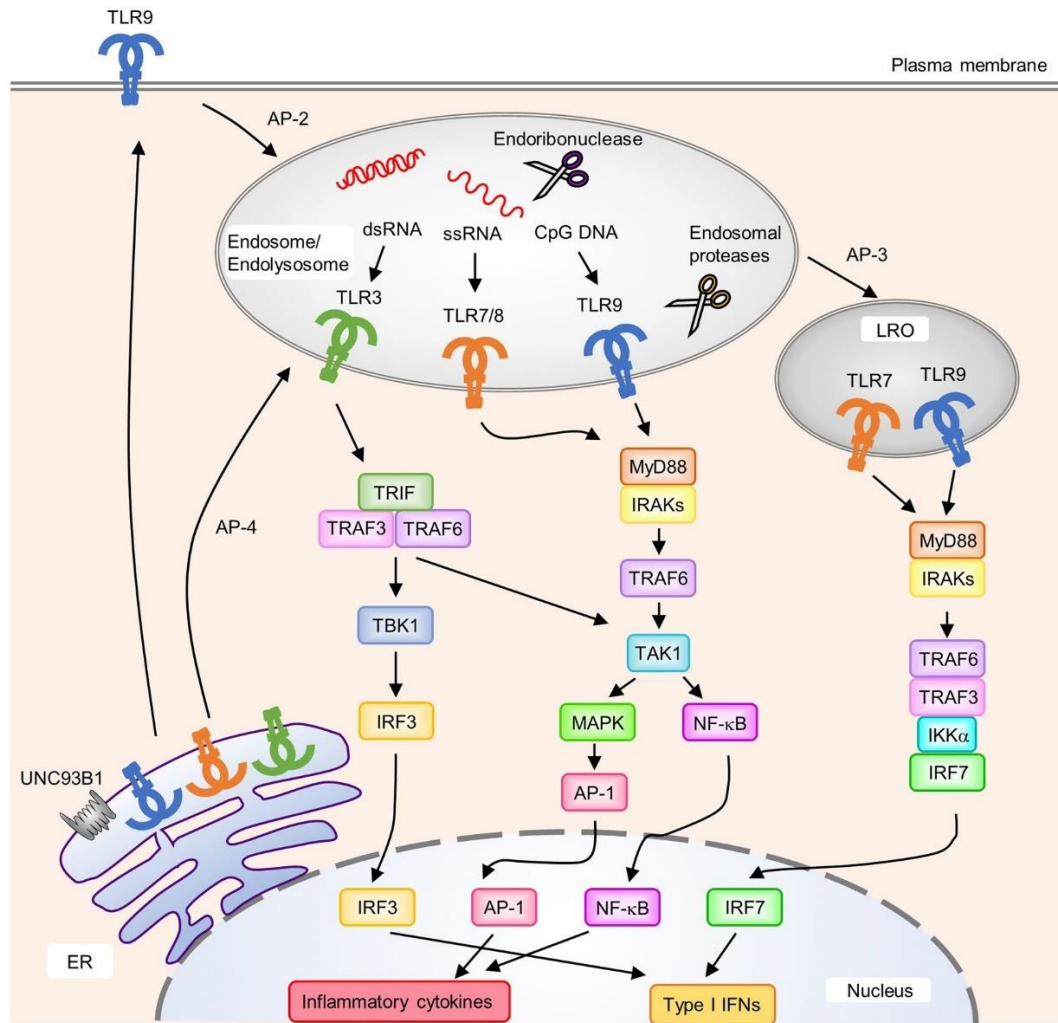


FIGURE 4 | Localization, intracellular transport, and signaling mechanisms of nucleic acid-sensing TLRs [99].

TLRs are produced in the ER and subsequently delivered to endosomes by UNC93B1. TLR9 requires the AP-2 complex to translocate from the cell surface to endosomes, whereas TLR7 interacts with the AP-4 complex to direct trafficking to endosomes. When cognate ligands are recognized, TLR7, TLR8, and TLR9 recruit MyD88 to activate downstream signaling pathways. MyD88 recruits IRAKs and TRAF6, which subsequently activate TAK1. Activated TAK1 activates AP-1 through MAPK, which initiates the transcription of pro-inflammatory cytokines. TAK1 also activates NF-κB, which in turn triggers the production of pro-inflammatory cytokines. It is thought that TLR7 and TLR9 in LRO make IRF7 active by joining with TRAF6, TRAF3, IKKα, and IRF7. This causes type I IFNs to be released. An AP-3 complex is required for the localization of TLR7 and TLR9 to LRO. TLR3 recruits TRIF to initiate downstream signaling pathways. To activate TBK1 and TAK1, TRIF recruits TRAF3 and TRAF6. TBK1 that is activated makes type I IFNs through IRF3, and TAK1 activated by NF-κB and AP-1 makes pro-inflammatory cytokines.

AP-1/2/3/4: Activator protein 1/2/3/4; CpG: cytosolic cytosine-phosphate-guanine; dsDNA: double stranded DNA; ER: endoplasmic reticulum; IFNs: interferons; IKKα: IκB kinase alpha; IRAKs: interleukin receptor-associated kinases; IRF3/7: interferon regulatory factor 3/7; LRO: lysosome-related organelle; MAPK: mitogen activated phosphokinase/protein kinase; MyD88: myeloid differentiation primary response gene 88; NF-κB: nuclear factor kappa-B; ssRNA: single stranded RNA; TAK1: transforming growth factor beta-activated kinase 1; TBK1: tank-binding kinase 1; TLRs: Toll-like receptors; TRAF3/6: tumor necrosis factor receptor-associated factor 3/6; TRIF: Toll-interleukin-1 receptor-domain-containing adapter-inducing interferon; UNC93B1: Unc-93 homolog B1 transmembrane protein

1.2.1.1 Types of CpG-ODNs

Mouse and human cell line investigations have indicated that unmethylated CpG sequences stimulate the immune system [100,101]. Three types of CpG DNA sequences are based on their chemical composition and immune cell-mediated responses. The chemical makeup of these sequences is crucial to their immunostimulatory effect on immune cells [102]. Liu and colleagues [102] studied how the three types of CpG-ODN affect the immune system's responses to antigens in different ways in mouse models. It was found that both B- and C-class CpG-ODNs caused a strong Th1-mediated immune response, with similar antibody and CD4⁺/CD8⁺ T cell responses. The A-class CpG-ODNs raised the cytotoxicity and antibody levels of CD8⁺ T cells, but they did not change the IgG1/IgG2a ratio or increase the number of CD4⁺ and CD8⁺ T cells that produced IFN- γ . Based on this, three CpG-ODN groups showed various levels of targeted protection against *Listeria monocytogenes*, an intracellular bacterium. These three CpG-ODN groups had similar effects on IL-12 production. This study may help to understand the adjuvant properties of three CpG-OND groups. These findings may also aid the CpG-ODN adjuvant strategy [103,104].

Currently, clinical trials have examined the therapeutic use of TLR9 agonists in several forms of cancer, such as colon, pancreatic, and breast malignancies [105-108]. Furthermore, continuous research is underway to evaluate the effectiveness of TLR9 agonist therapy on esophageal squamous cell cancer [109], melanomas [110], lymphomas [111,112], non-small cell lung carcinomas [113], renal malignancies, and androgen-resistant prostate cancers [114]. Mechanism of action of CpG in cellular processes are illustrated on **Figure 5**.

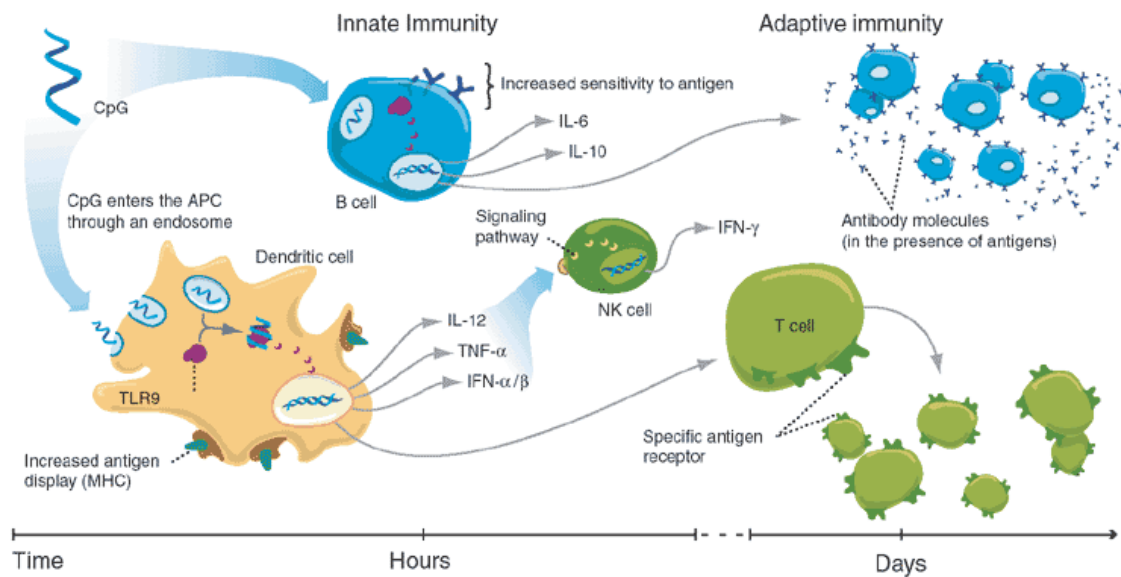


FIGURE 5 | Mechanism of action of CpG in cellular processes [115].

Most cell types take up DNA containing one or more CpG motifs through endocytosis, but only cells expressing the TLR9 receptor (B cells, plasmacytoid DCs (pDC), and several epithelial cells in humans) can activate it. TH1-like cytokine milieu is then made by these cells releasing IFN- α , IFN- β , IL-12, IP-10, and other cytokines and chemokines that support TH1. The secondarily activated NK cells secrete IFN- γ ; additionally, their antigen receptor increases the sensitivity of B cells to activation, and both B cells and plasmacytoid DCs express more costimulatory molecules, enhancing their capacity to trigger T-cell responses.

APC: antigen-presenting cell; CpG: cytosolic cytosine-phosphate-guanine; IFN- $\alpha/\beta/\gamma$: interferon alpha/beta/gamma; IL-6/10/12: interleukin 6/10/12; MHC: major histocompatibility complex; NK: natural killer; TNF α : tumor necrosis factor alpha; TLR9: Toll-like receptor 9

1.2.2 TLR9 in inflammation and malignancy

TLRs 3, 4, 5, 7 and 8 have been detected in colorectal cancers [116]. Human colon cancer cells HCT15, SW620, and HT29 express of several TLRs, including TLR7-9 [117-119]. The increased expression of TLRs in tumor cells appears to play a role in tumor growth by improving their capacity to survive and move within the tumor microenvironment, which is characterized by ongoing inflammation and PAMPs [120]. However, prior studies have shown that boosting TLRs and their associated mediators, such as type I IFNs, may have the ability to modify the balance between immunological tolerance and anti-tumor responses. Therefore, researchers have hypothesized a controversial role for *TLR* signaling pathways in cancer cells[121].

TLRs may promote tumors by conveying pro-inflammatory, anti-apoptotic, proliferative, or pro-fibrogenic signals to tumor cells or the tumor environment. TLRs are critical for inflammatory signaling via *MyD88*-dependent and *MyD88*-independent

pathways. The *NF-κB* pathway is critical for TLRs' tumor-promoting effects. TLR activation increases the production of inflammatory cytokines, such as IL-1β, TNFα and IL-6, which contribute to tumor growth. The increase occurs through the *NF-κB* pathway [121-123]. Apoptosis suppression involves the *TLR* signaling pathway. The *NF-κB* pathway is a key regulator of apoptosis, controlling gene expression and restricting pathways that induce it [124,125].

Tumor cells cannot frequently deliver antigens; therefore, they rely on specialized APCs like DCs to create effective immune responses. Cancer scientists are interested in DCs because they can induce significant anti-tumor immune responses. Cancer cell inhibitory signals frequently cause a lack of DC activation, which can lead to immunological tolerance by eliminating T cells or promoting Tregs [126]. This, in turn, promotes tumor growth. DCs triggered by TLR signaling can deliver antigens, activate T lymphocytes and directly kill tumor cells [127,128]. TLR5 activation on DCs and TLR9 stimulation of pDCs boost immune responses to cancer [129,130]. Signal transduction based on DNA sequence and methylation pattern activates TLR9. Nucleic acid structure affects their immunomodulatory capabilities, including their ability to activate or repress immune responses and promote or inhibit tumor development [119,131]. Synthesized CpG-ODN agonists have been shown to activate TLR9 and fight colon cancer in mouse xenograft models. According to research, TLR9 agonists can increase type I IFN production in DCs, resulting in cytotoxic DCs. This activates NK and cytotoxic T cells, causing a strong immune response to cancer [132,133]. These processes are shown in **Figure 6**.

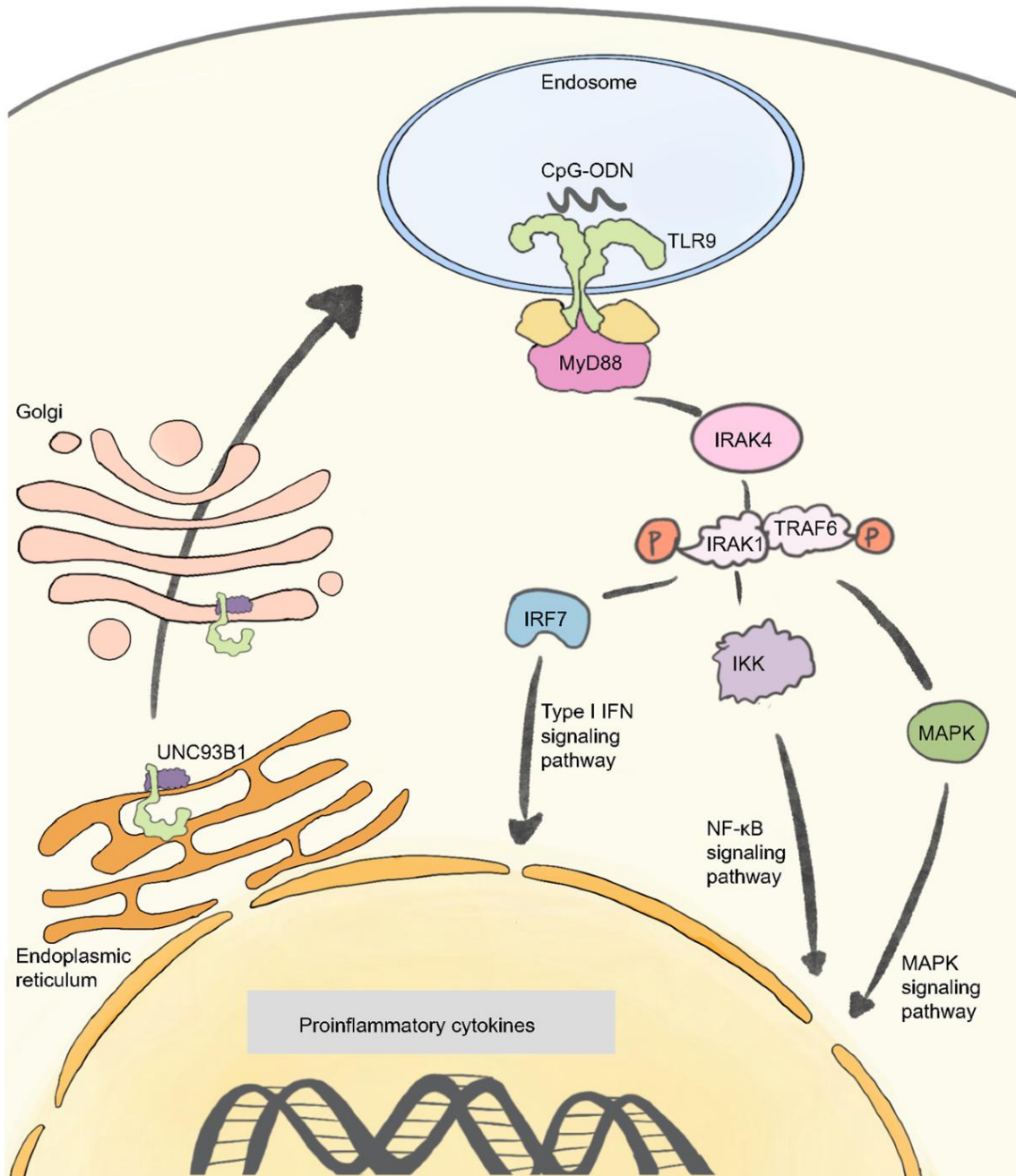


FIGURE 6 | The signaling pathways of TLR9 [134].

The binding of CpG-ODN to TLR9 activates the type I IFN signaling pathway, the NF- κ B signaling pathway, and the MAPK signaling pathway, which promotes the expression and secretion of pro-inflammatory cytokines in target cells.

CpG-ODN: CpG-oligodeoxynucleotide; IFN: interferon; IKK: I κ B kinase; IRAK1/4: interleukin receptor-associated kinase 1/4; IRF7: interferon regulatory factor 7; MAPK: mitogen activated phosphokinase/protein kinase; MyD88: myeloid differentiation primary response gene 88; NF- κ B: nuclear factor kappa-B; TRAF6: tumor necrosis factor receptor-associated factor 6; TLR9: Toll-like receptor 9; UNC93B1: Unc-93 homolog B1 transmembrane protein

1.3 Characteristics and process of autophagy

Autophagy, a well-conserved biological mechanism, encompasses numerous phases across the proteasomal breakdown route. Autophagy is a process that aids in the breakdown of excessive, damaged, or aged proteins and intracellular organelles. This is achieved by enclosing them within double-membraned vesicles called autophagosomes. Autophagosomes fuse with lysosomes/endosomes; their membranes break down and form autolysosomes [135].

Different types of autophagy have been distinguished according to the method by which cellular components are carried to lysosomes as well as their main physiological functions. The types of autophagy encompass macroautophagy, microautophagy, and chaperon-mediated autophagy. We can categorize autophagy into specific categories like lipophagy, ribophagy, nucleophagy, and mitophagy. These types entail the targeted breakdown of cytosolic proteins, lipids, and organelles such as ribosomes, nucleosomes, and mitochondria [135,136].

The term "macroautophagy," henceforth referred to as "autophagy," describes the non-discriminatory degradation of subcellular structures inside the cytoplasm [137]. These processes are illustrated in **Figure 7**.

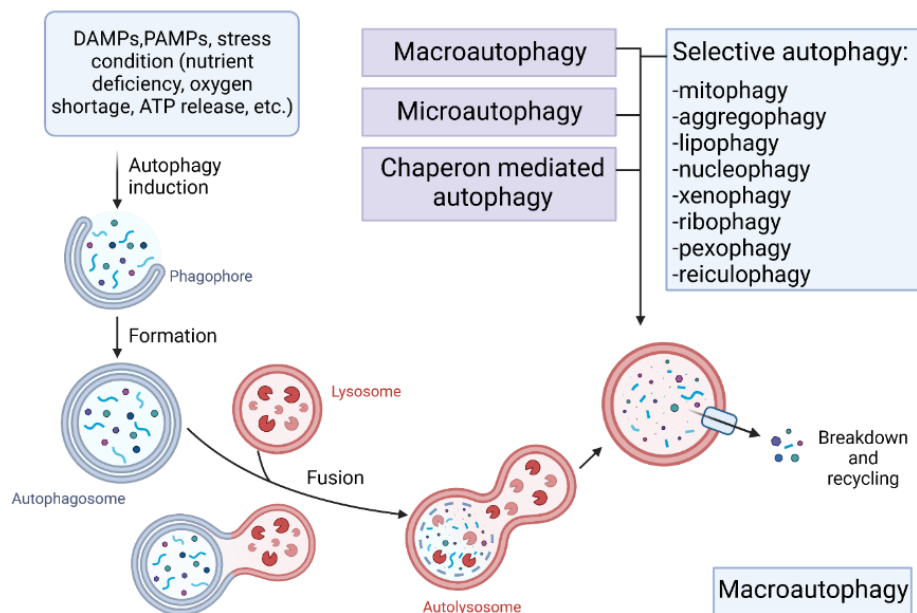


FIGURE 7 | The process of macroautophagy and the types of autophagy [138].

The image shows the formation of the autophagosome and the types of autophagy. (Created with BioRender.com)

ATP: adenosine-triphosphate; DAMP: danger-associated molecular pattern; PAMP: pathogen-associated molecular pattern

A few autophagy genes (*ATGs*) tightly regulate the complicated catabolic system, which involves multiple morphological steps. The encapsulation of molecules or particles for retention triggers the production of phagophores. Phagophores elongate and mature into autophagosomes. Finally, autophagosomes combine with lysosomes [135,137]. Multiple *ATG*-proteins, including the Ser/Thr kinases *ULK1/2 (ATG1)*, a complex of lipid kinases, and two additional ubiquitin-like conjugation systems, enable the multiple dynamic functions listed above [139]. After that, *BECN1*, the mammalian equivalent of *Atg6* in yeast, and the *ATG14* genes control the phagophore. The inhibitory class 1 canonical *PI3K/AKT/mTOR* pathway and the promoting *JNK1* pathway are additional regulators. The *ATG5-ATG12* complex, supported by *ATG16L1*, controls autophagosome formation. Additionally, *LC3/ATG8* is essential for autophagosome maturation. The ubiquitin-like systems *ATG10*, *ATG7*, and *ATG3* strictly regulate these processes. The *LC3* protein and *UVRAG* gene regulate cargo engulfment, autophagosome closure and lysosomal fusion [140,141].

LC3, unlike other autophagy pathway components, may degrade particles without producing a double membrane. This accelerates phagosome formation. Alternative autophagy signaling (*LAP*) is called noncanonical autophagy [142]. Stress-related cell death processes, including intrinsic and extrinsic apoptosis and autophagy, can interact in a complex way. The fate of a cell depends on these pathways' interaction and function [143]. The *ATG6/Beclin-1* and *Bcl-2/Bcl-xL* interact to modulate their communication, with *Bcl-2* suppressing autophagy. TLR adaptors such as *MyD88* and *TRIF* can dissociate this complex. Activating the *MAPK-JNK* cascade or translocating *HMGB-1* can also achieve this [140,143]. Autophagy and *NF-κB* signaling pathways interact in several ways, including positive and negative feedback loops, as **Figure 8** illustrates [141]. The tumor suppressor *p53* gene also controls autophagy. Depending on whether *p53* is in the nucleus or cytoplasm, it can activate or suppress autophagy [140,141].

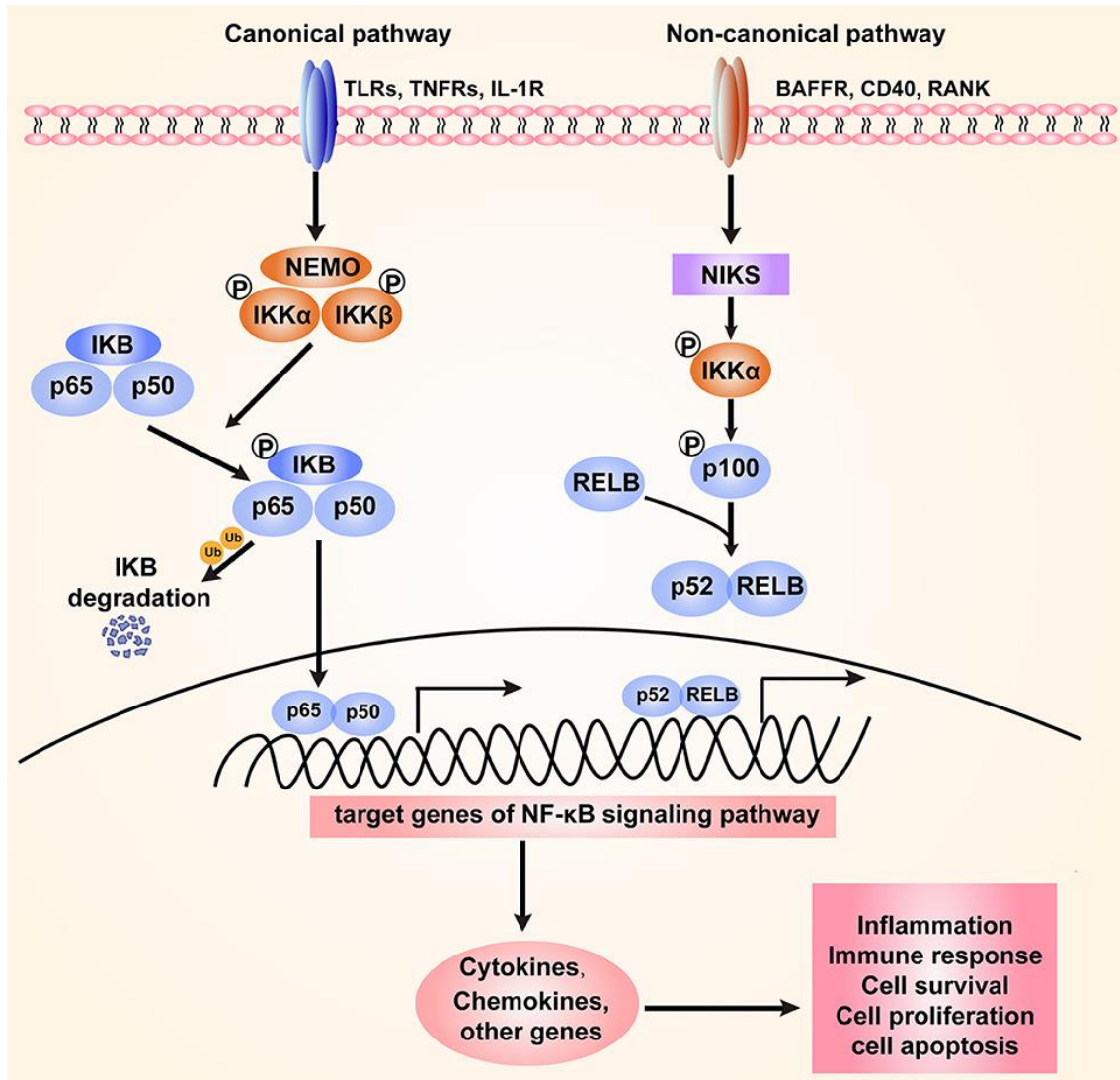


FIGURE 8 | The canonical and non-canonical NF-κB signaling pathways [144].

TLRs, TNFRs, and IL-1R activate the canonical pathway. This cascade activation results in the phosphorylation and destruction of the inhibitory protein IκB. Dissociation from the IκB-containing complex activates NF-κB, which then translocates into the nucleus. The non-canonical route relies on the activation of the NF-κB2 (p100)/RelB complex by BAFFR, CD40, and RANK. This cascade triggers the phosphorylation of NIK, which in turn phosphorylates IKKα. This activation leads to the translocation of the p52-RelB heterodimer to the nucleus. NF-κB signaling can change many cellular functions by affecting the expression of genes that code for cytokines, chemokines, and other things.

CD40: cluster of differentiation 40; BAFFR: B cell activating factor (BAFF) receptor; IL-1R: interleukin-1 receptor; IκB: kinase complex (IKK) that consists of two kinases (IKKα and IKKβ); IKKs: IκB kinases; NEMO: nuclear factor-kappa B essential modulator; NF-κB: nuclear factor kappa-B; NIK: NF-κB-inducing kinases; RANK: Receptor Activator of Nuclear Factor-kappa B; RELB: RelB gene product transcription factor; TLRs: Toll-like receptors; TNFRs: tumor necrosis factor receptor

Autophagy regulates cellular development, specialization, survival, and aging [145]. In addition, it affects inflammation and innate and adaptive immunological responses. Autophagy is essential and adaptable to cellular homeostasis. Several metabolic stress circumstances, such as lack of food and growth factor availability, can activate autophagy

to guarantee cell survival. Basal autophagy disruptions can lead to toxic chemical buildup and DNA damage, causing genomic instability. Most induced autophagy abnormalities impair cell survival [137,145].

Defective autophagy, which harms cells, has been related to cancer, neurological disorders, liver illnesses, viral diseases, aging and inflammatory conditions, including Crohn's disease [136,145-147].

Autophagy's dualistic "Janus" function is thought to have a role in carcinogenesis, as shown in **Figure 9**. This is because it can affect cancer cell survival and multiplication, especially in difficult conditions. Additionally, it can activate signaling pathways that kill cancer cells. Autophagy's effect on cellular defense or tumor cell growth depends on various internal and external factors. Specific tissue types, cellular environment, genetic makeup, and tumor advancement stage all have an impact on tumor growth. However, the relationship between autophagy and cancer networks is still unclear [145,146,148].

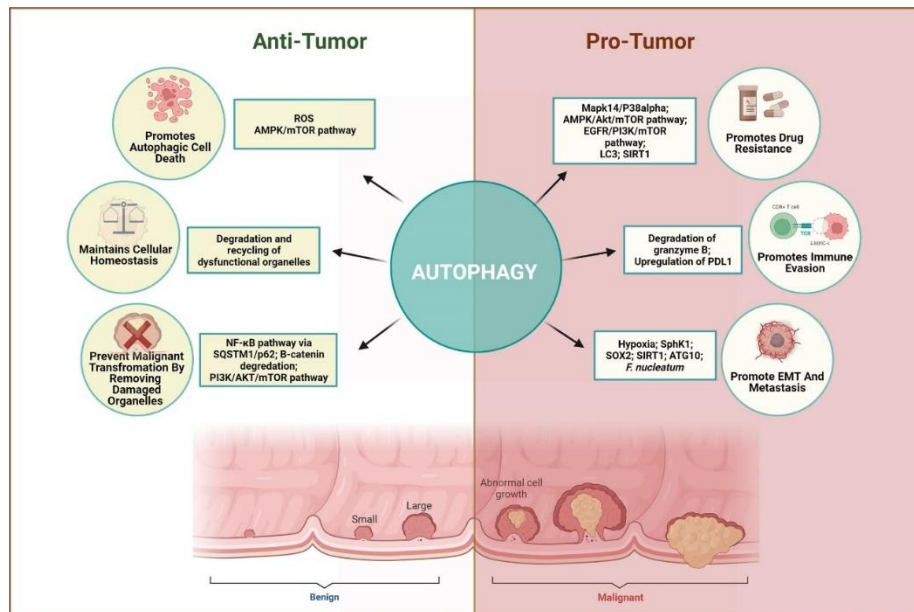


FIGURE 9 | The dual role of autophagy in CRC [149].

Autophagy has a complex and context-dependent role. On the one hand, it can protect against aberrant survival by promoting autophagic death of tumor cells, keeping homeostasis, and removing dysfunctional organelles in early stages, whereas on the other hand, it can promote tumor proliferation by supporting immune evasion, epithelial-mesenchymal transition (EMT), angiogenesis, and resisting the therapeutic effects when cancer has advanced.

AKT: Ak strain transforming; AMPK: AMP-activated protein kinase ; ATG10: autophagy-related gene 10; EGFR: epidermal growth factor receptor; EMT: epithelial–mesenchymal transition; LC3: microtubule-associated protein light chain 3; Mapk14: mitogen-activated protein kinase 14; MHC-I: major histocompatibility complex class-I; mTOR: mammalian target of rapamycin; NF-κB: nuclear factor kappa-B; PDL1: programmed death ligand 1; PI3K: phosphoinositide 3-kinase; ROS: reactive oxygen species; SIRT1: sirtuin 1; SOX2: SRY-related HMG-box transcription factor 2; SphK1: sphingosine kinase 1; SQSTM1: sequestosome 1; TCR: T cell receptor

1.3.1 Autophagy and TLR9 signaling in cancer

1.3.1.1 The role of TLRs in the regulation of autophagy

TLR-autophagy interactions generate innate immune responses [146]. The canonical type of TLRs can induce autophagy, according to recent studies. In addition, several TLRs induce LAP in macrophages, dendritic cells, and neutrophils. This suggests these pathways aid cellular defense [143,146,151,152]. Additionally, TLRs may intrinsically initiate autophagy. Phagocytosis is the main defensive mechanism of innate immunity. TLR signaling in macrophages activates transduction pathways that link the autophagic pathway to phagocytosis. **Figure 10** shows that autophagy can also affect TLR signaling [143,152,163].

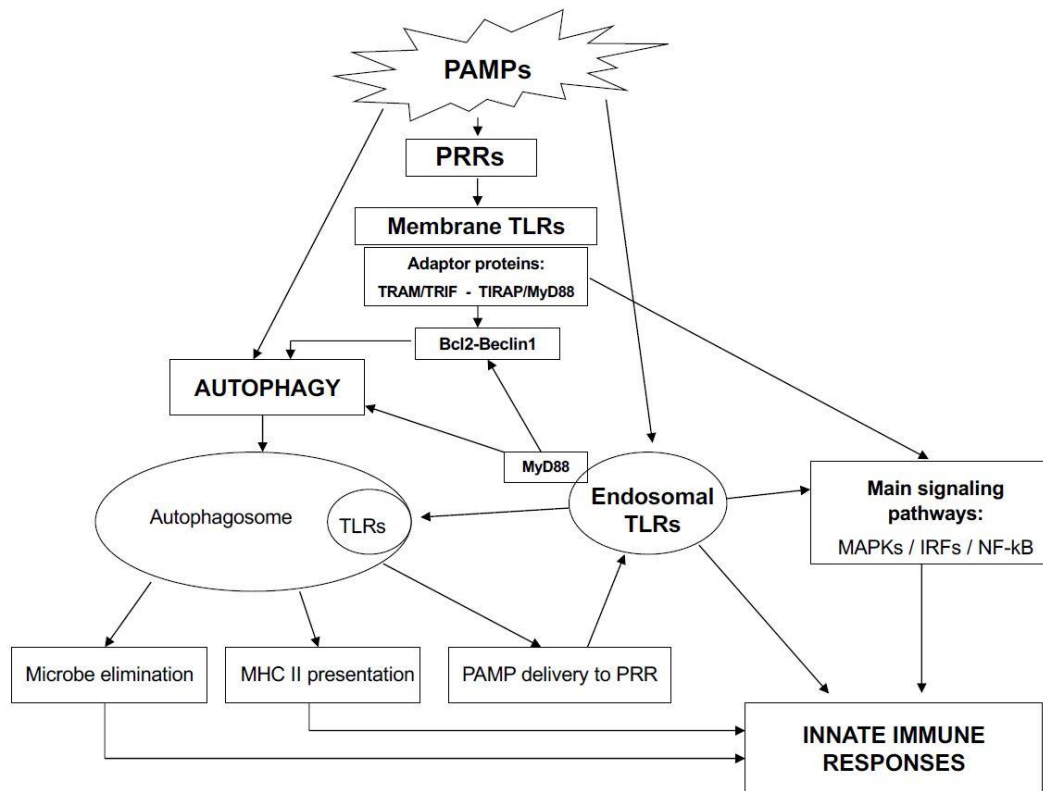


FIGURE 10 | Schematic illustration regarding the relation of PAMPs to (PRR) TLRs and autophagy in respect of signaling and regulatory loops [158].

PRR/TLR-ligands engage different adaptor proteins to initiate signaling. The association of *Bcl2* and *Beclin-1* with *MyD88* represents a basic molecular mechanism in linking TLR and autophagy signaling. Autophagy now is regarded as a recent output of TLR signaling deeply affecting innate immunity.

Bcl-2: B-cell lymphoma 2; IRF: interferon regulatory factor; MAPK: mitogen activated phosphokinase; MHC II: major histocompatibility complex class II; *MyD88*: myeloid differentiation primary response gene; NF-κB: nuclear factor-κB; PAMP: pathogen-associated molecular pattern; PRR: pattern recognition receptors; TIRAP: Toll-interleukin 1 receptor domain-containing adapter protein; TRAM: Toll-like receptor 4 adaptor protein; TLR: Toll-like receptor; TRIF: Toll-interleukin 1 receptor-domain-containing adapter-inducing interferon

However, the activation of TLR7 has not been shown to induce pDC autophagy [154]. Other immune system triggers do not induce autophagy in DCs, which naturally have strong autophagy. Instead, other signaling pathways may prevent autophagy [153]. TLRs initiate NF- κ B/MAPK (*ERK*, *p38*, *JNK*) and IRF3/7 signaling pathways [155]. *MyD88* and TRIF are the main adaptor proteins that activate autophagy after TLR activation [147,155,156]. After the TLR signaling pathway is activated, *Beclin-1* also joins with *MyD88* and TRIF, which separates it from the *Bcl-2* binding complex. Additionally, TRAF6 ubiquitination of *Beclin-1* increased TLR4-induced autophagy. In contrast, the deubiquitinating enzyme A20 had the opposite effect. The activation of *NF- κ B* in response to TLR stimulation may hinder autophagy regulation [155-157].

1.3.1.2 The role of autophagy in the regulation of TLRs

Autophagy protects cells from stress; thus, its role in regulating TLR-mediated pro-inflammatory responses is not surprising [159]. Inflammation is a major inhibitor of autophagy [152]. It directly affects inflammation by inhibiting adaptor proteins MyD88 and TRIF as well as killing invading microorganisms [160,161]. Aggregating TLR adaptors can generate large cytoplasmic aggregates. Autophagy mostly inhibits TLR signaling, which is important. This effect may be reversible in pDCs. [159]. Several autophagy proteins inhibit TLR-mediated signaling. In response to LPS-induced TLR4 stimulation, *ATG16L1*-deficient macrophages generate IL-1 and IL-18 due to increased caspase-1 activation [161]. In addition, *LC3B* or *Beclin-1* deficits impair macrophage autophagy, causing mitochondrial dysfunction. ROS production increased with accumulation [163].

In autophagosomes, autophagy sequesters endogenous viral or self-antigens to deliver them to MHC class II antigens. This method presents MHC II-restricted cytoplasmic antigens to T cells [163]. Contrary to common assumptions, autophagic machinery may transport PAMPs to endosomal TLRs, similar to antigen presentation. This suggests that autophagy enhances TLR-PAMP recognition and TLR-induced effects. **Figure 11** shows that autophagy may initiate an innate immune response before TLR activation [155].

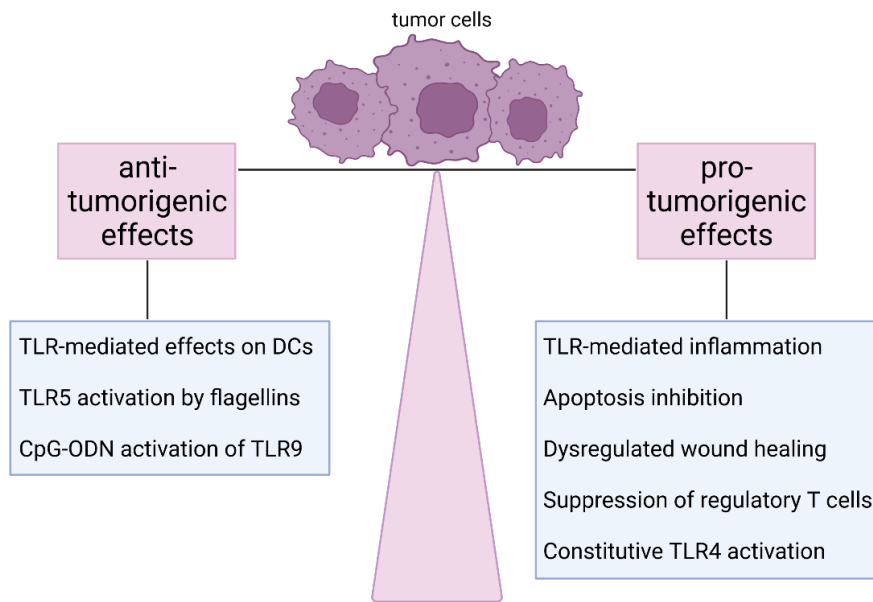


FIGURE 11 | The dual-faced role of TLR signaling in carcinogenesis [158].

While some direct and indirect actions of TLR-signaling act largely as an anti-tumorigenic factor, other effects may promote cancer development. (Created with [BioRender.com](https://www.biorender.com))

TLR: Toll-like receptor; DC: dendritic cell; CpG-ODN: CpG-oligodeoxynucleotide

1.3.1.3 The role of TLRs and autophagy in cancer

The relationship between *TLR* and autophagy signaling in cancer cells is poorly understood. LPS and polyinosine:polycytidylic acid (poly(I:C)) interact with TLR4 and TLR3 to activate autophagy in lung cancer cells, which increases the amount of cytokines and chemokines. Promoting *TRAF6* ubiquitination enhances cancer cell invasion and migration. The adaptor TRIF induces autophagy. However, autophagy suppression significantly inhibited *MAPK* and *NF- κ B* signaling pathways. These pathways' activation depends on TLR3 and TLR4. Thus, this alteration may be a viable lung cancer treatment [164].

In controlled experiments, GO activated TLRs and induced autophagy in CT26 colon cancer cells. Cancer cells ingested GO, stimulating autophagy and TLR4 and TLR9 activation. The *MyD88* and *TRAF6* adaptors were shown to regulate GO-induced autophagy. In mice, GO boosted autophagy, cellular death, and malignant cell immune responses while suppressing tumor development [165].

Many cancer cells express TLR9, which is activated by the identification of unmethylated CpG-ODNs, a subgroup of DAMPs. Proteomics analysis of tumor cells has

found that bacterial CpG patterns affect several proteins, including autophagic ones [166]. Many parallels exist between autophagy and the CpG-TLR9 pathway. The study found that colon, breast, and prostate tumor cell lines promote autophagy. By showing that this induction is TLR9-dependent, TLRs and cancer autophagy are linked [167]. Autophagy might cause cells to die and help the MHC II pathway present endogenous cytosolic proteins. Thus, bacterial CpG patterns may stimulate tumor antigen presentation in cancer, boosting the immune response. The data above provide unique insights into how bacterial CpG patterns affect TLR9-expressing tumor cells, revealing a new therapeutic approach [168].

1.4 cfDNA in tumors

Tumor-associated cfDNA's liquid biopsy capability makes it appealing for several therapeutic uses [169,170]. Despite its limitations, surgical biopsy/histology is the main cancer diagnostic method. This includes invasive and transient static cancers [171]. However, tumor cfDNA detection allows dynamic cancer development monitoring and genetic variety insights [172-174]. Recent genetic studies of plasma and tissue samples have shown considerable agreement, spurring more therapeutic research [175-178]. Early tumor cfDNA detection is a common method in various cancer types [179]. But cfDNA purification and handling are unstandardized. Centrifuges, purification kits, and blood collection tubes can impact cfDNA yield and analysis [180,181]. Therefore, more sensitive and reproducible procedures are needed. Screening using tumor cfDNA and conventional markers looks ideal [182-184]. Several studies have demonstrated that cfDNA can detect minor residual sickness after surgery or therapy in various cancer types. cfDNA is predictive because it predicts disease recurrence [185-187]. Tumor cfDNA genotyping is used in oncology for a variety of purposes. It helps choose the optimal treatment, track results, and uncover genetic factors that promote cancer and medication resistance. Clinical use of tumor cfDNA is imminent [188].

Chronic inflammation has been a hallmark of cancer since Colotta [189], Hanahan, and Weinberg [190,191] pioneered it. Numerous investigations have shown that people with various neoplastic diseases have higher cfDNA levels. One characteristic of cfDNA is its ability to cause inflammation. It is reasonable to explore cfDNA-induced inflammation's carcinogenic implications [192].

TLR9 cfDNA detection produces both positive and negative effects on tumor cells. CRC tissues overexpress TLR9. Through the *TLR9-MyD88* signaling pathway, cfDNA from colon cancer cells or the TLR9 agonist CpG-ODN2395 increased CRC cell growth, migration, invasion, and IL-8 production [192]. Findings show breast cancer secretes cfDNA primarily actively. Activating the *TLR9-NF-κB-cyclin D1* pathway with cfDNA can boost hormone-receptor-positive breast cancer cell proliferation [193]. The host's TLR9 recognizes tumor cfDNA to modulate the immune response to malignancies following chemotherapy, according to previous research. TLR9 helps DCs mature and migrate from the tumor microenvironment to nearby lymph nodes. These DCs stimulate lymph node tumor-specific cytotoxic T lymphocytes, generating powerful anti-tumor responses [194]. The processes described above are illustrated in **Figure 12**.

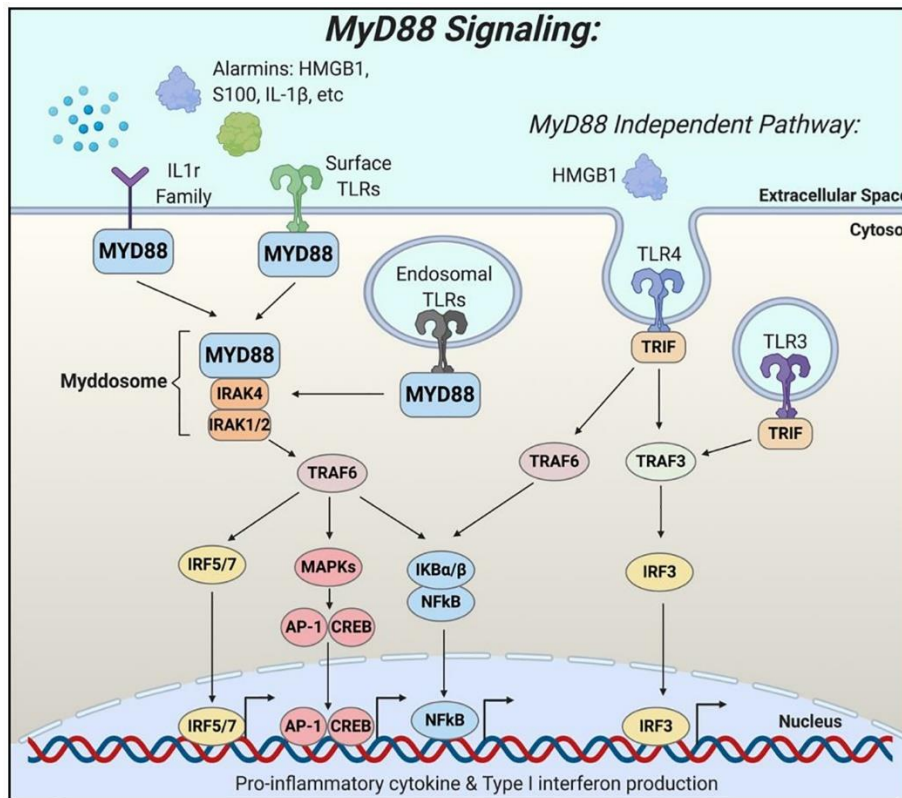


FIGURE 12 | MyD88 signaling pathways [195].

TLRs and cytokine receptors recognize alarmins, which activate MyD88 and trigger an immune response, in addition to cell-specific functions.

AP-1: activator protein 1; CREB: cAMP-response element binding protein; HMGB1: high mobility group box 1; IL-1r: interleukin-1 receptor; $\text{I}\kappa\text{B}\alpha/\beta$: kinase complex (IKK); IRAK1/2/4: interleukin receptor-associated kinases 1/2/4; IRF3/5/7: interferon regulatory factor3/5/7; MAPK: mitogen activated phosphokinase/protein kinase; MyD88: myeloid differentiation primary response gene 88; NF- κ B: nuclear factor kappa-B; TLRs: Toll-like receptors; TRAF6: tumor necrosis factor receptor-associated factor 6; TRIF: Toll-interleukin-1 receptor-domain-containing adapter-inducing interferon; S100: small acidic protein 100

In normal mitosis, the nucleosome competes with dsDNA to prevent cGAS activation. Thus, *cGAS-STING* signaling is incomplete. IRF3 phosphorylation and accumulation during mitotic arrest result from reduced *cGAS-STING* signaling. This reduces inflammation without increasing type 1 IFN. It induces apoptosis [196]. The cancer medicines taxol, paclitaxel, and taxane function in this manner. In some tumor types, overexpression of *cGAS-STING* reduces the infiltration of inflammatory immune cells, which worsens the prognosis [196,197]. Patients with lung cancer who had *cGAS* downregulation experienced a higher death rate [198]. Further research suggests that the *cGAS-STING* signaling pathway controls the immunological milieu of several tumor microenvironments. *STING* signaling pathway activation enhances protective benefits of immunotherapy and robust tumoricidal T-cell immune response [199,200]. NEAT1 suppresses the *cGAS-STING* signaling pathway and limits cytotoxic T cell entry into the tumor microenvironment in mice, encouraging tumor development [201].

AIM2 has anti-cancer benefits independent of inflammasome activity [62,202]. AIM2 includes colitis-associated cancer, hereditary nonpolyposis colorectal cancer, and cutaneous squamous cell carcinoma that have been chemically started [202-204]. AIM2 promotes non-small-cell lung cancer tumor development by altering mitochondrial dynamics [205,206]. AIM2 promotes oral squamous cell carcinoma, benign prostatic hyperplasia, and chemically-induced hepatic cell carcinoma [207–209]. Furthermore, AIM2 has been suggested to slow down the progression of HCC [210].

Genometastasis [211] is a popular theory that may explain metastasis-development experimental differences [212]. Cancer cfDNA with oncogene pieces can act like oncoviruses, providing an alternative metastatic route. Secretomes and horizontal DNA transfer between *in vitro* cells and species support the idea [213-216].

To demonstrate genometastasis, the cfDNA from human CRC was analyzed for *KRAS*, *p53*, and *HBB* gene mutant pieces. NIH-3T3 mouse tumor cells without the mutant gene pattern were subcutaneously implanted into NOD-SCID mice after 20 days of cfDNA incubation. Aggressive "transformed" mouse tumor cells have mutant *KRAS* genes. In another study, tumorous cfDNA in human adipose tissue stem cells did not cause gene alterations or cancer [212]. Cancer-derived cfDNA is implicated in malignant transformation in cell culture and animals [214,215,217,218].

Tumor development and metastasis are linked to increased NET production [219]. Granulocytes release DNA that binds and kills pathogens in the extracellular environment, synthesizing NET. This boosts cell adhesion, invasion, and immune system evasion [220]. DNA immobilizes and supports CCDC25 receptors. HMGB1, neutrophil elastase, ROS, and the TLR4-TLR9 pathway activate tumor cells [221]. However, evidence reveals tumor tissue NETs may be hazardous. NETs inhibit cancer cell proliferation by inducing apoptosis in Caco-2 and AML cells and suppressing melanoma cell migration and survival [222,223]. In a CT-26 mouse model of colorectal adenocarcinoma, oncolytic VSV caused neutrophil-dependent microvessel clot formation in tumor vessels. [224]. **Table 1** lists putative cfDNA effects on tumorigenesis.

TABLE 1 | The possible effects of cfDNA on tumor formation [86]

Harmful and beneficial impacts of cell-free DNA in tumors		
Protumor effects		Anti-tumor effects
TLR9-MyD88 + ODN2395	boosts cell growth, migration, invasion, and IL8 secretion [206]	modulates anti-tumor immunity in response to chemotherapy [208]
TLR9-NF-kB-Cyclin D1	stimulation of cell proliferation [207]	cfDNA sensing by TLR9 promotes maturation and migration of DCs to lymph nodes [208]
cGAS-STING overexpression	reduces intratumoral inflammatory cell infiltration [210] leads to poor prognosis [210]	
cGAS downregulation	increases mortality [211]	low expression of cGAS-STING ameliorates inflammation [209] enhances apoptosis [209]
cGAS-STING inhibition by NEAT1	promotes tumor growth [214]	STING activation improves the protective effects of immunotherapy [212] enhances T cell-mediated anti-tumor immunity [213]
AIM2 cfDNA sensing	modifies mitochondrial dynamics [218,219]	
cfDNA containing secretome	favors to supportive peritumoral milieu [229]	AIM2 (regardless of inflammasome activation) favors tumor cell survival [100,215-217]
horizontal DNA transfer	favors to supportive peritumoral milieu [227,228,230,231]	NET deposition displays cytotoxic effects [235,236] inhibits cell growth, migration, survival [235,236] induces apoptosis [235]
NET formation	enhances adhesion, invasion, immune escape [232] serves as a scaffold and trapping element [234]	
NET + TLR4-TLR9-HMBG1	activates neutrophils [234] activates tumor cells [234]	

1.5 HGFR: functions, relationship with autophagy and cancer

c-Met encodes the hepatocyte growth factor receptor (HGFR). Alpha and beta subunits of this transmembrane RTK protein are disulfide-bonded. In physiological circumstances, epithelial, muscle, hematopoietic, immunological, and neurological cells express HGFR. Many tumor and stromal cells express HGFR in cancer [225]. HGFR binds HGF. Fibroblasts and macrophages produce HGF, which has pleiotropic effects such as promoting cell survival, tissue preservation, regeneration, and anti-inflammatory effects [226]. HGF regulates cell motility, adhesion, and cytokine production [227].

There are two ways that HGFR can be activated: the canonical pathway involves other receptor dimerization, and the conventional pathway involves HGF binding and homodimerization [228]. Activation of HGFR promotes CRC malignancy by activating signaling pathways that influence cancer cell survival, proliferation, motility, migration, and invasion [229]. Metastasis through epithelial-to-mesenchymal transition necessitates signaling within and outside of this pathway [226]. By causing DNA double-strand breaks and perhaps lowering tumor hypoxia, HGFR inhibition made HT29 colorectal cancer cells more irradiable [230]. The HGF/HGFR system - as illustrated in **Figure 13** - can lead to tumor growth through transcriptional activation, gene amplification, mutation, or stimulation at the autocrine or paracrine level. Hepatocellular, pancreatic ductal, and colorectal malignancies activate HGF/HGFR [231]. This aberrant activation promotes the action of growth factors and oncogenic receptors, stimulating cell proliferation and metastasis [232]. Thus, HGF/HGFR inhibition is a promising targeted cancer therapy.

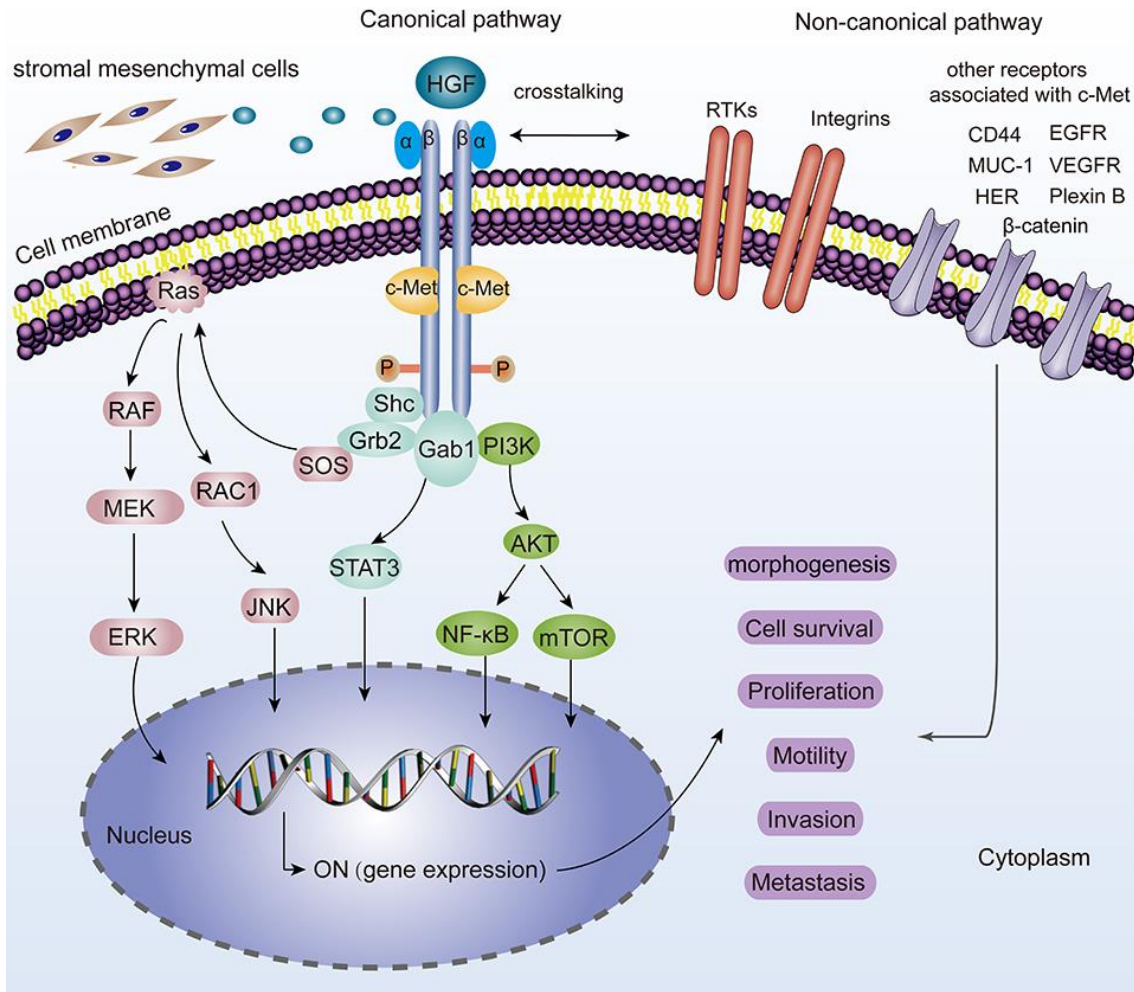


FIGURE 13 | The canonical and non-canonical pathways of HGF/c-Met (HGFR) [233].

The binding of HGF to c-Met results in the dimerization of two c-Met molecules, which triggers the autophosphorylation of tyrosine residues and activates many downstream signaling pathways, including MAPK/ERK, STAT3, and PI3K/AKT signaling. Phosphorylation of JNK also activates a variety of downstream substrates, including transcription factors like AP-1 and apoptosis-related Bcl-2, Bax, among others. All of these basically drive a plethora of cell phenotypes such as morphogenesis, survival, proliferation, motility, invasion, and metastasis. "ON" signifies the activation of gene expression. Other receptors, like EGFR, MUC-1, VEGFR, CD44, Plexin B1, HER, Integrin 64, β-catenin, and others, bind to c-Met and activate it. This leads to the activation of the non-canonical pathways.

AKT: Ak strain transforming; CD44: cluster of differentiation 44; c-Met: C mesenchymal epithelial transition factor; EGFR: epidermal growth factor receptor; ERK: extracellular signal-regulated kinase; Gab1: GRB2 associated binding protein 1; Grb2: growth factor receptor-bound protein 2; HER: human epidermal growth factor receptor; HGF: hepatocyte growth factor; JNK: C-jun N-terminal kinase; MEK: mitogen-activated extracellular signal-regulated kinase; mTOR: mammalian target of rapamycin; MUC-1: transmembrane glycoprotein mucin 1; NF-κB: nuclear factor kappa-B; P: phosphor; PI3K: phosphoinositide 3-kinase; RAC1: Ras-related C3 botulinum toxin substrate 1; RAF: rapidly accelerated fibrosarcoma; Ras: GTPase protein; RTKs: receptor tyrosine kinases; Shc: adaptor protein; STAT3: signal transducer and activator of transcription 3; SOS: sinusoidal obstruction syndrome; VEGFR: vascular endothelial growth factor receptor

Anti-HGF and anti-HGFR antibodies, as well as ATP-competitive and ATP-non-competitive small-molecule c-Met inhibitors [234,235]. It has been shown that the HGFR-EGFR interaction causes cancer [236]. Instead of being intrinsic, metastatic colorectal cancer acquires HGFR amplification after EGFR inhibition [237].

Evolution has preserved proteolysis. To maintain cellular homeostasis, damaged cellular components and energy are eliminated and recycled [238,239]. In preclinical trials, protective autophagy inhibition has been used alongside chemotherapies or targeted treatments to boost their effectiveness in certain cancers [240]. HGFR inhibition causes autophagy activation and inhibition in cancer cells [241,242]. Recent investigations have shown that HGFR-mediated autophagy requires the *HGFR/mTOR/ULK1* cascade. Targeting autophagy with therapeutic treatments may help HGFR-tyrosine kinases combat Met-amplified cancer cells [237,240,243].

A recent study has shown that *HGFR* gene DNA methylation changes over time affect the HGF/HGFR signaling cascade [244]. Additionally, DNA aptamers have beneficial chemical characteristics that can be used to build growth factor mimetics, particularly HGFR-targeting ones [245,246]. The discovery of powerful HGF-targeting drugs is crucial to cancer therapy. Inhibitory DNA aptamers that target human HGF may treat certain cancers [247].

1.6 IGF1R: functions, relationship with autophagy and cancer

IGF1R is a transmembrane receptor tyrosine kinase, which consists of an alpha and beta subunit. Insulin, IGF-1, and IGF-2 bind to IGF1R. The IGF1R- β receptor phosphorylates IRS1/2, SHC, and 14-3-3 after ligand stimulation. Downstream signaling pathways include *PI3K/AKT*, *JAK/STAT*, *Src*, *FAK*, and *RAS/MAPK*. **Figure 14** shows how these pathways regulate apoptosis and cell development genes [249,250]. Normal physiological growth, development, and nutrition include IGF1R in many tissues [251].

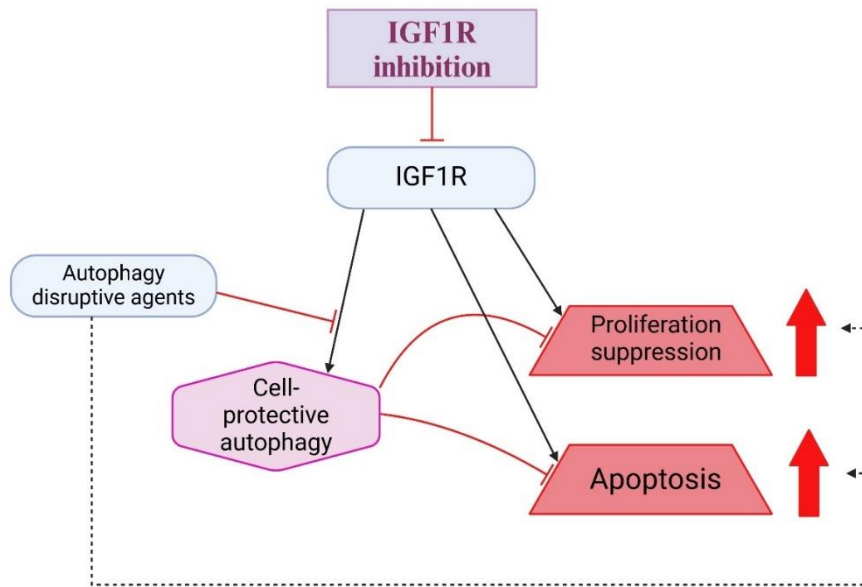


FIGURE 14 | Proposed model for the bi-directional IGF1R signaling-dependent modulation of the autophagic pathway [263].

IGF1R targeting via suppression of the "canonical" *PI3K/Akt/mTORC1* pathway stimulates the autophagy. In case of IGF1R inhibition the simultaneously induced cell-protective autophagy could promote cell proliferation and suppress apoptosis, thus via autophagy antagonize its own original actions on cells. If IGF1R inhibition is combined with autophagy disruptive agents autophagy can be blocked, hence cancer cell proliferation will be suppressed and apoptosis enhanced. (Created with [BioRender.com](https://www.biorender.com))
 IGF1R: insulin-like growth factor receptor 1

IGF1R activation in malignancies promotes carcinogenesis, maintains the altered phenotype, progresses cancer development, increases cell migration, causes epithelial-mesenchymal transition, and imparts treatment resistance [252,253]. Normal tissues exhibited lower *IGF1R* gene and protein expression than malignant CRC tissues [254]. Higher levels of IGF1R are associated with worse CRC outcomes [255]. IGF1R is involved in tumor growth and progression; hence, decreasing it has helped several malignancies [256]. Preclinical studies have demonstrated that anti-IGF1R monoclonal antibodies and small-molecule inhibitors have substantial anti-tumor effects [256], but clinical trials in non-selected cancer patients have failed. This suggests tumor cells can bypass IGF1R inhibition [238].

A previous study has shown that self-DNA configuration, including methylation status and fragment length, greatly affects TLR9-mediated signaling pathways [119]. Insufficient evidence exists on *TLR* signaling and the *IGF1R* pathway. A recent study suggests that CpG-ODN, a TLR9 ligand, stimulates intestinal epithelial IGF1 synthesis

[257]. IGF1 also supports intestinal homeostasis by stimulating macrophage production, which suppresses the immune system [258].

In moderate and chronic colon inflammation, mRNA and protein levels of IGF1R in epithelial cells rise [259]. This may help inflammation-related genetic defects in epithelial cells proliferate and survive. In acute murine colitis, IGF1-stimulated macrophages produced IL-10 to reduce intestinal immunological inflammation [257]. Scientists debate the biological importance of the *IGF1/IGF1R* axis in colonic inflammation [259].

Insulin and cell surface receptors, particularly the insulin receptor and IGF1R, assist cancer cells in survival and growth [261]. High blood insulin levels can alter the IGF-IGF1R axis, a well-known cancer route [262].

There is an interconnection between the *IGF1R* signaling pathway and the autophagy process [263]. In addition, inhibiting or stimulating IGF1R in cancer cells has had different effects on autophagy [264-266]. Autophagy-disrupting drugs and IGF1R inhibitors can improve triple-negative breast cancer treatment, according to recent studies. Recent studies have found that targeting cancers related to IGF1 signaling with IGF1R inhibitor-based drugs is a promising treatment idea (**Figure 15**) [267]. In various cancer stages, targeting IGF1R may be helpful. However, IGF1R pharmacological alteration may have extra physiologic consequences, so be cautious. The current finding reveals that IGF1R suppression may impair mTORC2 function. Reduced mTORC2 function impacts PKC α and β activity. Thus, cytoskeleton alteration and endocytosis rate affect autophagosome formation. *IGF1R* suppression affects autophagy in both ways [266]. Pharmacological inhibition of an *IGF1R* pathway effector and increased autophagy may work together. The data also imply that dual mTORC1/2 catalytic inhibitors may limit autophagy over time. This inhibition may impair cancer cell viability [268-270].

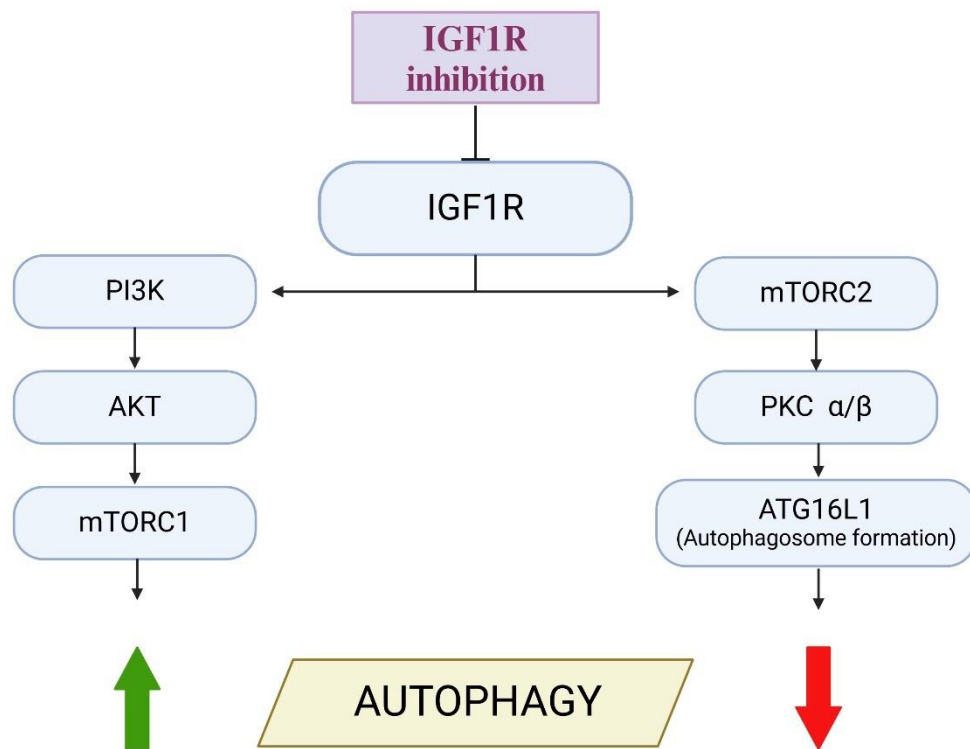


FIGURE 15 | Controversial therapeutic effects of IGF1R inhibition [263].

IGF1R targeting via suppression of the "canonical" *PI3K/Akt/mTORC1* pathway stimulates the autophagy process. However, it can also result in a reduced formation of autophagosomal precursors at the plasma membrane. IGF1R depletion inhibits mTORC2, which reduces the activity of PKC α and β . This finally negatively impacts autophagosome precursor formation. (Created with BioRender.com)

IGF1R: Insulin-like growth factor receptor 1; PI3K: phosphatidylinositol-3-kinase; PKC: protein kinase C; AKT: Akt strain transforming; mTORC1/2: mammalian target of rapamycin complex 1/2; ATG16L1: autophagy-related protein 16-1

The link between autophagy and cell cycle progression is unclear. Earlier studies found that mitotic cells are more resistant to autophagy-inducing stimuli such as mTOR inhibition [271]. Recent research examines the chemopreventive properties of *Boswellia serrata* gum resin's active constituent, AKBA. AKBA's particular interaction with oncogenic proteins explains this focus [272,273]. Epigenetic modification by AKBA suppresses CRC cell proliferation [274]. A potent natural analog of AKBA (BA145) triggers dose- and time-dependent autophagy in pancreatic cancer cells [275]. BA145-induced autophagy halted the G2/M cell cycle and decelerated cell proliferation. BA145 induced autophagy by blocking *mTOR*, which activated *Akt* via *IGF1R/PI3K*. Akt feedback attenuated BA145-induced autophagy, cell cycle, arrest and cell death. This

suggests single-target cancer treatments are ineffective [275]. **Figure 16** illustrates the mechanisms.

Increasing data shows that regulating autophagy and suppressing IGF and the *IGF1R* system may improve insulin-associated inflammatory and neoplastic diseases in the colon. However, manipulating the IGF1R-autophagy process pharmacologically, whether alone or in combination, may have unforeseen pathobiological effects.

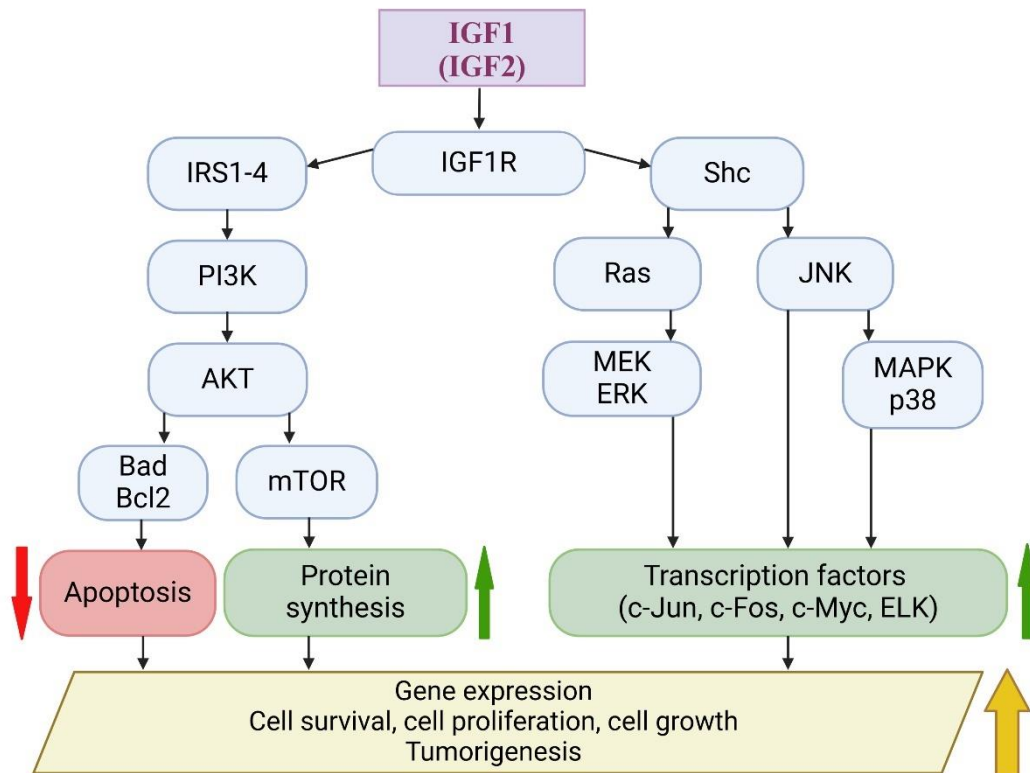


FIGURE 16 | The IGF/IGF1R axis: schematic representation of the composition and function [263].

Signaling of the IGF/IGF1R axis is mediated by IRS and Shc. *PI3K-AKT* activation is the predominant downstream event, but the *Ras/MEK/ERK* and *JNK/MAPK* pathways can also be activated. (Created with BioRender.com)

IGF: insulin-like growth factor; IGF1R: insulin-like growth factor receptor 1; IRS: insulin receptor substrate; PI3K: phosphatidylinositol-3-kinase; AKT: Ak strain transforming; mTOR: mammalian target of rapamycin; Bad: Bcl-2-associated death promoter; Bcl2: B-cell lymphoma 2; Shc: adaptor protein; Ras: GTPase protein; JNK: c-Jun N-terminal kinase; MEK: mitogen-activated extracellular signal-regulated kinase; ERK: extracellular regulated kinase; MAPK: mitogen-activated protein kinase; ELK: ETS domain-containing protein

2. OBJECTIVES

1. To select a human colorectal cancer adenocarcinoma cell line that is suitable for the combined application of cfDNA-induced TLR9-mediated autophagy and HGFR/IGF1R inhibition.

2. To investigate the complex biological effects of TLR9-mediated autophagy and HGFR inhibition induced by cfDNA:

How do cfDNA treatments with different properties (i.e., genomic, fragmented, or hypermethylated) affect the metabolic activity, proliferation, autophagy response, and stem cell phenotype of the selected colorectal cancer adenocarcinoma cell line?

3. To investigate the complex biological effects of TLR9-mediated autophagy and IGF1R inhibition induced by cfDNA:

How does genomic cfDNA treatment affect the metabolic activity, proliferation, autophagy response, and stem cell phenotype of the selected colon cancer adenocarcinoma cell line?

3. MATERIALS AND METHODS

3.1 Selection and maintenance of HT29 cell culture; self-DNA isolation

The selection of HT29 cells was made taking into account several aspects. There is basal TLR9 expression in HT29 cells, which is essential for induction with self-DNA [257]. Moreover, the *MyD88*-dependent and *MyD88*-independent *TLR* signaling pathways are intact in HT29 cells [277]. In HT29 cells, HGFR expression is high as compared to other CRC cell lines [278], and TLR and autophagy-mediated HGFR cross-activation is also present [167,279,280]. IGF1R expression in HT29 cells is moderate as compared to other CRC cell lines (e.g., SW480 or DLD-1) [281]. Also, in HT29 cells, elevated IGF2 expression can be detected, which is essential for both autocrine activation of IGF1R signaling and studying the effect of IGF1R inhibition [282]. HT29 cells adequately represent sporadic colon cancers [283].

Particular attention was paid to whether the inhibitors tested could cause proliferation inhibition in the given context. This graph (**Figure 17**) shows that in the DLD1 cell line, chloroquine treatment causes proliferation inhibition at concentrations as low as 10 μM , whereas in the HT29 cell line, proliferation inhibition occurs only at concentrations as high as 100 μM .

The application of inhibitors at given doses may not result in substantial suppression of cell growth. Beside HT29 cells, not all available colorectal cancer cell lines satisfy these criteria.

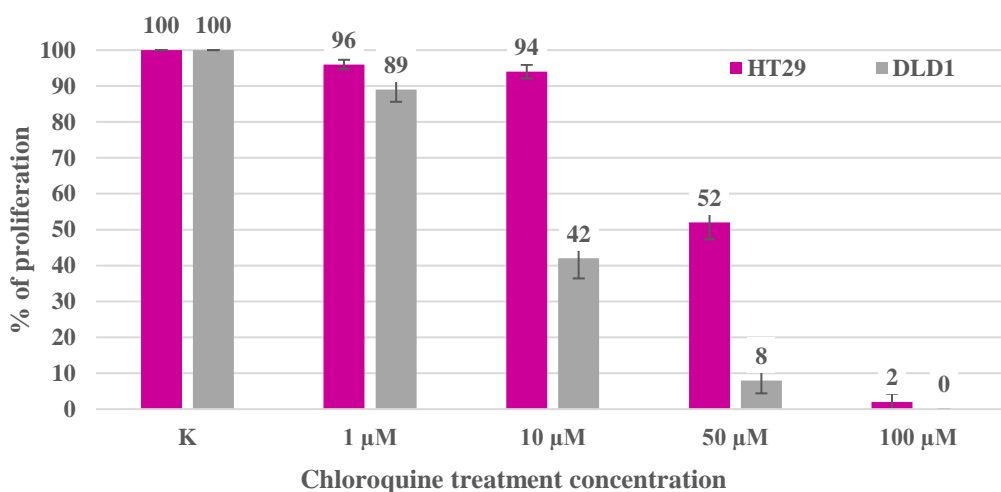


FIGURE 17 | Proliferation inhibition test on HT29 and DLD1 cell lines with chloroquine.

The HT29 undifferentiated colon adenocarcinoma cells were maintained in RPMI 1640 medium (Sigma-Aldrich, MO, USA) supplemented with 10% (v/v) fetal bovine serum (FBS; Standard Quality; PAA Laboratories GmbH, Austria), 125 µg/mL amphotericin B (Sigma-Aldrich, MO, USA), and 160 µg/mL gentamycin (Sandoz, Sandoz GmbH, Austria).

Genomic DNA was isolated from 5×10^7 steady-state, proliferating HT29 cells. DNA isolation was performed by using High Pure PCR template preparation kit containing proteinase K (Roche GmbH, Germany). The DNA samples were treated with 5 µL RNase A/T1 Mix (Thermo Fisher Scientific, Germany). DNA concentration was determined by Nanodrop (Thermo Fisher Scientific, Germany). Gel electrophoresis determined that the fragment length of gDNA was approximately 10.000 base pairs [119]. According to the bisulfite sequencing analysis of *Ogoshi et al.* [284], the basal methylation status of HT29 cells' CpG sites is as follows: 31.6 % in the low range; 11.6% in the middle; and 56.7% in the high range. According to the manufacturer's MALDI-TOF mass spectrometry measurements, the DNA samples were free of RNA, protein, or lipopolysaccharide contamination.

3.2 Fragmentation and hypermethylation of self-DNA

Genomic DNA was divided into three equal shares; the first one was neither fragmented nor hypermethylated (genomic DNA: gDNA). The second one was fragmented (fragmented DNA: fDNA) by ultrasonic fragmentation for 2 min. The third share was hypermethylated (methylated DNA: mDNA) using CpG methyltransferase (M.SssI) (New England Biolabs, Ipswich, USA). The length of the fragmented DNA shares was determined by agarose gel electrophoresis.

3.3 HT29 cell treatments

To incubate with the DNA samples, 5×10^5 HT29 cells were seeded in a 12-well plate with RPMI 1640 supplemented with amphotericin B, gentamycin, and FBS, as previously described. After 24 hours, the medium was changed to RPMI 1640, supplemented with gentamycin but lacking FBS. Separate aliquots of 15 µg of modified self-DNA were dissolved in 200 µL of sterile phosphate buffered saline (PBS).

At 37°C, HT29 cells were incubated with the various DNA samples in a humidified atmosphere containing 5% CO₂ and 95% O₂. Only 200 µL of sterile PBS was added to the control cells. Cells were washed twice with 5 mL of sterile PBS and resuspended in a final volume of 5 mL of PBS after 72 hours.

3.4 Inhibition of TLR9, HGFR, IGF1R signaling and autophagy

For inhibition of TLR9-, HGFR-, IGF1R-signaling or autophagy, HT29 cells were pretreated with TLR9 antagonist (5 µM ODN2088; Invivogen, CA, USA), or 4,4'-Diisothiocyanatostilbene-2,2'-disulfonic acid (DISU; 4 µM; D3514 Sigma-Aldrich, Budapest, Hungary; diluted in dimethyl sulfoxide/DMSO; Sigma-Aldrich Budapest, Hungary/), or picropodophyllin (P) (0.05 µM; BML-EI372-0001; EnzoLifeSciences, BioMarker Ltd., Gödöllő, Hungary; diluted in dimethyl sulfoxide/DMSO; Sigma-Aldrich Budapest, Hungary/) or chloroquine (10 µM; C6628 Sigma-Aldrich, Budapest, Hungary; diluted in DMSO) for 1 hour before treatments with DNAs. All treatments were performed in triplicate. **Table 2** displays the treatment plan for HT29 cells in the HGFR experiments, while **Table 3** displays the IGF1R experiments.

TABLE 2 | Treatment plan for HT29 cancer cells in the HGFR experiments [248].

g/f/mDNA: genomic/fragmented/hypermethylated deoxyribonucleic acid; ODN2088: CpG oligonucleotide; DISU: 4,4'-Diisothiocyanatostilbene-2,2'-disulfonic acid

Sample groups	gDNA	fDNA	mDNA	ODN2088 ("O")	DISU ("D")	Chloroquine ("C")
K						
O				+		
D					+	
C						+
Kg	+					
Kf		+				
Km			+			
gO	+			+		
gD	+				+	
gC	+					+
gOD	+			+	+	
gDC	+				+	+
fO		+		+		
fD		+			+	
fC		+				+
fOD		+		+	+	
fDC		+			+	+
mO			+	+		
mD			+		+	
mC			+			+
mOD			+	+	+	
mDC			+		+	+

TABLE 3 | Treatment plan for HT29 cancer cells in the IGF1R experiments [276].

gDNA: genomic deoxyribonucleic acid; ODN: O, CpG oligonucleotide; K: non-treated, control; P: picropodophyllin; C: chloroquine; Kg: gDNA control; gO: gDNA + ODN2088; gP: gDNA + picropodophyllin; gC: gDNA + chloroquine; gOP: gDNA + ODN2088 + picropodophyllin; gPC: gDNA + picropodophyllin + chloroquine

Sample groups	gDNA	ODN2088 ("O")	Picropodophyllin ("P")	Chloroquine ("C")
K				
O		+		
P			+	
C				+
Kg	+			
gO	+	+		
gP	+		+	
gC	+			+
gOP	+	+	+	
gPC	+		+	+

3.5 Cell viability and proliferation measurements

The use of the Alamar Blue assay served a dual purpose: partly to examine cell viability (metabolic activity) and partly to study cell proliferation [285].

The anti-proliferative effects of the 72-hour treatments were measured after a 4-hour incubation period using Alamar Blue (Thermo Fisher Scientific, Budapest, Hungary). The fluorescence was measured at 570–590 nm (Fluoroskan Ascent FL fluorimeter; Labsystems International Ltd., Budapest, Hungary), and the results were analyzed by Ascent Software.

As metabolic activity is not necessarily proportional to proliferative activity, manual cell counts (average cell numbers determined by using Bürker counting chambers) were also performed. Trypan Blue dye (302643 Sigma-Aldrich, Budapest, Hungary) was used to exclude dead cells.

3.6 Total mRNA isolation and NanoString analysis

Total mRNA from HT29 cells was extracted with the RNeasy Mini Kit (Qiagen, CA, USA) according to the prescription of the manufacturer. Quantitative (Nanodrop) and qualitative analysis (Bioanalyzer Pico 600 chip kit RNA program; RIN >8 in all cases) were performed.

To get the mRNA samples needed for gene expression tests on HT29 cells, the treated groups were multiplied three times. In HT29 samples, cell numbers ranged from 100,000 to 11,135,000 per well, and the recovered mRNA concentration ranged from 8 to 256 ng/ μ L per sample. mRNAs recovered from triplicates were pooled and used in the NanoString assay.

The custom mRNA Assay Evaluation panel (NA-SPRINT-CAR-1.0, nCounter SPRINT Cartridge) containing our custom gene code set (NA-XT-GXA-P1CS-04, nCounter GX Custom CodeSet) was designed by NanoString (the order was placed through Biomedica Hungaria Ltd., Budapest, Hungary). The NanoString experiments were carried out by RT-Europe Research Center Ltd. (Mosonmagyaróvár, Hungary; website: <http://rt-europe.org/>) as part of a contract work.

The selection criteria for examining the genes involved establishing an association between *c-Met/HGFR* or *IGF1R* and TLR9 signaling, apoptosis, cell proliferation, autophagy, and cancer cell stemness. **Supplementary Table 1** indicates the assayed genes with probe NSIDs.

3.7 Taqman real-time PCR analysis

For validating the NanoString gene expression analysis method, *mTOR* (ID: Hs00234508_m1), *ATG16L1* (ID: Hs01003142_m1), *LC3B* (ID: Hs00797944_s1), *BCNI* (ID: Hs01007018_m1), *HGFR* (ID: Hs01565584_m1), *IGF1R* (ID: Hs00609566_m1), *PI3KCA* (ID: Hs00907957_m1), *STAT3* (ID: Hs00374280_m1), *CD95* (ID: 4331182 Hs00236330_m1), and *TLR9* (ID: Hs00370913_s1) triplicated Taqman real-time polymerase chain reactions (PCRs) were used in an Applied Biosystems Micro Fluidic Card System. The measurements were performed using an ABI PRISM 7900HT Sequence Detection System as described in the user guide of products (<http://www.appliedbiosystems.com>, CA; United States). Gene expression levels for each individual sample were normalized to *GAPDH* (ID: Hs02786624_g1) expression. Mean relative gene expression was determined, and differences were calculated using the 2- Δ C(t) method. The whole cycle number was 45.

3.8 Immunocytochemistry for HGFR, IGF1R, CD133, TLR9 and autophagy

To detect *HGFR*, *IGF1R*, *CD133*, *TLR9*, and autophagy-associated *ATG16L2*, *Beclin-1*, and *LC3* protein expression, HT29 cell smears were incubated with rabbit polyclonal anti-Met culture supernatant antibody (1:100, Clone: C-12, Santa Cruz Biotechnology Inc.), anti-IGF1R monoclonal antibody (Chemicon International; Clone: 24-31; 1:50 dilution in PBS), anti-CD133/1-biotin antibody (1:100, Miltenyi, Germany), mouse anti-human monoclonal anti-TLR9 antibody (20 µg/mL; LS-B2341, clone: 26C593.2; LifeSpan BioSciences, WA, USA) and anti-ATG16L1-, anti-BECN1- and anti-MAP1LC3B antibodies (1:200, Antibody Verify, LA, USA) at 37°C for 1 hour. After three rounds of PBS rinsing, cell smears were treated for 40 minutes with an anti-rabbit EnVision polymerHRP conjugate kit (K4003, DAKO, Germany). Secondary immunodetection was performed according to the manufacturer's instructions using EnVision System Labeled Polymer-HRP K4001 (Anti-Mouse 1:1; DAKO, Germany). A Liquid DAB+ Substrate Chromogen System was used to convert the signal (DAKO, Germany). Smears of cells were then digitalized and analyzed using the CaseViewer software on a high-resolution PANNORAMIC 1000 FLASH DX instrument (3DHISTECH Ltd., Budapest, Hungary).

3.9 WES Simple and assessment of autophagic flux

The WES Simple (ProteinSimple 004-600, Minneapolis, MN, USA) method was also performed. A 12–230 kDa Separation Module (ProteinSimple SM-W004) was used for all the proteins (Phospho-mTOR (Ser2448) Rabbit Antibody /Cell Signaling; #2971; 1:50 dilution; 199 kDa/; mTOR (7C10) Rabbit mAb /Cell Signaling; #2983; 1:50; 200 kDa/; Anti-SQSTM1/p62 antibody [2C11] - BSA and Azide-free /Abcam; ab56416/; ATG16L1 (D6D5) Rabbit mAb /Cell Signaling; #8089; 1:50; 66-68 kDa/; Beclin-1 (D40C5) Rabbit mAb /Cell Signaling; #3495; 1:50; 60 kDa/; LC3B (D11) XP Rabbit mAb /Cell Signaling; #3868; 1:50; 14-16kDa/; Anti-β-actin (AC-74) Mouse mAb /Sigma Aldrich; A2228; 1:50; 48 kDa/; GAPDH (14C10) Rabbit mAb /Cell Signaling; #2118/) and either the Anti-Rabbit Detection Kit (ProteinSimple DM-001) or Anti-Mouse Detection Kit (ProteinSimple DM-002) was used, depending on the primary antibodies.

3.10 Cell counting and interpretation of immunoreactions

At 200x magnification, 10 fields of view and at least 100 cells (mainly 110 cells) per field of view were examined in a semiquantitative manner in each digitalized sample. The percentage of immunopositive and non-immunoreactive HT29 cells was determined. In the case of the TLR9 and HGFR immune responses, weak, moderate, and strong membrane staining and perinuclear cytoplasm staining were examined. In the case of the IGF1R immune response, weak, moderate, and strong membrane staining and perinuclear cytoplasm staining were examined. As for autophagy, weak, moderate, and strong *ATG16L1* and *Beclin-1* homogenous or spotted immunoreactions were detected in the cytoplasm. In the case of *LC3*, weak, moderate, and strong punctuated or spotted cytoplasmic immunoreactions were observed.

3.11 Transmission electron microscopy for evaluation of autophagy

For 60 minutes, HT29 cells in the wells were fixed in 2% glutaraldehyde (0.1M Millonig buffer, pH 7.4). The samples were post-fixed for 60 minutes at 4°C in the dark with 1% osmium tetroxide in 0.1 M sodium-cacodylate buffer. Cells were centrifuged and embedded in 10% gelatin in PBS (pH 7.4). The samples were embedded in Poly/Bed epoxy resin. Contrast staining of ultrathin sections (70-80 nm) with uranyl acetate and lead citrate, respectively. The JEM-1200EXII Transmission Electron Microscope was used to conduct ultrastructural analyses (JEOL, Akishima, Tokyo, Japan). In five HT29 cells per sample, the average number of autophagic vacuoles was counted (mean \pm SD/cell).

3.12 Semithin sections

From the HT29 cell blocks fixed for TEM semithin sections were cut for viewing by digital microscope. The sections were stained with toluidine blue (toluidine blue O 4 g, pyronin 1 g, and borax 5 g in distilled water). The average number of proliferative cells was counted in five fields of view per sample (mean \pm SD/sample).

3.13 Statistical analysis

At least three independent experiments were conducted. Data on cell viability, cell number, and proliferation were presented as means \pm SD. The χ^2 -test and Student's t-test were used for statistical analyses. $p < 0.05$ was considered statistically significant. In the case of immunocytochemistry, statistical analysis with one-way ANOVA and the Tukey HSD test was performed using R Core Team R version 3.5.3 (2019) [286].

Regarding NanoString gene expression analysis, after importing RCC files to the nSolver Analysis Software, quality checking was performed. Then agglomerative cluster heat maps were created. The Euclidean distance metric was used to calculate the distance between two samples (or genes) as the square root of the sum of squared differences in their log count values. The average linkage method was used to calculate the distance between two clusters. In the case of the WES Simple, the area of the tested proteins was multiplied by the values of the β -actin area for graphical representation.

4. RESULTS

4.1 Cell viability and proliferation measurements (HGFR studies)

Treatment of HT29 cells with gDNA alone, ODN2088, DISU, chloroquine, or all three together increased their metabolic activity. However, cell viability was significantly reduced when TLR9 or autophagy inhibitor treatments combined with gDNA were also combined with DISU.

gDNA administration, as opposed to metabolic activity, inhibited the proliferation of HT29 cells. The co-treatment of ODN2088 and DISU significantly reduced the inhibitory effect of gDNA on cell proliferation. When treated alone, ODN2088 or DISU in combination with gDNA reduced the inhibitory effect of gDNA on cell proliferation. However, when combined, these treatments showed significantly enhanced efficacy. The co-treatment of gDNA, DISU, and chloroquine demonstrated the most efficacious suppression of HT29 cell proliferation, accompanied by elevated metabolic activity.

In isolation, fDNA treatment marginally enhanced cell viability; however, when combined with a TLR9 inhibitor, it substantially augmented metabolic activity; furthermore, it exhibited a moderate increase when combined with chloroquine or DISU. However, in the case of fDNA/ODN2088 and fDNA/chloroquine combinations, the metabolic activity of HT29 cells was reduced by DISU to the same extent as in the fDNA control samples.

The fDNA control samples produced a marginal increase in HT29 cell proliferation, which subsequently declined to varying degrees upon combination with both treatments. After DISU administration, the decrease in cell proliferation remained largely unchanged in the fDNA/ODN2088 combination. However, DISU in combination with fDNA and chloroquine had a minor effect on HT29 cell proliferation.

mDNA exhibited the greatest increase in cellular metabolic activity among all DNA varieties. In comparison to the mDNA control, the level of metabolic activity exhibited no change (DISU, ODN2088/DISU) or increased (ODN2088, chloroquine) throughout the interventions; it only decreased significantly when DISU and chloroquine were administered concurrently.

A marginal reduction in cell proliferation was observed in response to mDNA treatment; a decline was observed in response to all treatments, most notably autophagy

inhibition. With mDNA/DISU or mDNA/ODN2088/DISU regimens, however, a substantial increase in cell proliferation was observed. Notably, when mDNA, ODN2088, and DISU were co-administered, there was a concurrent increase in cell proliferation and a substantial reduction in metabolic activity. The data pertaining to cell proliferation, viability, and cell count are presented in **Table 4** and **Figure 18**.

TABLE 4 | Numerical data of metabolic activity, cell number and proliferation (HGFR studies) [248].

*represents significant alteration as compared to K (control), non-treated sample ($p < 0.05$; $n = 3$).
g/f/mDNA: genomic/fragmented/hypermethylated deoxyribonucleic acid; O: ODN2088 CpG oligonucleotide; D: DISU; C: chloroquine; SD: standard deviation

Sample	Metabolic activity mean % (\pm SD)	Average cell number (\pm SD)	Proliferation % (\pm SD)
K	100 \pm 1.1	800,000 \pm 8,800	100 \pm 1.1
O	120.17 \pm 4.5*	760,000 \pm 32,680	95 \pm 4.3
D	111.41 \pm 3.8	810,000 \pm 25,920	101.25 \pm 3.2
C	116.23 \pm 2.9*	775,000 \pm 31,775	96.87 \pm 4.1
Kg	127.51 \pm 3.1*	220,000 \pm 9,900	27.5 \pm 4.5*
Kf	112.61 \pm 2.2	855,000 \pm 31,635	106.87 \pm 3.7
Km	147.87 \pm 3.4*	720,000 \pm 19,440	90 \pm 2.7*
gO	139 \pm 3.1*	270,000 \pm 3,780	33.75 \pm 1.4*
gD	134.44 \pm 2.7*	310,000 \pm 6,510	38.75 \pm 2.1*
gC	123.55 \pm 3.1*	230,000 \pm 4,370	28.75 \pm 1.9*
gOD	75.75 \pm 2.6*	690,000 \pm 24,840	86.25 \pm 3.6*
gDC	90.99 \pm 3.3	100,000 \pm 1,600	12.5 \pm 1.6*
fO	198.02 \pm 4.7*	745,000 \pm 23,840	93.12 \pm 3.2
fD	120.87 \pm 3.7*	665,000 \pm 21,945	83.12 \pm 3.3*
fC	121.18 \pm 2.5*	560,000 \pm 13,440	70 \pm 2.4
fOD	99.61 \pm 3.7	730,000 \pm 26,280	91.25 \pm 3.6
fDC	107.62 \pm 3.2	640,000 \pm 17,920	80 \pm 2.8*
mO	155.15 \pm 4.1*	740,000 \pm 25,160	92.5 \pm 3.4
mD	141.85 \pm 3.9*	875,000 \pm 36,750	109.37 \pm 4.2
mC	183.48 \pm 4.6*	560,000 \pm 16,240	70 \pm 2.9*
mOD	90.12 \pm 2.5	1,140,000 \pm 60,420	142.5 \pm 5.3*
mDC	92.34 \pm 3.1	580,000 \pm 9,860	72.5 \pm 1.7*

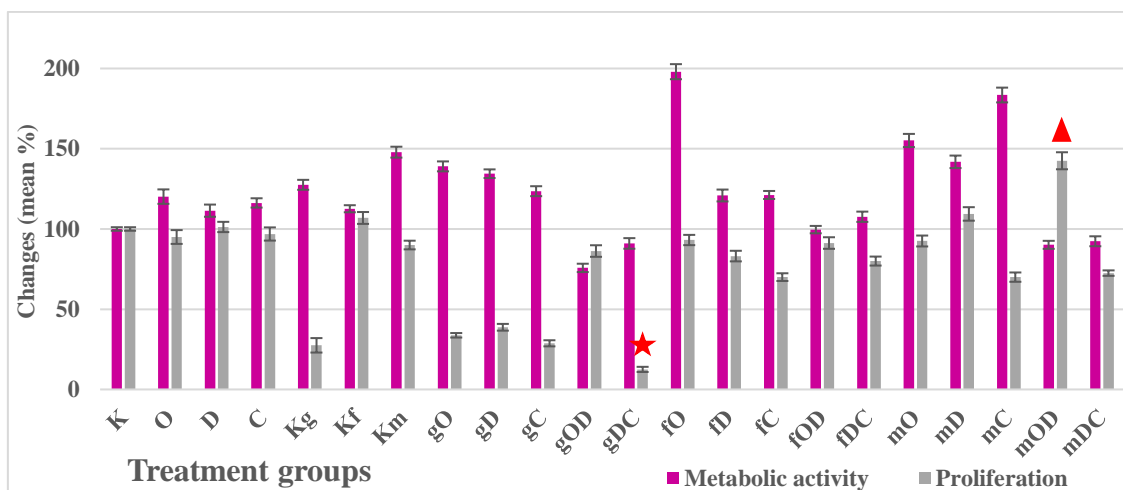


FIGURE 18 | Changes in the metabolic activity (magenta) and proliferation (grey) of the studied cell groups under the influence of each treatment combination in HGFR studies [248].

The red star indicates the lowest (group gDC), while the red triangle indicates the highest proliferative activity (group mOD).

g/f/m: genomic/fragmented/hypermethylated DNA; K: control; O: ODN2088 CpG oligonucleotide; D: DISU; C: chloroquine

4.2 Cell viability and proliferation measurements (IGF1R studies)

The metabolic activity of the HT29 cells was significantly ($p < 0.05$) increased in all treatment groups except the gOP combination as compared to K (control, non-treated cells). The P treatment exhibited the highest metabolic activity.

The Kg treatment group of cells had significantly lower ($p < 0.05$) cell proliferation compared to K.

When gDNA, ODN2088, picropodophyllin, and chloroquine were co-treated (i.e., gO, gP, gC), effective inhibition of HT29 cell proliferation with high metabolic activity was observed. The combination of gDNA, ODN2088, and picropodophyllin (i.e., gOP) raised proliferative activity back to levels close to those of the non-treated control group.

Viability, cell number, and proliferation data are illustrated in **Table 5** and **Figure 19**.

TABLE 5 | Numerical data of metabolic activity, cell number and proliferation (IGF1R studies) [276].
 *represents significant alteration as compared to K (control), non-treated sample ($p < 0.05$; $n=3$).
 g: genomic DNA; O: ODN2088 CpG oligonucleotide; P: picropodophyllin; C: chloroquine; SD: standard deviation

Sample	Metabolic activity mean % (\pm SD)	Average cell number (\pm SD)	Proliferation % (\pm SD)
K	100 \pm 1.1	800,000 \pm 8,800	100 \pm 1.1
O	120.17 \pm 4.5	760,000 \pm 32,680	95 \pm 4.3
P	142.15 \pm 4.7*	810,000 \pm 25,920	101.25 \pm 1.8
C	116.23 \pm 2.9	775,000 \pm 30,775	96.87 \pm 4.1
Kg	127.51 \pm 3.1	220,000 \pm 9,900	27.5 \pm 4.5*
gO	139 \pm 3.1*	270,000 \pm 3,780	33.75 \pm 1.4*
gP	119.57 \pm 3.2	270,000 \pm 7,020	33.75 \pm 2.6*
gC	123.55 \pm 3.1	230,000 \pm 4,370	28.75 \pm 1.9*
gOP	91.3 \pm 2.4	660,000 \pm 16,500	82.5 \pm 2.5
gPC	127.38 \pm 2.8	250,000 \pm 9,250	31.25 \pm 3.7*

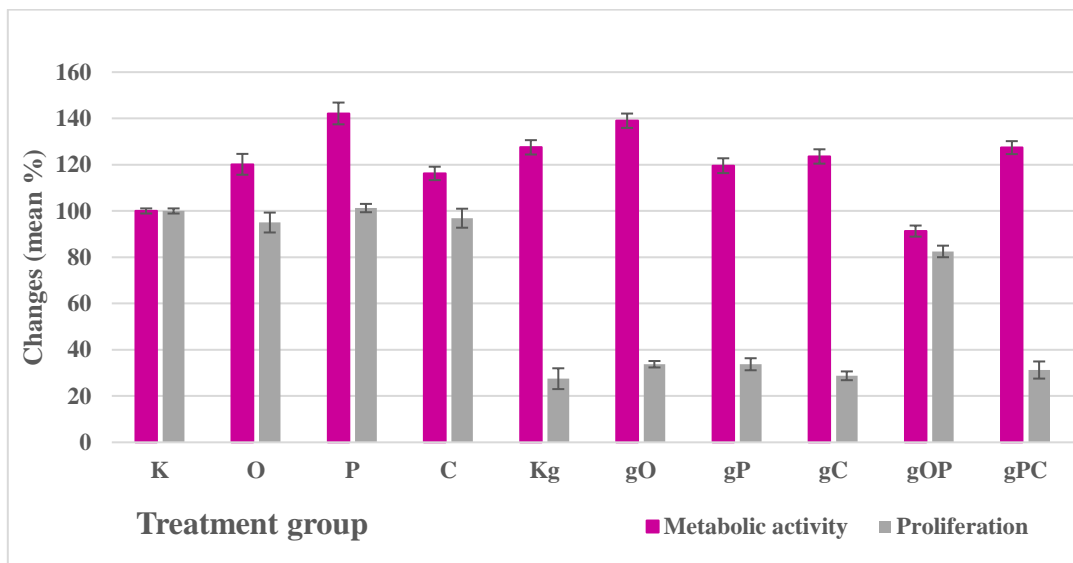


FIGURE 19 | Changes in the metabolic activity (magenta) and proliferation (grey) of the studied cell groups under the influence of each treatment combination in IGF1R studies[276].
 g: genomic DNA; K: control; O: ODN2088 CpG oligonucleotide; P: picropodophyllin; C: chloroquine

4.3 NanoString and Taqman gene expression analyses (HGFR studies)

In relation to the expression of TLR9 mRNA, the application of g-, f- and mDNA treatments led to *TLR9* upregulation in comparison to the untreated control cells (**Figure 20/A**). *HGFR* gene expression was not upregulated in response to gDNA treatment when compared to the untreated control group. However, fDNA and mDNA treatments upregulated *HGFR* gene expression. When not incubated with gDNA, the gene expression profile remained comparable to that observed in the control samples (**Figure 20/A**). With the exception of IL1- β , all observed transcripts exhibited increased mRNA expression in response to fDNA administration. Genes associated with extrinsic and intrinsic apoptosis, including *Bcl-2*, *CD95*, and caspase-3, exhibited significant upregulation. Genes related to autophagy (*ULK1*), TLR9 signaling (*TRAF6*), c-Met signaling/anti-apoptotic factors (*PI3K* and *HGFR*), and apoptosis (*CD95L*) showed moderate upregulation. Conversely, genes related to autophagy (*ATG16L1*, *MAP1LC3B*, *Beclin-1*), pro-apoptotic mechanisms (*AMPK*), *HGFR* signaling, and *STAT3* displayed only modest upregulation (**Figure 20/A**). When incubated with mDNA, the anti-apoptotic *Bcl-2* gene exhibited significant upregulation. Conversely, the autophagy-related (*MAP1LC3B*), TLR9-signaling (*IL8*, *MyD88*), pro-apoptotic (*MAPK*), anti-apoptotic (*Akt*), and c-Met-signaling (*HGFR*) genes displayed moderate overexpression (**Figure 20/A**).

In relation to the impact of modified DNA treatments and combined *HGFR* inhibition on canonical and non-canonical *HGFR* signaling, it was observed that the concurrent administration of DISU and gDNA led to upregulation of *STAT3* and *CD95*, a marginal upregulation of *PI3K*, and a downregulation of *HGFR* expression (**Figure 20/B**). The simultaneous administration of fDNA and DISU increased the expression of *HGFR*, decreased the expression of *STAT3* and *PI3K*, and did not change the expression of *CD95* (**Figure 20/C**). The co-administration of DISU and mDNA resulted in increased expressions of *STAT3* and *HGFR* as well as decreased expressions of *PI3K* and *CD95* (**Figure 20/D**).

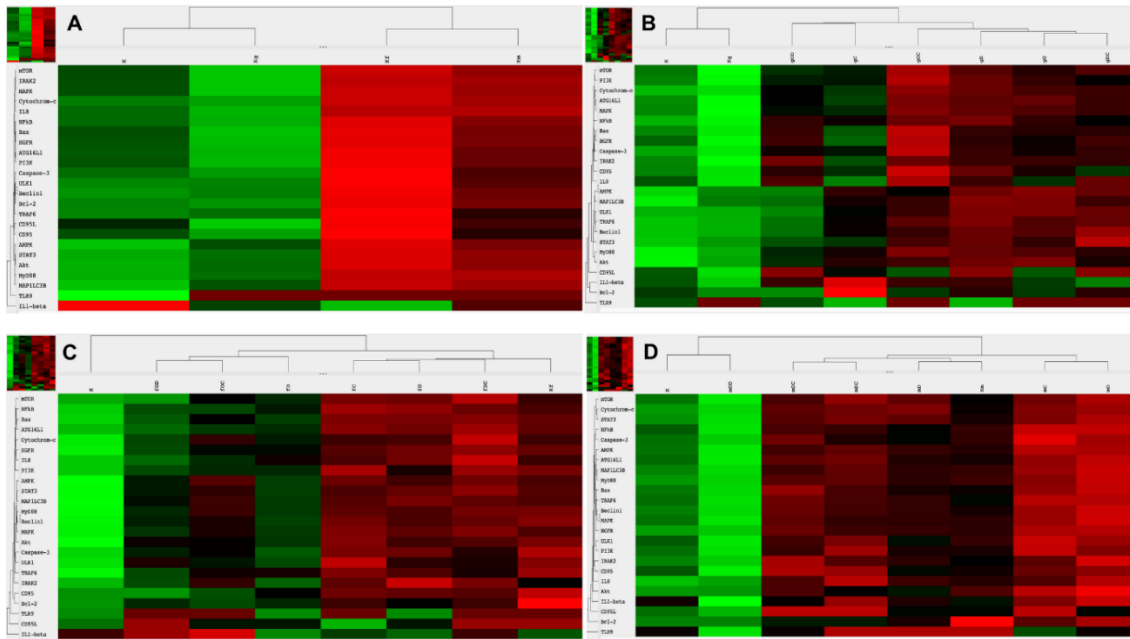


FIGURE 20 | Heatmap visualization of the NanoString gene expression analyses in HGFR studies [248].

A. Gene expression changes of modified DNA treatments as compared to control, non-treated HT29 cells. Gene expression alterations in HT29 cell after incubation with gDNA (**B.**), fDNA (**C.**) and mDNA (**D.**). g/f/m: genomic/fragmented/hypermethylated DNA; K: control; O: ODN2088 CpG oligonucleotide; D: DISU; C: chloroquine; red: overexpression, green: downregulation

Due to the fact that cfDNA treatment influences both *TLR9*-signaling and the autophagy apparatus, we also examined how inhibition of *TLR9*-signaling or autophagy modifies the effect of concurrent *HGFR* inhibition and modified DNA treatment. Co-administration of all types of modified DNAs and DISU decreased the expression of genes implicated in canonical and non-canonical *HGFR* signaling by inhibiting *TLR9* signaling (**Figure 21/A**). The co-administration of gDNA and DISU, along with the inhibition of autophagy, did not affect the overexpression of *STAT3*, but it did reduce the expression of all other genes implicated in *c-Met* signaling (**Figure 21/A**). The simultaneous introduction of DISU and chloroquine along with fDNA or mDNA significantly increased the expression of each component of *HGFR* signaling (**Figure 21/A**).

In regard to genes associated with autophagy, the concurrent administration of *HGFR* inhibition and modified DNA treatments led to the upregulation of *ATG16L1*, *MAP3K4*, *Beclin-1* and *ULK1*, with the exception of fDNA and *Beclin-1*, and mDNA and *ULK1*, for which there was no significant alteration in gene expression when compared to the control group (**Figure 21/B**). The concurrent inhibition of *HGFR*, modified DNA, and *TLR9* led

to the downregulation of all genes associated with autophagy when gDNA or mDNA were utilized for treatment. Conversely, *MAPLC3B*, *Beclin-1*, and *ULK1* showed upregulation and incubation with fDNA did not result in any alteration in the expression of *ATG16L1*. Combining DISU, chloroquine, and modified DNAs led to the upregulation of all autophagy-associated genes (**Figure 21/C**).

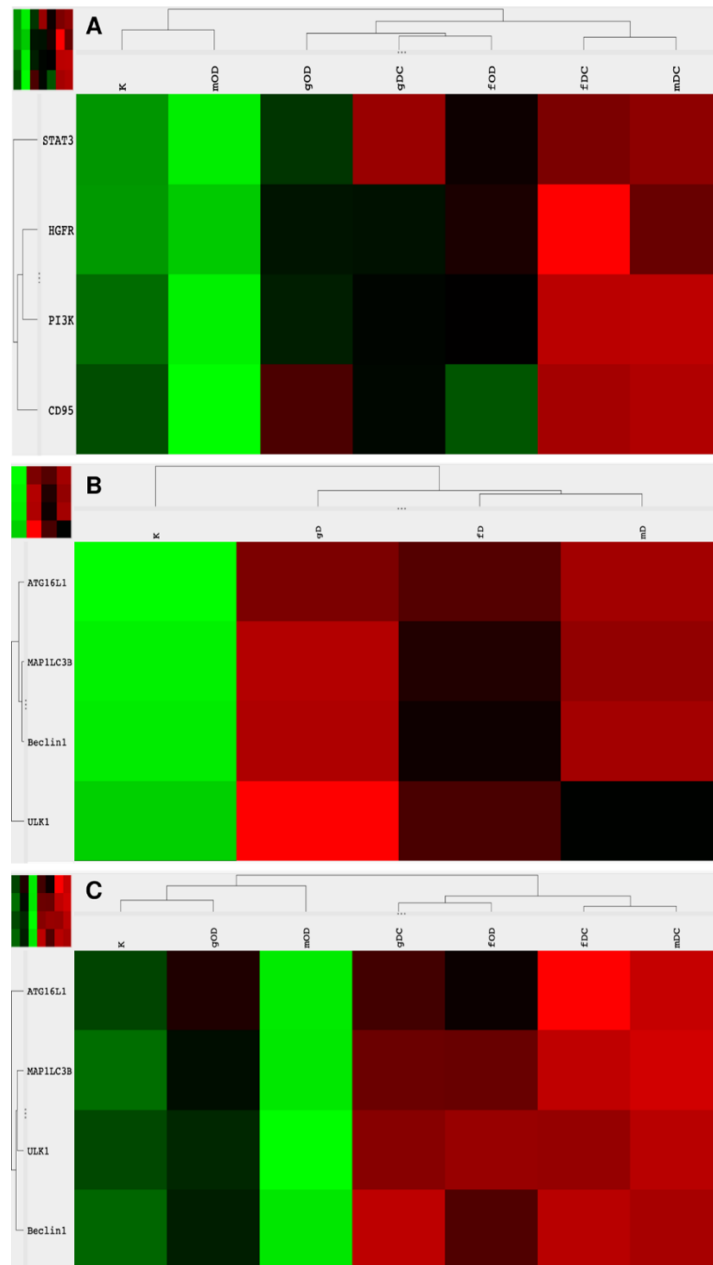


FIGURE 21 | Heatmap visualization of the NanoString gene expression analyses in HGFR studies: alterations in c-Met signaling pathways and autophagy [248].

Gene expression changes of combined treatments with modified DNAs, ODN2088, DISU, or chloroquine. g/f/m: genomic/fragmented/hypermethylated DNA; K: control; O: ODN2088 CpG oligonucleotide; D: DISU; C: chloroquine; red: overexpression, green: downregulation

The Taqman RT-PCR results confirmed the identification of changes in gene expression by NanoString/nCounter analysis. **Figure 22** provides a summary of the fold changes and **Supplementary Table 2** of SD values of the gene expressions that were analyzed.

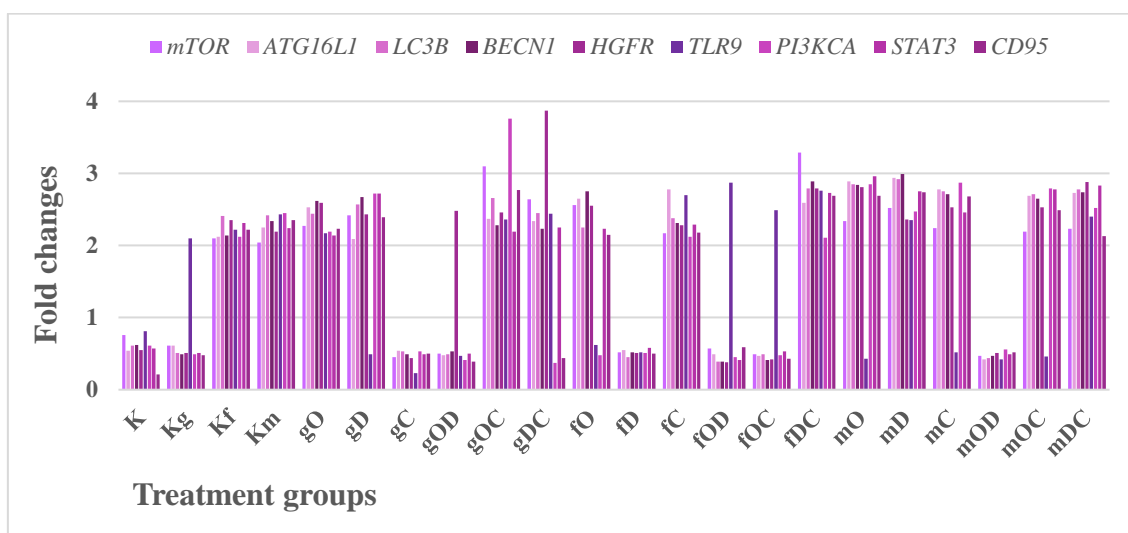


FIGURE 22 | Graphical visualization of the Taqman fold changes in HGFR studies [248].

Conventional Taqman RT-PCR confirmed the Nanostring results, with examined genes observed in all treatment groups ($p < 0.05$; $n = 3$).

g/f/m: genomic/fragmented/hypermethylated DNA; K: control; O: ODN2088 CpG oligonucleotide; D: DISU; C: chloroquine

4.4 NanoString and Taqman gene expression analyses (IGF1R studies)

In terms of TLR9 mRNA expression, gDNA treatment led to an upregulation of TLR9 in comparison to the untreated control cells. In comparison to the untreated control, gDNA treatment had no effect on the expression of the *IGF1R* gene. When not incubated with gDNA, the gene expression profile was comparable to that observed in the control samples.

With respect to the impact of gDNA treatment and combined IGF1R inhibition on the expression of *IGF1R* signaling elements, a marginal increase in *IGF1R* expression was observed; however, there was no significant alteration in the expressions of *MAPK*, *PI3K*,

and *Akt*. The combination of gDNA with ODN2088 or chloroquine significantly overexpressed all examined genes, except for *TLR9* in gC and *Bcl-2* in gO.

Due to the fact that cell-free DNA treatment influences both *TLR9* signaling and the autophagy apparatus, we also investigated how inhibiting *TLR9* signaling or autophagy modifies the effect of concurrent IGF1R inhibition and gDNA treatment.

TLR9 signaling-related (e.g., *MyD88*, *NF-κB*), autophagy-related (e.g., *ATG16L1*, *Beclin-1*, *MAP1LC3B*, *ULK1*, *Ambra-1*), autophagy suppressor/anti-apoptotic (e.g., *PI3K*, *Akt*, *mTOR*) and autophagy activator/pro-apoptotic (e.g., *MAPK*, *AMPK*, *Bax*) gene expressions increased most significantly when gDNA was combined with picropodophyllin and chloroquine, with the exception of *TLR9* and *Bcl-2*. Conversely, the utilization of gDNA in conjunction with ODN2088 and picropodophyllin led to a widespread suppression of the examined genes, except for *TLR9* and *Bcl-2*. All four treatment combinations (gP, gC, gO, and gPC) increased the activity of the gene CD133, which is associated with cancer stemness. **Figure 23** depicts the visible modifications in gene expression. The Taqman RT-PCR results confirmed the identification of changes in gene expression by NanoString/nCounter analysis. **Figure 24** and **Supplementary Table 3** present a summary of the fold changes of the analyzed gene expressions.

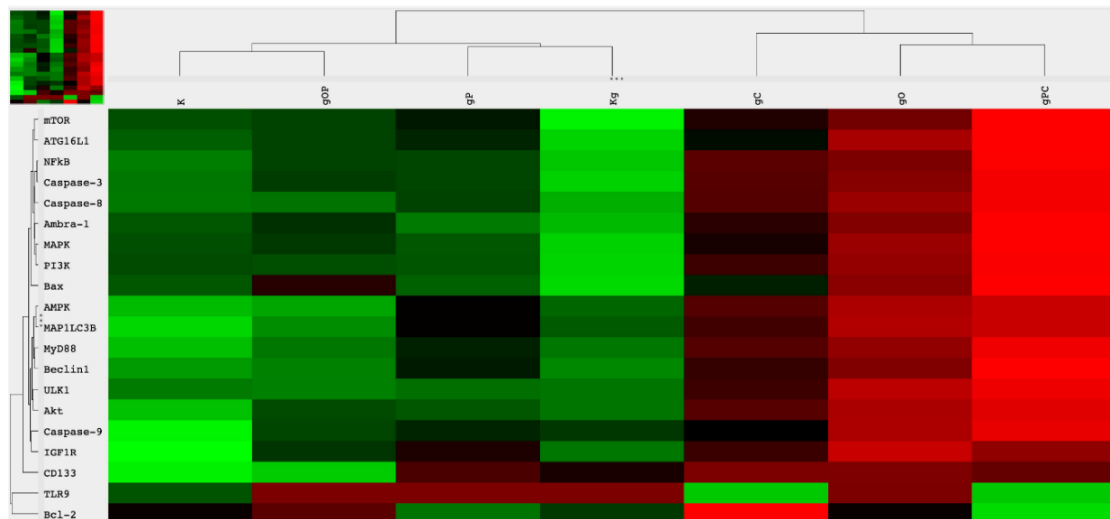


FIGURE 23 | Heatmap visualization of the NanoString gene expression analysis in IGF1R studies [276].

Gene expression alterations in HT29 cells after incubation with genomic self-DNA.

g: genomic DNA; K: control; O: ODN2088 CpG oligonucleotide; P: picropodophyllin; C: chloroquine; red: overexpression, green: downregulation

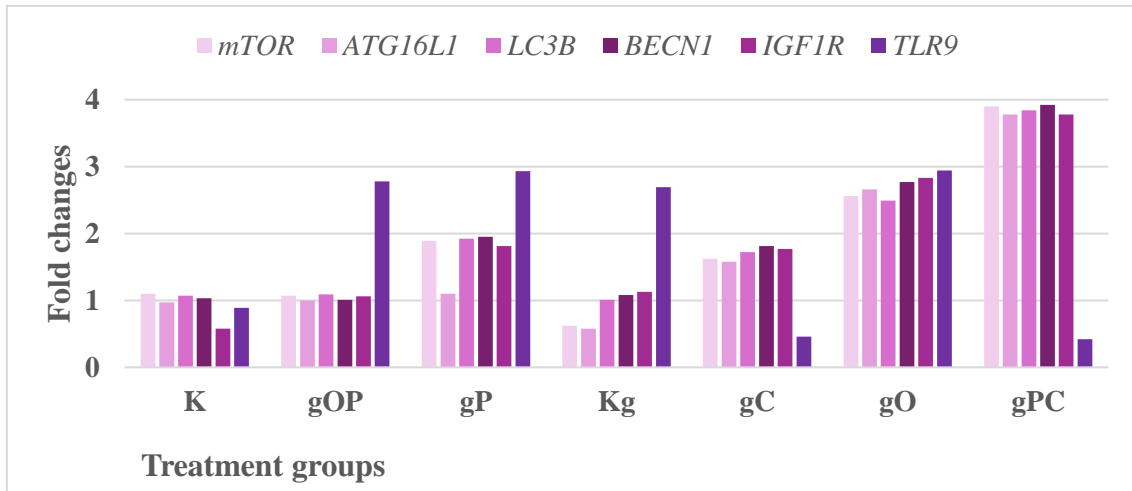


FIGURE 24 | Graphical visualization of the Taqman fold changes in IGF1R studies [276]. The gene expression fold changes were in correlation with the NanoString gene expression results ($p < 0.05$; $n = 3$).
g: genomic DNA; K: control; O: ODN2088 CpG oligonucleotide; P: picropodophyllin; C: chloroquine

4.5 Immunocytochemistry and WES Simple (HGFR studies)

We performed immunocytochemistry in specific instances to validate gene expression findings at the protein level.

Untreated control HT29 cells showed mild to moderate TLR9 immunopositivity. TLR9 protein expression ranging from moderate to strong was observed subsequent to incubation with g-, f- and mDNAs. HGFR immunocytochemistry revealed a mild immunoreaction in control and gDNA-treated samples, while fDNA and mDNA treatments produced a strong immunopositivity. In relation to autophagy, the expression of ATG16L1, Beclin-1, and LC3 proteins was significantly increased in response to f- and mDNAs; moderate to strong immunoreactions were observed in these cases, in contrast to the untreated control group and HT29 cells treated with gDNA (**Figure 25**). The outcomes of the immunochemistry assay reflected those of the NanoString and Taqman gene expression assays.

Variations in LC3B protein levels among the groups under investigation were consistent with changes in gene expression as measured by NanoString and Taqman as well as immunocytochemistry. In relation to autophagy, the protein levels of LC3B and p62 indicate that the combined application of DNA treatments (g, f and m) and DISU amplifies the inhibitory effect of chloroquine, specifically by inducing a greater inhibition

of autophagy. Conversely, the suppression of autophagy results in protein accumulation via the inhibition of LC3B and p62 degradation. **Figure 26** illustrates the outcomes of the WES Simple.

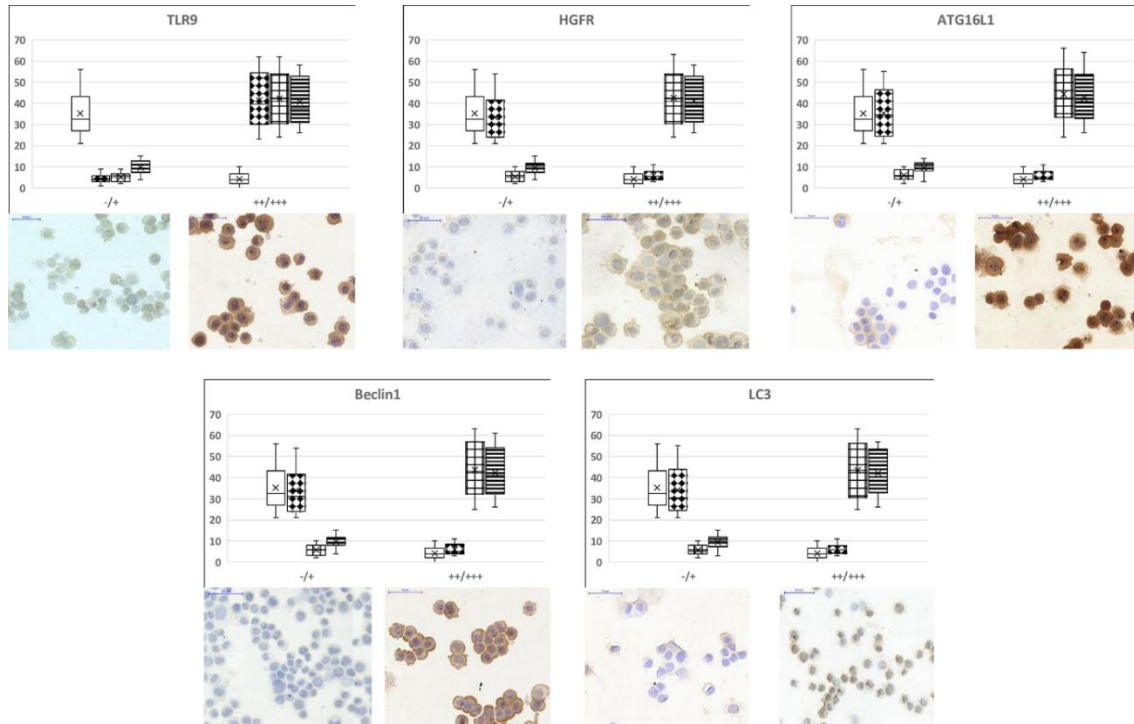


FIGURE 25 | TLR9, HGFR and autophagy-related protein immunocytochemistry results in HGFR studies [248].

The box and whisker plots represent the one-way ANOVA results of immunocytochemistry analyses. The percentage of non-immunoreactive and weakly immunopositive (“-/+”), as well as moderately and strongly immunopositive (“++/+++”) HT29 cells within the treatment groups was visualized. Under the plots representative “-/+” and “++/+++” image inserts can be seen ($p < 0.05$; $n = 3$). Scale bars represent 50 μm. Empty boxes: control, non-treated cells; diamond dots boxes: gDNA treatment; square grid boxes: fDNA treatment; striped boxes: mDNA treatment

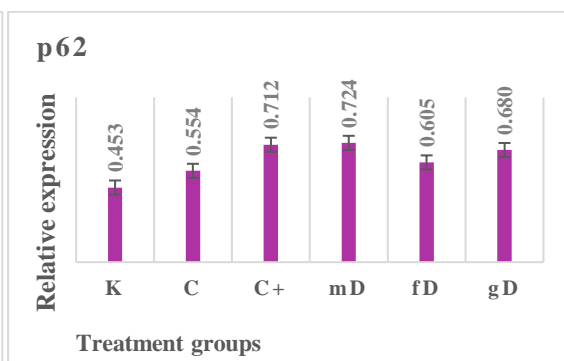
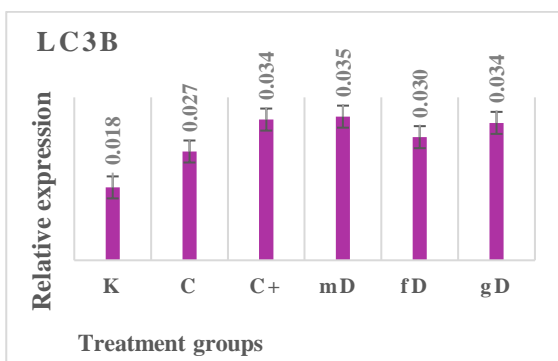
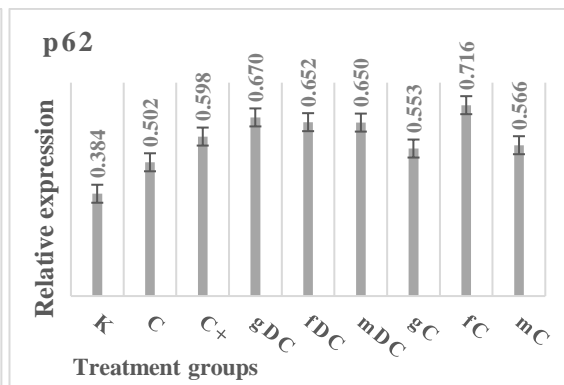
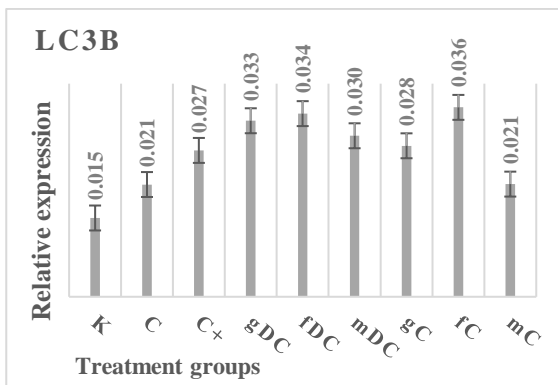
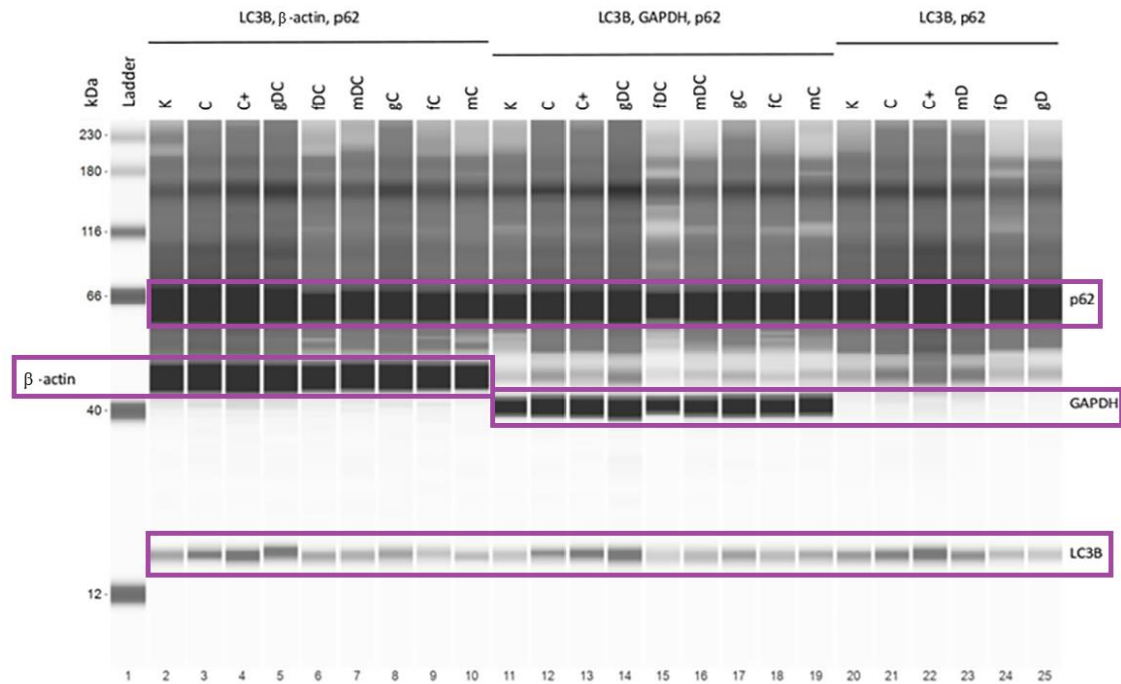


FIGURE 26 | Results of the p62/sequestrome 1 and LC3B WES Simple in HGFR studies [248]. The figure is a representative blot image. The graphs show the expression of proteins: the area of the tested proteins was multiplied by the values of the β -actin area ($p < 0.05$; $n = 3$). g/f/m: genomic/fragmented/hypermethylated DNA; K: control; C: chloroquine (10 μ M); C+: chloroquine (50 μ M) D: DISU

4.6 Immunocytochemistry and WES Simple (IGF1R studies)

We carried out immunocytochemistry on autophagy-related genes (*ACTN16L1*, *Beclin-1*, and *MAP1LC3B*) associated with IGF1R in order to validate protein-level gene expression results. The correlation between the gene expression results and the distribution of non-immunoreactive and weakly immunopositive ("-/+") HT29 cells, as well as moderately and strongly immunoreactive ("++/+++") cells, was the initial observation. An increased degree of moderate to strong immunopositivity was observed in the case of IGF1R subsequent to incubation with gO, gC, and gPC. Concerning autophagy, the gO and pPC groups exhibited the most pronounced upregulation of ATG16L1 protein expression, which was followed by the Kg, gP, and gOP interventions. The gO and gPC treatment groups showed the highest proportion of strong Beclin-1 and LC3 immunoreactivity, followed by the gP and gC treatments. We conducted an analysis of the NanoString gene expression results to determine whether or not each treatment group contained an HT29 cell expressing CD133 protein. CD133-positive cells were observed in the gO, gP, gC, and gPC treatment groups only in a dispersed manner. **Figure 27** illustrates the representative immunocytochemistry images and the outcomes of the one-way ANOVA test. **Supplementary Figure 1** illustrates the results of the Tukey HSD test.

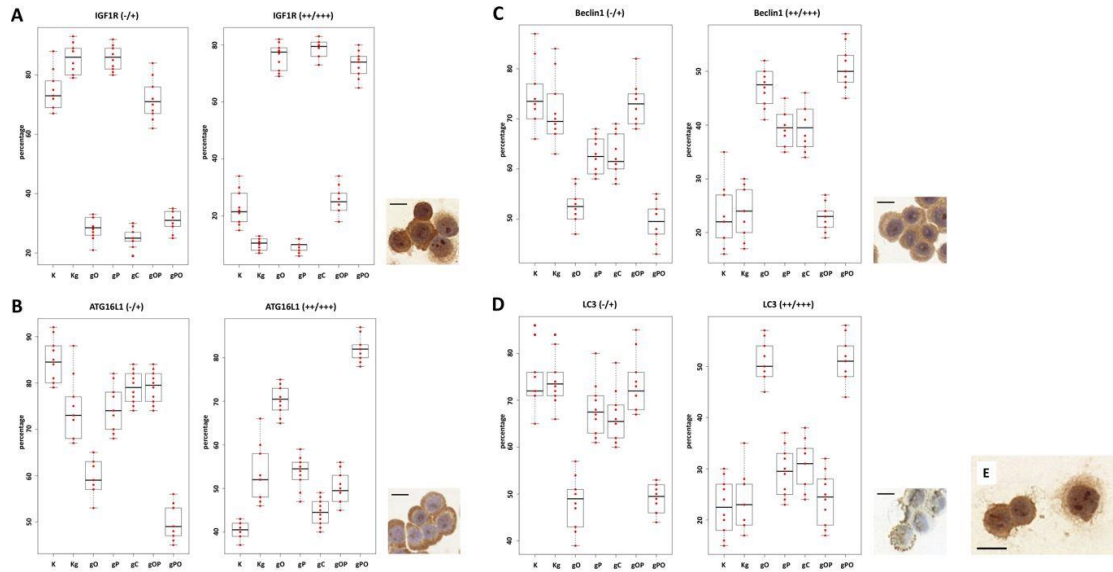


FIGURE 27 | One-way ANOVA results of IGF1R, ATG16L1, Beclin1, and LC3 immunocytochemistry analyses in IGF1R studies [276].

The percentages of non-immunoreactive and weakly immunopositive (“-/+”), as well as moderately and strongly immunopositive (“+/+/+/+”) HT29 cells within the treatment groups were plotted on box and whisker plots ($p < 0.05$; $n = 3$). (A) The boxplots for IGF1R. The right upper inserts represent the moderate to strong IGF1R immunopositivity (at $\times 200$ magnification; the scale bar indicates $10 \mu\text{m}$). The boxplots and representative immunostainings for ATG16L1 (B), Beclin1 (C) and LC3B (D) are also visualized. (E) Right lower insert represents CD133 positive HT29 cells ($\times 200$ magnification; the scale bar indicates $10 \mu\text{m}$). g: genomic DNA; K: control; O: ODN2088 CpG oligonucleotide; P: picropodophyllin; C: chloroquine

The inclusion of picropodophyllin in our experimental setup on gDNA-treated cells led to a comparatively modest reduction in the expression of *PI3K*, *Akt*, *AMPK*, and *mTOR* genes. This reduction may have had an inhibitory effect on autophagy initiation. *mTOR* has to be active if autophagy is inhibited; therefore, a WES Simple was also conducted. In the K, Kg, and gP groups, the gene expression results were linked to the levels of mTOR, phospho-mTOR, and autophagy-related proteins, as well as the activity of phospho-mTOR (Figure 28).

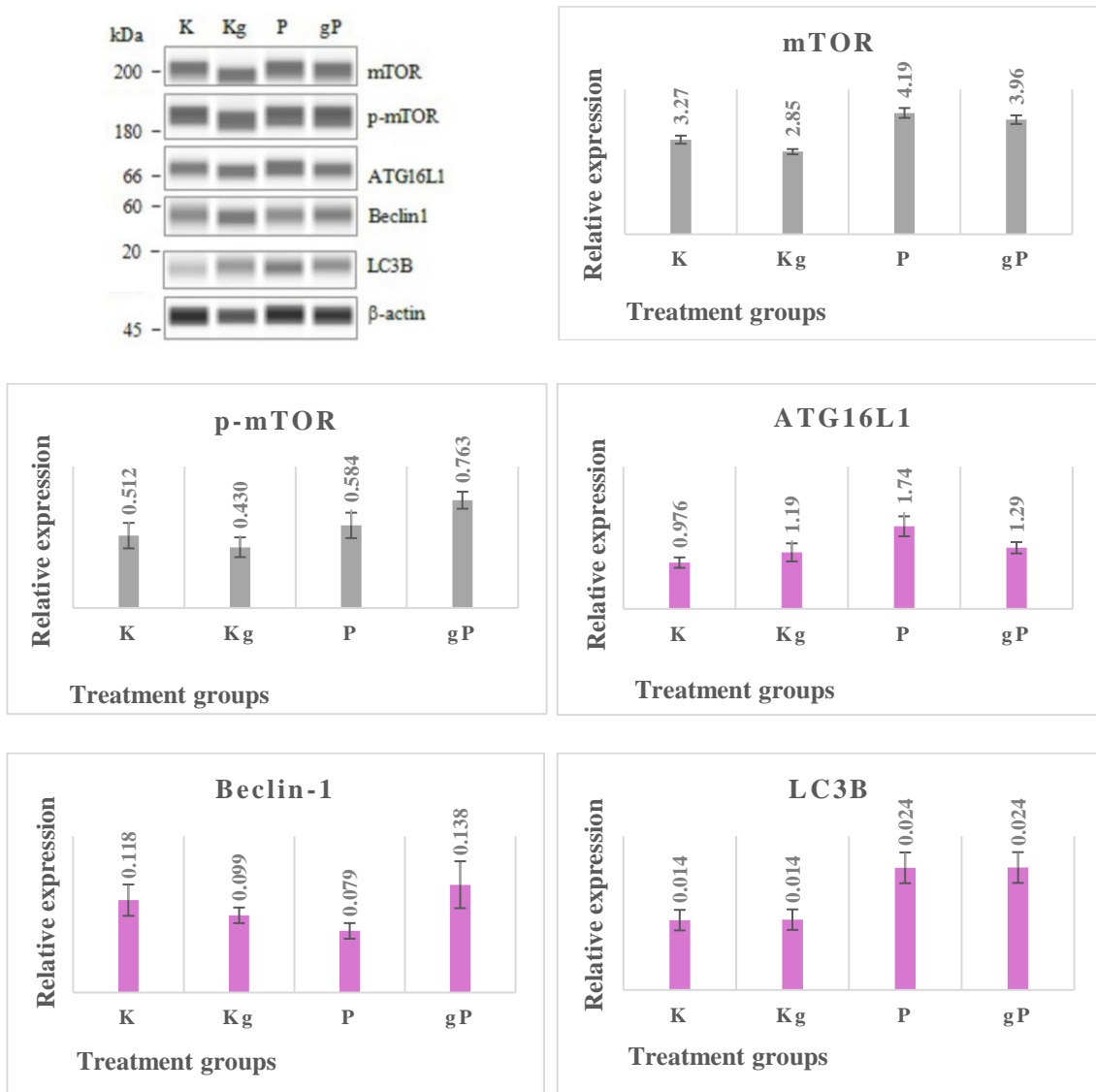


FIGURE 28 | WES Simple analyses of selected proteins in IGF1R studies [276].

According to protein expression values normalized to β -actin (bar graphs), the mTOR and phospho-mTOR (p-mTOR) protein activities (grey), as well as the autophagy-related protein (ATG16L1, Beclin-1, LC3B) expressions (purple) were in relation to the gene expression results ($p < 0.05$; $n = 3$).

g: genomic DNA; K: control; P: picropodophyllin

4.7 Transmission electron microscopy (HGFR studies)

In the cytoplasm of control, untreated, metabolically active HT29 cells, autophagic vacuoles (AV) were seen (3 ± 1 pcs/cell), which showed the same phenotype as chloroquine-treated controls (4 ± 1.5 pcs/cell), indicating the occurrence of macroautophagy. The incidence of AVs was higher in DISU (6 ± 1.8 pcs/cell) and ODN2088 (7 ± 1.4 pcs/cell) compared to control cells. A more pronounced form of macroautophagy was observed upon incubation with gDNA (6 ± 2 pcs/cell). Additionally, the simultaneous administration of chloroquine (7 ± 1.6 pcs/cell), ODN2088 (9 ± 1.2 pcs/cell), and DISU (7 ± 2 pcs/cell) further promoted the presence of intensive autophagy. After the administration of fDNA (5 ± 1.8 pcs/cell), multivesicular bodies (MVBs) and AVs both appeared. The autophagy process was significantly enhanced by the combined effect of ODN2088 and fDNA (12 ± 2 pcs/cell) (fD: 6 ± 1.4 pcs/cell; fC: 4 ± 2.3 pcs/cell). However, the cells disintegrated when administered with fDNA and any inhibitor simultaneously. After incubation with mDNA (7 ± 1.3 pcs/cell), the cells showed chromatin condensation and blebbing, in addition to disorganization. The introduction of chloroquine into mDNA (5 ± 1.6 pcs/cell) led to the formation of MVBs. However, the combination of mD (7 ± 1.4 pcs/cell) improved cell survival, and the activated macroautophagy appeared to aid in the maintenance of cellular fitness. The combination of mO generated the fewest number of AVs (2 ± 1.3 pcs/cell). Following this, autophagy was detected to a different extent in each cohort of HT29 cells. **Figure 29** illustrates the representative microstructural alterations.

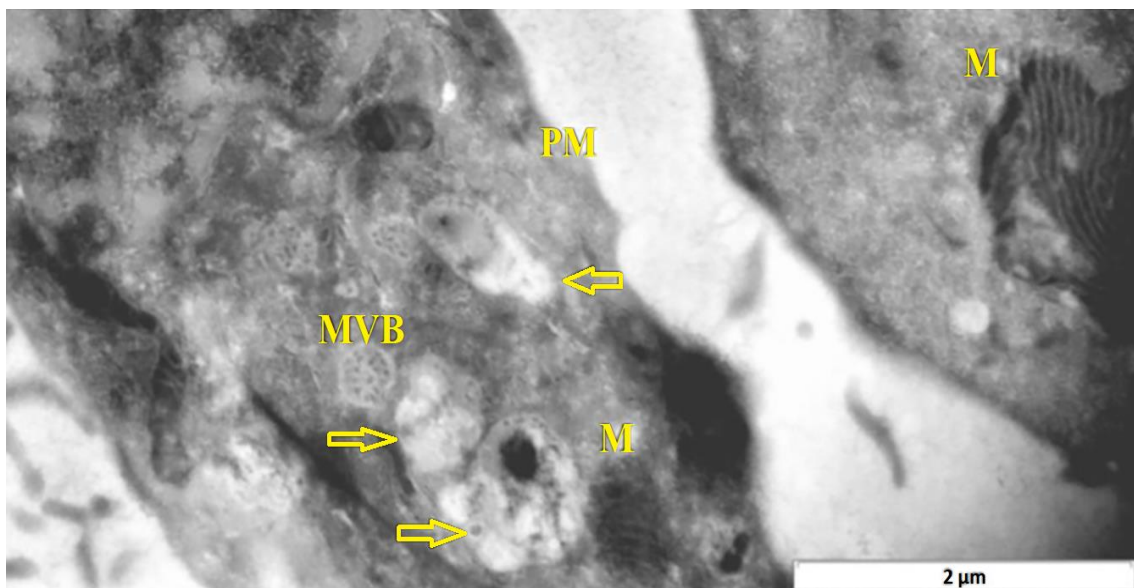
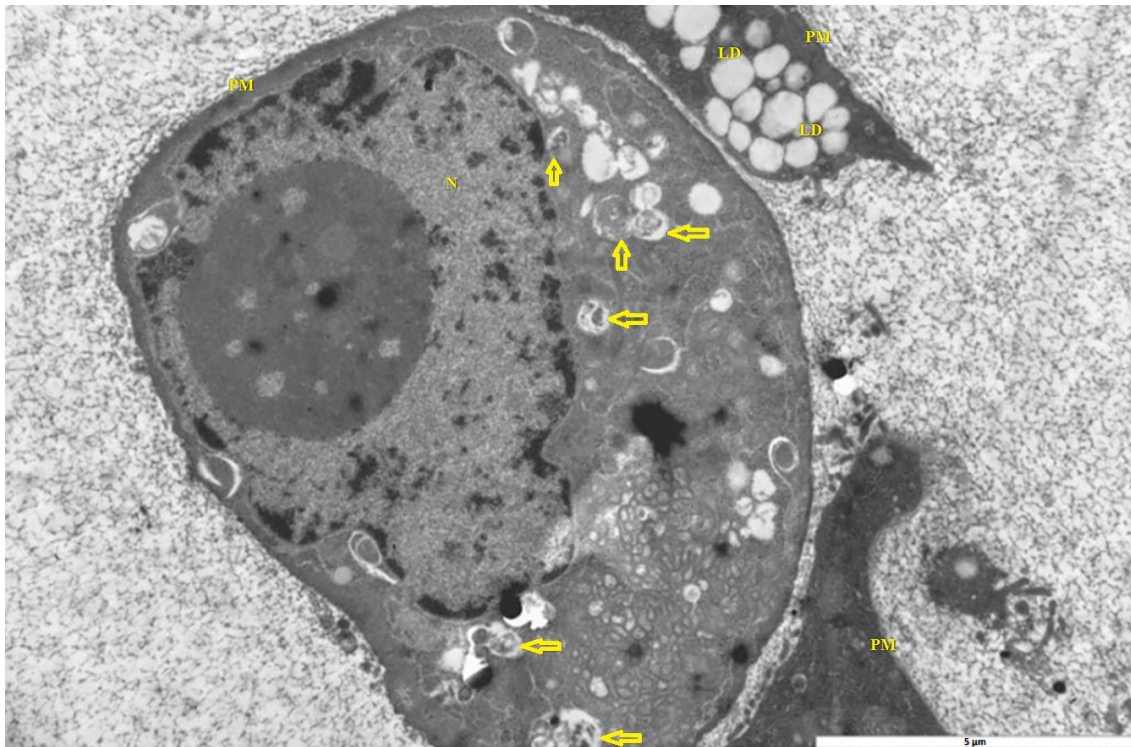


FIGURE 29 | Transmission electron microscopy results of HGFR inhibition [248].

The representative images highlight the autophagy-related structural changes in HT29 cells (from top to down: disorganized nucleus with chromatin condensation plus autophagic vacuoles (scale bar: 5 μ m); autophagic vacuoles with multivesicular body (scale bar: 2 μ m)). (p<0.05; n=3).

Arrows: autophagic vacuoles; MVB: multivesicular body; PM: plasma membrane; N: nucleus; M: mitochondria; LD: lipid droplet

4.8 Transmission electron microscopy (IGF1R studies)

Control, non-treated, metabolically active HT29 cells (3 ± 1 pcs/cell), similarly to chloroquine-treated controls (4 ± 1.5 pcs/cell), displayed autophagic vacuoles (AVs) in the cytoplasm, indicating macroautophagy. The frequency of AVs in ODN2088 (7 ± 1.4 pcs/cell) control cells was higher as compared to control. However, in picropodophyllin-treated control cells, AVs were only scattered (0.5 ± 0.5 pcs/cell). Incubation with gDNA resulted in the appearance of a more intense macroautophagy (6 ± 2 pcs/cell), and co-administration of ODN2088 (10 ± 2.2 pcs/cell) or chloroquine (5 ± 1.5 pcs/cell) also favored the presence of intense autophagy, represented by disorganized cell structure along with chromatin condensation and blebbing. The combination of gDNA with picropodophyllin and/or ODN2088, similarly to non-treated control cells, resulted in a low number of AVs (2 ± 1.5 pcs/cell in gP; 3 ± 1 pcs/cell in gOP). On the contrary, gPC co-treatment caused an intense macroautophagy (11 ± 2.6 pcs/cell). The gP combination resulted in the detection of multivesicular bodies (MVBs). Thus, the presence of autophagy was observed in each group of HT29 cells but to different extents. The representative microstructural changes together with the numerical data can be seen in **Figure 30**.

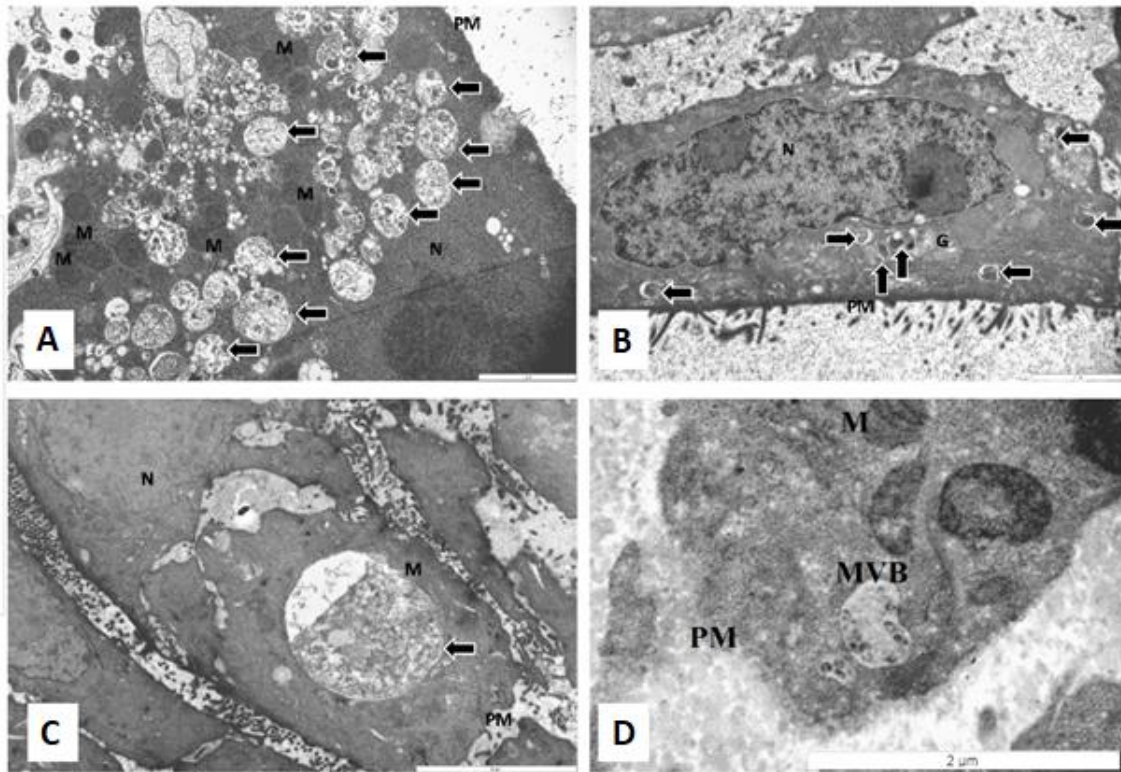


FIGURE 30 | Transmission electron microscopy results of IGF1R inhibition [276].

The representative image inserts highlight the autophagy-related structural changes in HT29 cells; (A) large number of AVs in gPC (scale bar: 2 μ m); (B) large late-stage AV in gO (scale bar: 5 μ m); (C) disorganized nucleus with chromatin condensation (scale bar: 2 μ m); (D) multivesicular body in gP (scale bar: 2 μ m). ($p < 0.05$; $n = 3$).

Arrows: autophagic vacuoles; MVB: multivesicular body; PM: plasma membrane; N: nucleus; M: mitochondria

4.9 Semithin sections (HGFR studies)

In certain cases, semithin sections were also examined to determine whether the decrease in cell numbers following treatment with modified self-DNAs and/or inhibitors of TLR9, HGFR, or autophagy was due to increased cell mortality or decreased proliferation activity. When incubated with mDNAs, gDNAs, or fDNAs, the number of proliferating cells was directly proportional to the incidence of proliferation. Co-administration of gDNA with DISU and chloroquine resulted in exceptionally reduced proliferative activity. The combination of mDNA with ODN2088 and DISU led to increased proliferative activity, as shown in **Figure 31 A-F**.

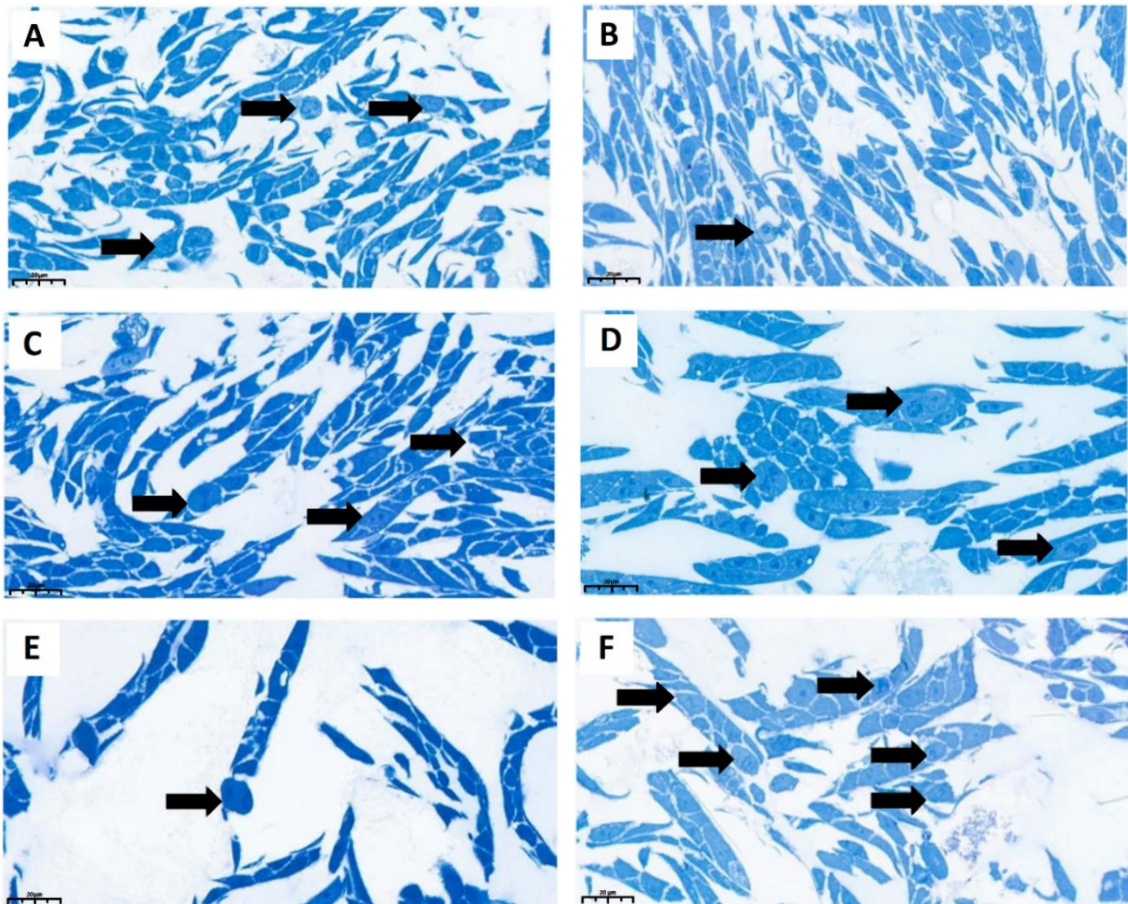


FIGURE 31 | Signs of proliferative activity in HT29 cells in HGFR studies [248].

In case of gDNA, DISU and chloroquine co-treated, the number of cell divisions was decreased. After mDNA, ODN2088 and DISU treatment, the proliferation activity of HT29 cancer cells increased. Arrows indicate cell divisions; scale bar represents 20 μm ; $p < 0.05$; $n = 3$.

K (A); gDNA (B); fDNA (C); mDNA (D); gDC (E); mOD (F)

4.10 Semithin sections (IGF1R studies)

In order to ascertain whether the alterations in cell counts subsequent to interventions involving genomic DNA and/or inhibitors of *TLR9*, *IGF1R*, or autophagy were attributable to decreased proliferation activity or increased cell mortality, semi-thin sections of specific cases were also analyzed. Using gDNA for incubation led to a direct correlation between the number of cells obtained and the incidence of proliferation. Co-administration of gDNA with picropodophyllin and/or chloroquine resulted in exceptionally diminished proliferative activity. **Figure 32 A-C** illustrates that increased proliferative activity was observed when gDNA was combined with ODN2088 and picropodophyllin. Combining gDNA with ODN2088 and picropodophyllin led to increased proliferative activity, as shown in **Figure 32 A-C**.

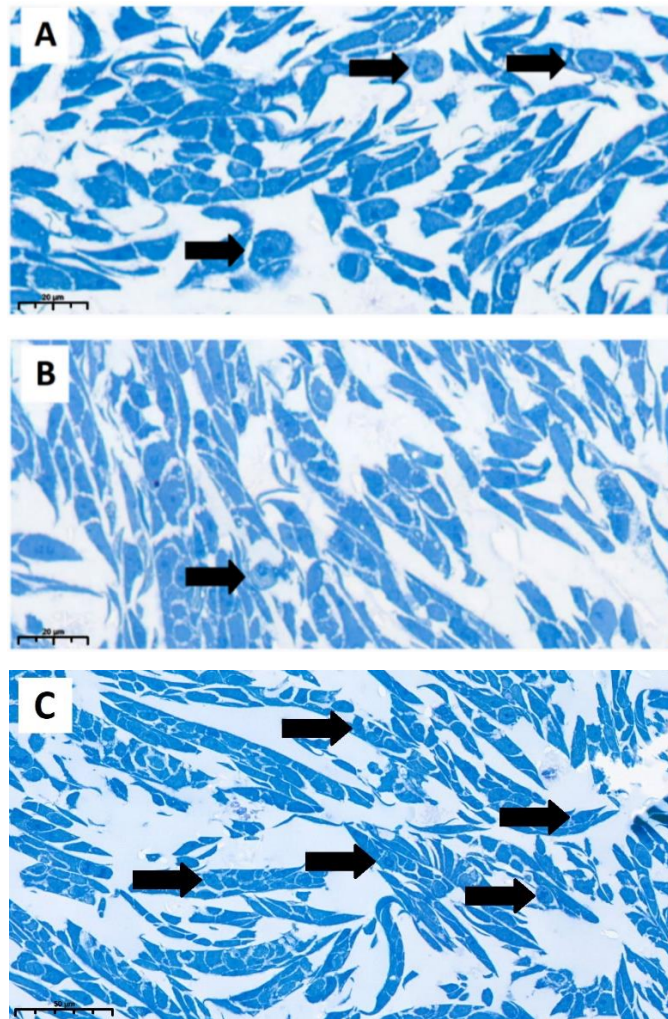


FIGURE 32 | Cell divisions in HT29 cells in IGF1R studies [276].
A Control, non-treated cells; (B) gDNA-treated control cells; (C): larger number of cell divisions in gOP sample. Arrows indicate cell divisions; scale bar represents 20 µm; $p < 0.05$; $n = 3$.

5. DISCUSSION

5.1 The interconnection of TLR9-mediated autophagy response and HGFR signaling

Our aim was to determine the impact on HT29 cell viability and proliferation of inhibiting TLR9 signaling, autophagy, and/or HGFR signaling in conjunction with intact or modified tumor self-DNA treatment.

Initially, we evaluated the impact of self-DNA-induced TLR9 signaling modulation on the survival of HT29 cells. It is established knowledge that cfDNA sequences can be detected in human blood, urine, saliva, and feces [1]. The methylation status or fragmentation of cfDNAs may encode information about their origin [287,288]. Concerning their source, cfDNAs can be classified into various groups. Endogenous cfDNA sequences originate from cellular and tissue components, whereas exogenous sequences are predominantly obtained from sources such as the host microbiome, infectious agents, the embryo, and diet [288-291].

TLRs are the innate immune system's receptors. DNA can be detected by TLR9 from both exogenous and endogenous sources [292]. Self-DNA structural modifications (i.e., fragment length and methylation status) have been shown to significantly influence the activation of TLR9-mediated signaling pathways [119,293].

The constitutive expression of TLR9 mRNA in HT29 cells was previously documented [294]. The expression of TLR9 mRNA is minimal at baseline, but it is significantly upregulated through incubation with CpG-ODN or tumorous self-DNA [119,294]. Additionally, we also observed that the expression of the TLR9 gene was augmented in cell populations that were exposed to genomic, fragmented, or hypermethylated self-DNAs, in comparison to the control group of untreated HT29 cells.

Autophagy can be induced in tumor cell lines (e.g., colon, breast, and prostate malignancies) in a manner dependent on the expression of TLR9 induced by CpG-ODNs [167]. Gene expression changes in glyceraldehyde-3-phosphate dehydrogenase (GAPDH) and the production of reactive oxygen species (ROS) may act as signals between TLRs and autophagy [295-297]. *TLR9* and autophagy have several features in common, including their respective impacts on cellular survival and demise, their involvement in innate immunity, the facilitation of MHC class II antigen presentation,

their interactions within endosomes, the beneficial influence of class III *PI3K* on their signaling, and the inhibitory effects of common substances (hydroxychloroquine, 3-methyladenine, and bafilomycin A1) [167]. A close relationship between TLR9 signaling and the autophagy response has been demonstrated to have remarkable effects on the survival of HT29 cells treated with modified self-DNA [293].

In our research, treatments with modified self-DNA altered HT29 cells' metabolic activity and proliferation to varying degrees. It is noteworthy that the noted decrease in the expression levels of all genes tested was attributed to gDNA, while an increase in the expression levels of fragmented and hypermethylated DNAs was observed. This may be the result of the investigated components of the *TLR9* signaling pathway demonstrating both pro- and anti-survival effects [293,298-302] and the activation of this complex signaling pathway by self-DNA sequences with distinct modifications [293].

In all cases where cells were treated with modified self-DNAs, inhibiting *TLR9* signaling led to increased metabolic activity. Incubation with genomic and hypermethylated DNAs resulted in a reduction in cell division, whereas treatment with fragmented DNA marginally enhanced cell proliferation. The reduction of *TLR9* signaling nevertheless nullified the impact of self-DNA treatments. Aside from the role of distinct levels of TLR9 signaling activation, the differential expression of pro- and anti-apoptotic genes can be hypothesized to be in the background of this observation [303-307].

The subsequent procedures involved examining the impact of changes in the interaction between the *HGFR* and *TLR9* signaling pathways on the survival of HT29 cells. There is a lack of information available about this intricate signaling crosstalk. The activation of TLR2 and TLR5 in epithelial cells has been shown to recently induce phosphorylation of RTKs that are involved in the growth, repair, and carcinogenesis of the epithelium. In addition to all epidermal growth factor receptor (EGFR) family members, TLR stimulation can also activate other RTKs, including HGFR [167]. Chemotactic stimuli and *TLR-MyD88* signaling have the potential to activate extracellular signal-regulated kinases (ERKs). Growth hormones can stimulate ERKs, which in turn can stimulate RTKs. Specifically, both *TLR-MyD88*-dependent and *TLR-MyD88*-independent ERK activation in macrophages infected with *Toxoplasma gondii* has been described [308]. Given that *MyD88* is a crucial component of the *TLR9* signaling pathway,

the possibility of a molecular connection between the *TLR9* and *HGFR* signaling pathways cannot be ruled out.

Our findings indicate that self-DNA treatment has a tendency to increase *MyD88* expression and that *HGFR* inhibition does not alter or further enhance this effect. We found a correlation between *MyD88* overexpression and increased HT29 cell proliferation. Recent research indicates that *MyD88* inhibits apoptosis in colon carcinoma cells via the *Ras/Erk* pathway but not via the *NF-κB* pathway [309]. A comparable alteration in the expression of caspase-3 was noted to that of *MyD88*. Inhibited apoptosis-induced compensatory cell proliferation, which is significantly influenced by caspases (e.g., caspase-3), may therefore account for a portion of the observed changes in HT29 cell proliferation [310].

Additionally, we investigated the impact of the interaction between *TLR9* and *HGFR* signaling on HT29 cell proliferation and autophagy. Strict regulation of RTK trafficking is essential for maintaining homeostasis. RTKs prevent access to degradation pathways in human malignancies [311]. Besides growth factor RTKs, signaling cascades and nutrient availability fluctuations have been demonstrated to regulate autophagy [312]. It was discovered that autophagy mediated by *LC3C* regulates HGF/*HGFR*-stimulated migration and invasion in HeLa cancer cells in a selective manner [279]. In relation to the interaction between *HGFR* signaling and autophagy machinery in colorectal cancer cell lines, recent research has revealed that basal autophagy, independent of mTORC1 positively regulates the phosphorylation levels of multiple RTKs, including *HGFR*. Furthermore, research has shown that genetic inhibition of basal autophagy reduces *Akt* activation mediated by mTORC2 but has no discernible impact on mTORC1 activity. Additionally, it has been shown that autophagy regulates mTORC2 and positively mediates the phosphorylation of *HGFR*; the impaired *HGFR* phosphorylation in autophagy-deficient cells was due to decreased mTORC2 activation [280].

All types of modified self-DNA treatments increased autophagy gene expression, but it was fDNA administration that specifically increased cell growth. Autophagy was disrupted due to the accumulation of p62 and LC3B proteins caused by the combination of DISU and DNA. In contrast to DNA alone, the combined effect of DISU and DNA was antithetical to that of DNA in relation to cell proliferation. In recent times, scholars have uncovered a multifaceted reciprocal association between autophagy-master regulator

kinases and autophagy-associated proteins [313]. HGFR and β 1-integrin colocalize with compartments that are positive for *Beclin-1* and/or *LC3B*. Additionally, in response to HGF stimulation, a concentration of phosphorylated ERK1/2 localizes alongside HGFR in endomembranes associated with autophagy [314]. HGFR has also been seen to partially colocalize with LC3B-positive perinuclear vesicles, which may have an effect on its phosphorylation. This is because HGFR phosphorylation is only enhanced under autophagy-competent conditions [280], which is precisely when chloroquine-mediated accumulation of autophagosomes occurs. As a result, autophagic vesicles may serve as signaling platforms through which mTORC2 regulates HGFR phosphorylation [313].

The most significant inhibition of cellular proliferation was observed when gDNA, DISU, and chloroquine were utilized concurrently. An instance of *STAT3* overexpression was identified, which is implicated in non-canonical *c-Met* signaling. *STAT3* activity in colon carcinoma cells is stimulated by IL-6 or promoted by cancer cell multiplication by a constitutively active *STAT3* mutant [315]. Based on these factors, *STAT3* stimulates cellular proliferation. IL-6 production is also stimulated by TLR9 activation [316], which is advantageous for *STAT3* activation. Conversely, *LC3B* exhibited upregulation within this cohort of HT29 cells. The threshold for *LC3B* activation rises in the event of *LC3B* upregulation, a factor that can regulate pro-apoptotic function [317]. It is not impossible that the effect of *LC3B* on stopping cell growth overpowered the effect of *STAT3* expression on encouraging cell growth in this case, resulting in a significant decrease in cell growth. Additionally, we observed the accumulation of *LC3B* and *p62* proteins in the gDC group. This implies that autophagy dysfunction was the consequence of the combined therapeutic interventions. Proliferation ability is enhanced when there is an excessive accumulation of *p62* in tumor cells, which is characterized by cell cycle initiation and inhibition of apoptosis [318]. On the contrary, a recent study [319] found that in CRC patients, high expression of LC3B dot-like and p62 dot-like cytoplasmic proteins (which indicate impaired autophagy) was associated with the best prognosis. These results indicate that inhibiting autophagy is associated with a reduction in cell proliferation. It is important to note, however, that while previous studies have documented chloroquine's ability to eliminate cancer cells without inhibiting autophagy [320-322], the 10 μ M chloroquine we utilized in this study merely inhibited autophagy without impacting the proliferation of HT29 cells. On this basis, it is possible to

hypothesize that the concurrent administration of gDNA and DISU along with chloroquine contributed to the observed reduction in cell proliferation within the gDC group.

In gastric adenocarcinoma cells, it was discovered that the induced form of cytoprotective autophagy in response to HGFR inhibition or a combination of HGFR and autophagy inhibition can lead to a substantial reduction in cell viability [323]. It has been demonstrated that the administration of HGF and mTOR agonist MHY1485 can inhibit autophagy induction as well as the dephosphorylation of *ULK1* and *mTOR*, which occurs in response to HGFR inhibitor treatment. This suggests that the HGFR inhibitors induced autophagy via the *HGFR-mTOR-ULK1* molecular cascade. It is noteworthy that HGFR inhibitors exhibited additional suppression of cell survival and tumor growth in Met-amplified cancer cells when autophagy was inhibited. Therefore, HGFR inhibitor-mediated autophagy appears to be mediated by the *HGFR-mTOR-ULK1* cascade; therefore, HGFR inhibitors combined with autophagy inhibitors may represent a promising therapeutic approach for Met-amplified malignancies [240].

Concurrent administration of mDNA, ODN2088, and DISU detected a maximum degree of cellular proliferation. Remarkably, in this instance, both canonical and non-canonical *HGFR* signaling pathway expression was reduced, in addition to autophagy-related gene expression. It has been shown that decreased autophagy promotes cell proliferation through an unidentified mechanism [324-326]. Genetic silencing of critical autophagy proteins (e.g., *Beclin-1*, *Ambra 1*) in mice has been shown to result in increased cell proliferation [326]. It is not impossible to rule out the possibility that the combination of treatments used regulated the autophagy/cell proliferation interaction epigenetically. Furthermore, with respect to the genes that were evaluated, the predominant overexpression detected was that of *CD95L* and IL-8. Apoptosis can be induced by *CD95L* through its cognate receptor, *CD95*. In recent times, there has been further insight into the ability of *CD95L* to stimulate cell migration, differentiation, and proliferation [327]. It was discovered that EGFR transactivation by IL-8 stimulated cell proliferation in non-small cell lung cancer [328]. There is a significant degree of cross-talk between *HGFR* and *EGFR* [236]. Intense proliferation in the mOD HT29 cell group may be caused not only by overexpression of *CD95L* and IL-8 but also by *HGFR/EGFR* cross-signaling, according to these findings. By impeding *TLR9* and/or *HGFR* signaling pathways and

autophagy, respectively, modified tumor self-DNAs enable the development of novel anti-cancer therapies. Further research should be conducted to examine the impacts of concurrently administering these compounds to alternative tumor cell lines and animal models.

In the absence of stromal cells, HT29 cells have been shown to secrete small extracellular vesicle complexes resembling multivesicular bodies (MVBs) in recent research [329]. The ultrastructural changes observed in this investigation highlight the potential involvement of autophagy in either cellular protection or cell death promotion. The cell populations in which MVBs were identified exhibited upregulation of the *Beclin-1* and *PI3K* genes. This implies that, subsequent to the development of amphisomes, autolysosomal degradation may also occur via the interplay between the autophagosome and multivesicular body pathways [330]. The amphisome functions as a prelysosomal compartment that facilitates the convergence of the endocytic and autophagic pathways [331,332]. There are numerous possible outcomes for the contents of amphisomes, including extracellular release or lysosomal degradation. Both exosome biogenesis and autophagy are essential mechanisms for enhancing stress tolerance and maintaining cellular homeostasis [333]. Modulating these functions in cancer cells may reveal feasible therapeutic targets.

5.2 The interconnection of TLR9-mediated autophagy response and IGF1R signaling

By analyzing the proliferation and metabolic activity of HT29 colon cancer cells, we sought to determine how inhibition of IGF1R affects the way in which tumor-derived self-DNA influences TLR9 signaling and autophagy behavior.

Initially, we assessed the impact of TLR9 signaling modulation induced by self-DNA on the survival of HT29 cells. Initially, we evaluated the effect of self-DNA-induced TLR9 signaling modulation on the survival of HT29 cells. Beyond its application in cancer diagnostics, cfDNA has the potential to stimulate tumorigenesis and "genometastasis" as well as affect the immune response [334]. By activating signaling pathways through the interaction of cfDNA with specific cell receptors (including TLRs) or by increasing the transcriptional levels of multiple genes in a manner analogous to that observed with DNA aptamers, these biological effects can be induced [335].

In relation to HT29 cell proliferation and metabolic activity, we observed that gDNA treatment, with or without ODN2088, picropodophyllin, or chloroquine, had variable degrees of impact on cell survival. It is noteworthy that incubation solely with gDNA resulted in a reduction in the expression level of all genes examined (with the exception of TLR9). On the other hand, combining gDNA with inhibitors (specifically O, C, and PC) resulted in an increase in gene expression. This is partly explained by the survival-promoting and inhibitory effects of the gDNA-induced *TLR9* signaling pathway [293,298-302]. ODN2088 inhibited TLR9 signaling, resulting in an increase in cellular metabolic activity while not significantly affecting cell proliferation. Treatment with gDNA exclusively led to a significant reduction in cellular proliferation. In addition to gDNA-treated cells, ODN2088 exhibited a propensity to counteract the anti-proliferative effect of gDNA. This phenomenon may be attributed to variations in the expression levels of critical *TLR* signaling molecules, including *MAPK*, *PI3K*, or *NF-κB*, which may have significant functions [336].

The subsequent procedures involved examining the impact of alterations in the interplay between the *IGF1R* and *TLR9* signaling pathways on the survival of HT29 cells. Inhibition of IGF1R increased the metabolic activity of HT29 cells but had no discernible effect on proliferation, according to our findings. Treatment with gDNA (and its combination with O, P, C, and PC regimens) reduced cell division by a significant margin. Conversely, gDNA concurrently inhibited *IGF1R* and *TLR9* signaling (i.e., gOP), nullifying the suppression of cell proliferation. A noteworthy inconsistency was identified in the context of this matter: autophagy and apoptosis-related genes exhibited downregulation, whereas *Bcl-2* was found to be overexpressed. *Bcl-2* overexpression exerts anti-apoptotic and autophagy-suppressive effects, as evidenced by the increased number of cell divisions and decreased level of AVs in the gOP treatment group. In addition to regulating programmed cell death during tissue repair and development, *Bcl-2* may also possess oncogenic properties [337] by impeding cell proliferation rather than promoting it. CpG-ODN-induced TLR9 activation can increase IGF1 expression in intestinal epithelial cells [257]. Furthermore, intracellular IGF1 stimulates *Bcl-2* expression via the *IGF1R* and *EGFR* pathways [337]. Based on the findings, the combination of gDNA and picropodophyllin was able to inhibit the overexpression of *Bcl-2*. Nevertheless, the introduction of ODN2088 resulted in the upregulation of *Bcl-2*,

likely through a cross-talk between the *TLR9/EGFR* and *IGF1R/EGFR* signaling pathways [337,338]. Therefore, the concurrent application of IGF1R inhibitors and tumorous self-DNA may have anti-proliferative (therapeutic) implications. However, concurrent inhibition of TLR9 may negate this advantageous consequence (**Supplementary Figure 2**).

Additionally, we investigated the impact of the interaction between *TLR9* and *IGF1R* signaling on HT29 cell proliferation and autophagy. In this study, IGF1R inhibition decreased autophagy and mitigated the pro-autophagic effects of gDNA treatment and TLR9 signaling inhibition. In contrast, concomitant administration of chloroquine inhibited picropodophyllin, resulting in an increase in autophagy.

Prior research has demonstrated that cellular autophagy can occur through the inhibition of *PI3K/Akt*, leading to a subsequent downregulation of *AMPK/mTOR* [339,340]. It was observed that the administration of gDNA led to the suppression of these genes, ultimately resulting in a diminished capacity to inhibit autophagy initiation.

Activation of the IGF1R can stimulate the *PI3K/Akt* and *MAPK* signaling pathways, which are regulated by the phosphorylation of IRS1 and IRS2 subsequent to ligand binding [341,342]. The *PI3K/Akt* pathway activates the mTOR pathway, which regulates protein synthesis and cell proliferation via downstream effectors [342]. *AMPK* activity can be inhibited by IGF1R through the action of Akt1, which phosphorylates an AMPK inhibitory site [343] (**Supplementary Figure 2**). Recent research has identified picropodophyllin as an on-target, potent inducer of autophagic flux [283].

The experimental findings revealed that the introduction of picropodophyllin into gDNA-treated cells led to inhibitory effects on autophagy initiation and ultimately resulted in a reduced quantity of AVs, despite the relatively minor reductions in *PI3K*, *Akt*, *AMPK*, and *mTOR* gene expression. On the other hand, pharmacological inhibition of TLR9 resulted in the accumulation of AVs (compared to gP), suggesting that ODN2088 reduced the anti-autophagic effect of the gP combination. Considering that TLR9 maintains autophagic flux [344], this occurrence is also rational.

It has been discovered that chloroquine inhibits cell proliferation by impeding late-stage autophagy and inducing apoptosis mediated by mitochondria [345]. Although the gP combination exhibited anti-autophagic properties, the introduction of chloroquine (referred to as gPC) led to a substantial upregulation of autophagy and a reduction in cell

proliferation. Based on these, we think that the complex balance between the factors that stop and start autophagy has a major impact on the final biological outcome. The different effects of P, O, and C treatments on HT29 cell proliferation and autophagy, both alone and together, show that the IGF1R-related and unrelated autophagy machinery have a "Janus-faced" effect on cell proliferation, in addition to the *TLR9-IGF1R-Bcl-2* molecular link.

We also examined what happened to the HT29 stem-like phenotype when autophagy and IGF1R were inhibited. High levels of autophagy and low levels of cell proliferation were seen in the groups that were given inhibitors (gP, gC, gO, and gPC). These groups also had CD133-positive cells. This shows that blocking *IGF1R* and/or autophagy may be therapeutically ineffective. Unbalanced *IGF1R* signaling has the potential to stimulate cancer cell proliferation and initiate cancer reprogramming in various tumor tissues [250,346]. It has been demonstrated recently that *IGF1R* facilitates epithelial-mesenchymal transition and cancer stem cell properties by activating *Akt* [347,348]. Moreover, various cell types recognize autophagy for its role in promoting stem cell viability [349]. When IGF1R is inhibited, protective autophagy may be induced concurrently, which may stimulate cell proliferation and inhibit apoptosis. Thus, it counteracts its own initial biological effects on cells via autophagy [236]. The combination of IGF1R inhibition and autophagy-disruptive agents has the potential to impede autophagy, thereby impeding the proliferation of cancer cells and augmenting apoptosis [236]. The autophagy process in CD133-positive HT29 stem cells could not be detected because these cells were scattered in the cell smear and could not be distinguished on TEM sections. The only information available is that the HT29 treatment groups have an autophagy flux that promotes the development of the CD133 phenotype. Notwithstanding this, future research should undoubtedly focus on evaluating the autophagic flux within HT29 stem-like cells that express CD133. Based on the results of our experiments, it is likely that autophagy induced by different combinations of gDNA and inhibitors used cannot prevent HT29 cell death. Additionally, it may compel stem-like HT29 cells that are positive for CD133 to promote their own survival. Curcumin was discovered to promote the proliferation and autophagic survival of colon cancer stem cells [63], providing support for this hypothesis. This discovery indicates that autophagy

confers a survival advantage, allowing colorectal cancer progenitor cells to persist indefinitely [351].

We investigated the correlation between autophagy and IGF1R inhibition in relation to ultrastructural alterations using TEM. MVB signals were identified in HT29 cells that were treated with gP. At least three potential causes can be identified for this phenomenon. The first is that receptors (such as the receptor tyrosine kinase IGF1R) can be rapidly recycled back to the plasma membrane via "back fusion" from early endosomes. As luminal acidification increases during the maturation of the early endosome, its biochemical composition alters. MVBs, or intraluminal vesicles, are ultimately produced [348]. *IGF1R* can be delivered for recycling at this stage. Second, endocytosed IGF1R-containing MVBs are capable of fusing with the plasma membrane and releasing their cargo as exosomes. Reports indicate that cells secrete IGF1R in this manner [250,347,348]. Thirdly, recent research has shown that HT29 cells are capable of releasing MVB-like small extracellular vesicle complexes [349] in the absence of stromal cells. The observed ultrastructural changes in our research highlight the potential involvement of autophagy in either cellular protection or the induction of cell death. The gP cell group, which exhibited the presence of MVBs alongside autophagic vacuoles, demonstrated an upregulation of autophagy-related protein expression (*Beclin-1*, *ATG16L1*, *LC3B*) in comparison to the non-treated control cells. Based on the findings, it is probable that autolysosomal degradation occurs subsequent to the development of amphisomes through the interplay between the autophagosome and multivesicular body pathways [350]. The amphisome serves as a junction between the endocytic and autophagic pathways [351,352], operating as a prelysosomal compartment. There are numerous possible outcomes for the contents of amphisomes, including extracellular release or lysosomal degradation. Both exosome biogenesis and autophagy are essential mechanisms for enhancing stress tolerance and maintaining cellular homeostasis [329-331,353,354]. Modulating these functions in cancer cells may reveal feasible therapeutic targets.

6. CONCLUSIONS

In conclusion, the purpose of this research was to determine how modified tumorous self-DNA treatments affected the survival and proliferation of HT29 colon cancer cells through the intricate interplay of *HGFR/IGF1R*, *TLR9* signaling, and autophagy inhibition.

Concerning the HGFR inhibitory experiments, we have demonstrated that the nature of the DNA modification influences the reduction in cell proliferation. By employing TLR9 blocking, this effect has been reversed. A marginal increase in *MyD88* expression was observed in response to self-DNA treatments. HT29 cell proliferation was observed to be augmented in conjunction with the upregulation of *MyD88*. Similarly, caspase-3 expression exhibited alterations consistent with those of *MyD88*. Therefore, incubation with modified self-DNAs was able to inhibit apoptosis-induced proliferation of compensating HT29 cells. All forms of self-DNA modification upregulate autophagy-related gene expression. DISU inhibited the proliferation-reducing effects of genomic and hypermethylated DNAs, whereas fragmented DNA showed the opposite effect. The most significant inhibition of cellular proliferation was observed when gDNA, DISU, and chloroquine were utilized concurrently. The inhibitory effect of *LC3B* may have compensated for the proliferation-stimulating effect of *STAT3* overexpression in this instance, suggesting that the *HGFR* inhibitor-mediated autophagy process involves the *HGFR-mTOR-ULK1* molecular cascade. The maximum degree of cellular proliferation was detected upon the simultaneous administration of mDNA, ODN2088, and DISU. In this case, we saw that autophagy-related genes and both canonical and non-canonical *HGFR* signaling pathways were less expressed. In addition, the observed ultrastructural alterations provide further evidence for the context-dependent function of autophagy and HGFR inhibition on cell survival and proliferation.

Regarding the studies into the effects of IGF1R inhibition, it was found that giving tumorous self-DNA, picropodophyllin, HT29 cells, or chloroquine together changes metabolic activity and proliferation in different ways. Inhibiting *TLR9* signaling negatively impacts the effect of self-DNA treatment on cell proliferation. The concurrent administration of *IGF1R* inhibitors and tumor-derived self-DNA exhibits anti-proliferative properties. However, concomitant inhibition of *TLR9* signaling undermines this advantageous effect. It has been observed that the intricate equilibrium between

inhibitory and promotional factors in autophagy significantly influences its ultimate intensity and biological consequences. The distinct impacts of picropodophyllin, ODN2088, and chloroquine, either individually or in combination, on HT29 cell proliferation and autophagy indicate that the *IGF1R*-associated and non-*IGF1R*-associated autophagy machinery exhibit a "Janus-faced" nature with regard to their influence on cell proliferation, in addition to the *TLR9-IGF1R-Bcl-2* molecular linkage. Autophagy induced by various combinations of tumorous self-DNA and inhibitors may not be adequate to prevent the irreversible demise of HT29 cells; however, it may enable the survival of certain CD133-positive stem-like cancer cells, thereby promoting the recurrence of colorectal cancer. We also observed ultrastructural alterations that support the notion that autophagy and *IGF1R* inhibition influence cell survival and proliferation in a context-dependent manner.

Inhibitors that target autophagy, *TLR9*, *HGFR/IGF1R*, and/or autophagy signaling in combination would be instrumental in the advancement of personalized anti-tumor treatments. Nonetheless, further *TLR9*-expressing cell lines should be utilized to validate our current investigations. Additional research is required to examine the biological effects of self-DNA fragments that have been modified, as factors such as fragment length or methylation status may impact the results of the experiments.

7. SUMMARY

Self-DNA-induced TLR9 signaling and autophagy response in HT29 colon cancer cells were closely related, affecting cell survival and differentiation. Interfering with *HGFR* hinders autophagy and promotes colorectal cancer. *IGF1R* activation drives colorectal cancer development and progression. Debate surrounds the effect of IGF1R inhibition on autophagy. The exact methods by which *HGFR* or *IGF1R* suppression affects *TLR9*/autophagy signaling in HT29 cancer cells are unclear. We investigated how suppressing *HGFR* or *IGF1R* impacts *TLR9*-autophagy signaling in HT29 cells. We examined how these components interact by measuring cell proliferation, metabolism, TLR9, HGFR, IGF1R, and autophagy inhibitory tests. Gene expression, immunocytochemistry, transmission electron microscopy and WES Simple autophagy flux measurements were also examined.

In HGFR inhibitory tests, we found that *MyD88* and *caspase-3* promoted HT29 cell growth. Incubation with self-DNAs may decrease apoptosis-induced compensatory cell growth. HGFR inhibition blocks the proliferation-reducing impact of genomic and hypermethylated DNA, while fragmented DNA is unaffected. Chloroquine, HGFR inhibitor, and genomic DNA showed the least cell proliferation. The *HGFR-mTOR-ULK1* molecular cascade may be implicated in HGFR inhibitor-mediated autophagy since *LC3B* inhibited *STAT3* overexpression and reversed its proliferation-stimulating action. When given together, hypermethylated DNA, TLR9, and HGFR inhibitors increased cell proliferation the most. Autophagy-related genes and conventional and non-canonical *HGFR* signaling pathways were downregulated. Ultrastructural alterations support the context-dependent effect of HGFR inhibition and autophagy on cell survival and proliferation. In IGF1R inhibitory assays, tumor-derived self-DNA and IGF1R inhibitors have anti-proliferative potential. *TLR9* signaling inhibition reverses this effect. Picropodophyllin, ODN2088, and chloroquine all had different effects on HT29 cell proliferation and autophagy. This suggests that autophagy mechanisms have "Janus-faced" effects on cell proliferation, depending on whether they are linked to or not linked to the *IGF1R*. Self-DNA and inhibitors do not promote autophagy, but they let CD133-positive stem-like HT29 cells survive. In the development of more individualized anti-tumor therapies for colorectal cancer, the discovery of novel forms of combined inhibitors of *HGFR* or *IGF1R*, autophagy, and/or *TLR9* signaling would be instrumental.

8. REFERENCES

- [1] Mandel P, Metais P. Les acides nucléiques du plasma sanguin chez l'homme [Nuclear Acids In Human Blood Plasma]. C R Seances Soc Biol Fil. 1948 Feb;142(3-4):241-243. French.
- [2] Tan EM, Schur PH, Carr RI, Kunkel HG. Deoxybonucleic acid (DNA) and antibodies to DNA in the serum of patients with systemic lupus erythematosus. J Clin Invest. 1966 Nov;45(11):1732-1740.
- [3] Leon SA, Shapiro B, Sklaroff DM, Yaros MJ. Free DNA in the serum of cancer patients and the effect of therapy. Cancer Res. 1977 Mar;37(3):646-650.
- [4] Lo YM, Corbetta N, Chamberlain PF, Rai V, Sargent IL, Redman CW, Wainscoat JS. Presence of fetal DNA in maternal plasma and serum. Lancet. 1997 Aug 16;350(9076):485-487.
- [5] Palomaki GE, Kloza EM, Lambert-Messerlian GM, Haddow JE, Neveux LM, Ehrich M, van den Boom D, Bombard AT, Deciu C, Grody WW, Nelson SF, Canick JA. DNA sequencing of maternal plasma to detect Down syndrome: an international clinical validation study. Genet Med. 2011 Nov;13(11):913-920.
- [6] Hill M, Barrett AN, White H, Chitty LS. Uses of cell free fetal DNA in maternal circulation. Best Pract Res Clin Obstet Gynaecol. 2012 Oct;26(5):639-654.
- [7] Banfalvi G, Szyfter K, Antoni F. Analysis of 5'-ends of short DNA fragments excreted by phytohemagglutinin stimulated lymphocytes. Biochem Biophys Res Commun. 1984 Jan 13;118(1):140-146.
- [8] Ranucci R. Cell-Free DNA: Applications in Different Diseases. Methods Mol Biol. 2019;1909:3-12.
- [9] Spisák S, Solymosi N, Ittész P, Bodor A, Kondor D, Vattay G, Barták BK, Sipos F, Galamb O, Tulassay Z, Szállási Z, Rasmussen S, Sicheritz-Ponten T, Brunak S, Molnár B, Csabai I. Complete genes may pass from food to human blood. PLoS One. 2013 Jul 30;8(7):e69805.

- [10] Bronkhorst AJ, Ungerer V, Holdenrieder S. The emerging role of cell-free DNA as a molecular marker for cancer management. *Biomol Detect Quantif*. 2019 Mar 18;17:100087.
- [11] Shin SH, Park WY, Park D. Characterization of DNA lesions associated with cell-free DNA by targeted deep sequencing. *BMC Med Genomics*. 2021 Jul 28;14(1):192.
- [12] Muraio A, Aziz M, Wang H, Brenner M, Wang P. Release mechanisms of major DAMPs. *Apoptosis*. 2021 Apr;26(3-4):152-162.
- [13] Fenech M, Kirsch-Volders M, Natarajan AT, Surralles J, Crott JW, Parry J, Norppa H, Eastmond DA, Tucker JD, Thomas P. Molecular mechanisms of micronucleus, nucleoplasmic bridge and nuclear bud formation in mammalian and human cells. *Mutagenesis*. 2011 Jan;26(1):125-132.
- [14] Kustanovich A, Schwartz R, Peretz T, Grinshpun A. Life and death of circulating cell-free DNA. *Cancer Biol Ther*. 2019;20(8):1057-1067.
- [15] Bronkhorst AJ, Wentzel JF, Aucamp J, van Dyk E, du Plessis L, Pretorius PJ. Characterization of the cell-free DNA released by cultured cancer cells. *Biochim Biophys Acta*. 2016 Jan;1863(1):157-165.
- [16] Martignano F. Cell-Free DNA: An Overview of Sample Types and Isolation Procedures. *Methods Mol Biol*. 2019;1909:13-27.
- [17] Kılınç N, Onbaşılar M, Çayır A. Evaluation of circulating cell-free nucleic acids in health workers occupationally exposed to ionizing radiation. *Environ Sci Pollut Res Int*. 2022 Jun;29(27):40543-40549.
- [18] Zhong Y, Fan Q, Zhou Z, Wang Y, He K, Lu J. Plasma cfDNA as a Potential Biomarker to Evaluate the Efficacy of Chemotherapy in Gastric Cancer. *Cancer Manag Res*. 2020 May 5;12:3099-3106.
- [19] Kadam SK, Farmen M, Brandt JT. Quantitative measurement of cell-free plasma DNA and applications for detecting tumor genetic variation and promoter methylation in a clinical setting. *J Mol Diagn*. 2012 Jul;14(4):346-356.

- [20] Hassan S, Shehzad A, Khan SA, Miran W, Khan S, Lee YS. Diagnostic and Therapeutic Potential of Circulating-Free DNA and Cell-Free RNA in Cancer Management. *Biomedicines*. 2022 Aug 22;10(8):2047.
- [21] MacKinnon HJ, Kolarova TR, Katz R, Hedge JM, Vinopal E, Lockwood CM, Shree R, Delaney S. The impact of maternal autoimmune disease on cell-free DNA test characteristics. *Am J Obstet Gynecol MFM*. 2021 Nov;3(6):100466.
- [22] Feng CS, Lu BY, Ju HH, Pan WJ. The failure of non-invasive prenatal testing due to maternal dermatomyositis. *Prenat Diagn*. 2019 Oct;39(11):958-961.
- [23] Zhang S, Shu X, Tian X, Chen F, Lu X, Wang G. Enhanced formation and impaired degradation of neutrophil extracellular traps in dermatomyositis and polymyositis: a potential contributor to interstitial lung disease complications. *Clin Exp Immunol*. 2014 Jul;177(1):134-141.
- [24] Hashimoto T, Ueki S, Kamide Y, Miyabe Y, Fukuchi M, Yokoyama Y, Furukawa T, Azuma N, Oka N, Takeuchi H, Kanno K, Ishida-Yamamoto A, Taniguchi M, Hashiramoto A, Matsui K. Increased Circulating Cell-Free DNA in Eosinophilic Granulomatosis With Polyangiitis: Implications for Eosinophil Extracellular Traps and Immunothrombosis. *Front Immunol*. 2022 Jan 12;12:801897.
- [25] Giaglis S, Daoudlarian D, Voll RE, Kyburz D, Venhoff N, Walker UA. Circulating mitochondrial DNA copy numbers represent a sensitive marker for diagnosis and monitoring of disease activity in systemic lupus erythematosus. *RMD Open*. 2021 Dec;7(3):e002010.
- [26] Camuzi Zovico PV, Gasparini Neto VH, Venâncio FA, Soares Miguel GP, Graça Pedrosa R, Kenji Haraguchi F, Barauna VG. Cell-free DNA as an obesity biomarker. *Physiol Res*. 2020 Jul 16;69(3):515-520.
- [27] Marcatti M, Saada J, Okereke I, Wade CE, Bossmann SH, Motamedi M, Szczesny B. Quantification of Circulating Cell Free Mitochondrial DNA in Extracellular Vesicles with PicoGreen™ in Liquid Biopsies: Fast Assessment of Disease/Trauma Severity. *Cells*. 2021 Apr 6;10(4):819.

- [28] Otawara M, Roushan M, Wang X, Ellett F, Yu YM, Irimia D. Microfluidic Assay Measures Increased Neutrophil Extracellular Traps Circulating in Blood after Burn Injuries. *Sci Rep*. 2018 Nov 19;8(1):16983.
- [29] Baumann AK, Beck J, Kirchner T, Hartleben B, Schütz E, Oellerich M, Wedemeyer H, Jaeckel E, Taubert R. Elevated fractional donor-derived cell-free DNA during subclinical graft injury after liver transplantation. *Liver Transpl*. 2022 Dec;28(12):1911-1919.
- [30] Urosevic N, Merritt AJ, Inglis TJJ. Plasma cfDNA predictors of established bacteraemic infection. *Access Microbiol*. 2022 Jun 14;4(6):acmi000373.
- [31] Jing Q, Leung CHC, Wu AR. Cell-Free DNA as Biomarker for Sepsis by Integration of Microbial and Host Information. *Clin Chem*. 2022 Sep 1;68(9):1184-1195.
- [32] Sugawara T, Fujita SI, Kuji T, Ishibashi N, Tamai K, Kawakami Y, Takekoshi K. Dynamics of Specific cfDNA Fragments in the Plasma of Full Marathon Participants. *Genes (Basel)*. 2021 Apr 30;12(5):676.
- [33] Breitbach S, Tug S, Simon P. Circulating cell-free DNA: an up-coming molecular marker in exercise physiology. *Sports Med*. 2012 Jul 1;42(7):565-86.
- [34] Konuralp Atakul B, Koc A, Adiyaman D, Kuyucu M, Sahingoz Yildirim AG, Saka Guvenc M, Erdogan KM, Sengul B, Oztekin DC. Could high levels of cell-free DNA in maternal blood be associated with maternal health and perinatal outcomes? *J Obstet Gynaecol*. 2020 Aug;40(6):797-802.
- [35] Bianchi DW, Chudova D, Sehnert AJ, Bhatt S, Murray K, Prosen TL, Garber JE, Wilkins-Haug L, Vora NL, Warsof S, Goldberg J, Ziainia T, Halks-Miller M. Noninvasive Prenatal Testing and Incidental Detection of Occult Maternal Malignancies. *JAMA*. 2015 Jul 14;314(2):162-169.
- [36] Ashoor G, Syngelaki A, Poon LC, Rezende JC, Nicolaides KH. Fetal fraction in maternal plasma cell-free DNA at 11-13 weeks' gestation: relation to maternal and fetal characteristics. *Ultrasound Obstet Gynecol*. 2013 Jan;41(1):26-32.
- [37] Han DSC, Ni M, Chan RWY, Chan VWH, Lui KO, Chiu RWK, Lo YMD. The Biology of Cell-free DNA Fragmentation and the Roles of DNASE1, DNASE1L3, and DFFB. *Am J Hum Genet*. 2020 Feb 6;106(2):202-214.

- [38] Leffler J, Ciacma K, Gullstrand B, Bengtsson AA, Martin M, Blom AM. A subset of patients with systemic lupus erythematosus fails to degrade DNA from multiple clinically relevant sources. *Arthritis Res Ther*. 2015 Aug 13;17(1):205.
- [39] Barra GB, Santa Rita TH, de Almeida Vasques J, Chianca CF, Nery LF, Santana Soares Costa S. EDTA-mediated inhibition of DNases protects circulating cell-free DNA from ex vivo degradation in blood samples. *Clin Biochem*. 2015 Oct;48(15):976-981.
- [40] Bodaño A, Amarelo J, González A, Gómez-Reino JJ, Conde C. Novel DNASE I mutations related to systemic lupus erythematosus. *Arthritis Rheum*. 2004 Dec;50(12):4070-4071.
- [41] Duvvuri B, Lood C. Cell-Free DNA as a Biomarker in Autoimmune Rheumatic Diseases. *Front Immunol*. 2019 Mar 19;10:502.
- [42] Hartl J, Serpas L, Wang Y, Rashidfarrokhi A, Perez OA, Sally B, Sisirak V, Soni C, Khodadadi-Jamayran A, Tsirigos A, Caiello I, Bracaglia C, Volpi S, Ghiggeri GM, Chida AS, Sanz I, Kim MY, Belmont HM, Silverman GJ, Clancy RM, Izmirly PM, Buyon JP, Reizis B. Autoantibody-mediated impairment of DNASE1L3 activity in sporadic systemic lupus erythematosus. *J Exp Med*. 2021 May 3;218(5):e20201138.
- [43] Felux J, Erbacher A, Breckler M, Hervé R, Lemeiter D, Mannherz HG, Napirei M, Rammensee HG, Decker P. Deoxyribonuclease 1-Mediated Clearance of Circulating Chromatin Prevents From Immune Cell Activation and Pro-inflammatory Cytokine Production, a Phenomenon Amplified by Low Trap1 Activity: Consequences for Systemic Lupus Erythematosus. *Front Immunol*. 2021 Mar 4;12:613597.
- [44] Gaipl US, Beyer TD, Heyder P, Kuenkele S, Böttcher A, Voll RE, Kalden JR, Herrmann M. Cooperation between C1q and DNase I in the clearance of necrotic cell-derived chromatin. *Arthritis Rheum*. 2004 Feb;50(2):640-649.
- [45] Fredi M, Bianchi M, Andreoli L, Greco G, Olivieri I, Orcesi S, Fazzi E, Cereda C, Tincani A. Typing TREX1 gene in patients with systemic lupus erythematosus. *Reumatismo*. 2015 Jun 30;67(1):1-7.
- [46] Gillmore JD, Hutchinson WL, Herbert J, Bybee A, Mitchell DA, Hasserjian RP, Yamamura K, Suzuki M, Sabin CA, Pepys MB. Autoimmunity and glomerulonephritis in

mice with targeted deletion of the serum amyloid P component gene: SAP deficiency or strain combination? *Immunology*. 2004 Jun;112(2):255-264.

[47] Ogden CA, Kowalewski R, Peng Y, Montenegro V, Elkon KB. IGM is required for efficient complement mediated phagocytosis of apoptotic cells in vivo. *Autoimmunity*. 2005 Jun;38(4):259-264.

[48] Janko C, Franz S, Munoz LE, Siebig S, Winkler S, Schett G, Lauber K, Sheriff A, van der Vlag J, Herrmann M. CRP/anti-CRP antibodies assembly on the surfaces of cell remnants switches their phagocytic clearance toward inflammation. *Front Immunol*. 2011 Dec 2;2:70.

[49] Saevarsdottir S, Steinsson K, Ludviksson BR, Grondal G, Valdimarsson H. Mannan-binding lectin may facilitate the clearance of circulating immune complexes--implications from a study on C2-deficient individuals. *Clin Exp Immunol*. 2007 May;148(2):248-253.

[50] Stortz JA, Hawkins RB, Holden DC, Raymond SL, Wang Z, Brakenridge SC, Cuschieri J, Moore FA, Maier RV, Moldawer LL, Efron PA. Cell-free nuclear, but not mitochondrial, DNA concentrations correlate with the early host inflammatory response after severe trauma. *Sci Rep*. 2019 Sep 20;9(1):13648.

[51] Hauser CJ, Otterbein LE. Danger signals from mitochondrial DAMPS in trauma and post-injury sepsis. *Eur J Trauma Emerg Surg*. 2018 Jun;44(3):317-324.

[52] Kumar V. The Trinity of cGAS, TLR9, and ALRs Guardians of the Cellular Galaxy Against Host-Derived Self-DNA. *Front Immunol*. 2021 Feb 11;11:624597.

[53] Wang H, Zang C, Ren M, Shang M, Wang Z, Peng X, Zhang Q, Wen X, Xi Z, Zhou C. Cellular uptake of extracellular nucleosomes induces innate immune responses by binding and activating cGMP-AMP synthase (cGAS). *Sci Rep*. 2020 Sep 21;10(1):15385.

[54] Ishikawa H, Barber GN. STING is an endoplasmic reticulum adaptor that facilitates innate immune signalling. *Nature*. 2008 Oct 2;455(7213):674-678.

[55] Ishikawa H, Ma Z, Barber GN. STING regulates intracellular DNA-mediated, type I interferon-dependent innate immunity. *Nature*. 2009 Oct 8;461(7265):788-792.

- [56] Hooy RM, Sohn J. The allosteric activation of cGAS underpins its dynamic signaling landscape. *Elife*. 2018 Oct 8;7:e39984.
- [57] Luecke S, Holleufer A, Christensen MH, Jønsson KL, Boni GA, Sørensen LK, Johannsen M, Jakobsen MR, Hartmann R, Paludan SR. cGAS is activated by DNA in a length-dependent manner. *EMBO Rep*. 2017 Oct;18(10):1707-1715.
- [58] Liu S, Cai X, Wu J, Cong Q, Chen X, Li T, Du F, Ren J, Wu YT, Grishin NV, Chen ZJ. Phosphorylation of innate immune adaptor proteins MAVS, STING, and TRIF induces IRF3 activation. *Science*. 2015 Mar 13;347(6227):aaa2630.
- [59] Chen H, Sun H, You F, Sun W, Zhou X, Chen L, Yang J, Wang Y, Tang H, Guan Y, Xia W, Gu J, Ishikawa H, Gutman D, Barber G, Qin Z, Jiang Z. Activation of STAT6 by STING is critical for antiviral innate immunity. *Cell*. 2011 Oct 14;147(2):436-446.
- [60] Abe T, Barber GN. Cytosolic-DNA-mediated, STING-dependent proinflammatory gene induction necessitates canonical NF- κ B activation through TBK1. *J Virol*. 2014 May;88(10):5328-5341.
- [61] Saitoh T, Fujita N, Hayashi T, Takahara K, Satoh T, Lee H, Matsunaga K, Kageyama S, Omori H, Noda T, Yamamoto N, Kawai T, Ishii K, Takeuchi O, Yoshimori T, Akira S. Atg9a controls dsDNA-driven dynamic translocation of STING and the innate immune response. *Proc Natl Acad Sci U S A*. 2009 Dec 8;106(49):20842-20846.
- [62] Liang Q, Seo GJ, Choi YJ, Kwak MJ, Ge J, Rodgers MA, Shi M, Leslie BJ, Hopfner KP, Ha T, Oh BH, Jung JU. Crosstalk between the cGAS DNA sensor and Beclin-1 autophagy protein shapes innate antimicrobial immune responses. *Cell Host Microbe*. 2014 Feb 12;15(2):228-238.
- [63] Motwani M, Pesiridis S, Fitzgerald KA. DNA sensing by the cGAS-STING pathway in health and disease. *Nat Rev Genet*. 2019 Nov;20(11):657-674.
- [64] Latz E, Schoenemeyer A, Visintin A, Fitzgerald KA, Monks BG, Knetter CF, Lien E, Nilsen NJ, Espevik T, Golenbock DT. TLR9 signals after translocating from the ER to CpG DNA in the lysosome. *Nat Immunol*. 2004 Feb;5(2):190-198.
- [65] Miyake K, Shibata T, Fukui R, Sato R, Saitoh SI, Murakami Y. Nucleic Acid Sensing by Toll-Like Receptors in the Endosomal Compartment. *Front Immunol*. 2022 Jun 23;13:941931.

- [66] Miyake K. Nucleic acid-sensing Toll-like receptors: beyond ligand search. *Adv Drug Deliv Rev.* 2008 Apr 29;60(7):782-785.
- [67] De Nardo D, Balka KR, Cardona Gloria Y, Rao VR, Latz E, Masters SL. Interleukin-1 receptor-associated kinase 4 (IRAK4) plays a dual role in myddosome formation and Toll-like receptor signaling. *J Biol Chem.* 2018 Sep 28;293(39):15195-15207.
- [68] Singer JW, Fleischman A, Al-Fayoumi S, Mascarenhas JO, Yu Q, Agarwal A. Inhibition of interleukin-1 receptor-associated kinase 1 (IRAK1) as a therapeutic strategy. *Oncotarget.* 2018 Sep 7;9(70):33416-33439.
- [69] Dong W, Liu Y, Peng J, Chen L, Zou T, Xiao H, Liu Z, Li W, Bu Y, Qi Y. The IRAK-1-BCL10-MALT1-TRAF6-TAK1 cascade mediates signaling to NF-kappaB from Toll-like receptor 4. *J Biol Chem.* 2006 Sep 8;281(36):26029-26040.
- [70] Wu ZH, Wong ET, Shi Y, Niu J, Chen Z, Miyamoto S, Tergaonkar V. ATM- and NEMO-dependent ELKS ubiquitination coordinates TAK1-mediated IKK activation in response to genotoxic stress. *Mol Cell.* 2010 Oct 8;40(1):75-86.
- [71] Pohar J, Kužnik Krajnik A, Jerala R, Benčina M. Minimal sequence requirements for oligodeoxyribonucleotides activating human TLR9. *J Immunol.* 2015 Apr 15;194(8):3901-3908.
- [72] Pohar J, Lainšček D, Ivičak-Kocjan K, Cajnko MM, Jerala R, Benčina M. Short single-stranded DNA degradation products augment the activation of Toll-like receptor 9. *Nat Commun.* 2017 May 22;8:15363.
- [73] Pohar J, Yamamoto C, Fukui R, Cajnko MM, Miyake K, Jerala R, Benčina M. Selectivity of Human TLR9 for Double CpG Motifs and Implications for the Recognition of Genomic DNA. *J Immunol.* 2017 Mar 1;198(5):2093-2104.
- [74] Barton GM, Kagan JC, Medzhitov R. Intracellular localization of Toll-like receptor 9 prevents recognition of self DNA but facilitates access to viral DNA. *Nat Immunol.* 2006 Jan;7(1):49-56.
- [75] Jansen MP, Emal D, Teske GJ, Dessing MC, Florquin S, Roelofs JJ. Release of extracellular DNA influences renal ischemia reperfusion injury by platelet activation and formation of neutrophil extracellular traps. *Kidney Int.* 2017 Feb;91(2):352-364.

- [76] Aslam R, Speck ER, Kim M, Crow AR, Bang KW, Nestel FP, Ni H, Lazarus AH, Freedman J, Semple JW. Platelet Toll-like receptor expression modulates lipopolysaccharide-induced thrombocytopenia and tumor necrosis factor-alpha production in vivo. *Blood*. 2006 Jan 15;107(2):637-641.
- [77] Panigrahi S, Ma Y, Hong L, Gao D, West XZ, Salomon RG, Byzova TV, Podrez EA. Engagement of platelet toll-like receptor 9 by novel endogenous ligands promotes platelet hyperreactivity and thrombosis. *Circ Res*. 2013 Jan 4;112(1):103-112.
- [78] Lugrin J, Martinon F. The AIM2 inflammasome: Sensor of pathogens and cellular perturbations. *Immunol Rev*. 2018 Jan;281(1):99-114.
- [79] Wang B, Tian Y, Yin Q. AIM2 Inflammasome Assembly and Signaling. *Adv Exp Med Biol*. 2019;1172:143-155.
- [80] Matyszewski M, Morrone SR, Sohn J. Digital signaling network drives the assembly of the AIM2-ASC inflammasome. *Proc Natl Acad Sci U S A*. 2018 Feb 27;115(9):E1963-E1972.
- [81] Morrone SR, Matyszewski M, Yu X, Delannoy M, Egelman EH, Sohn J. Assembly-driven activation of the AIM2 foreign-dsDNA sensor provides a polymerization template for downstream ASC. *Nat Commun*. 2015 Jul 22;6:7827.
- [82] Banerjee I, Behl B, Mendonca M, Shrivastava G, Russo AJ, Menoret A, Ghosh A, Vella AT, Vanaja SK, Sarkar SN, Fitzgerald KA, Rathinam VAK. Gasdermin D Restrains Type I Interferon Response to Cytosolic DNA by Disrupting Ionic Homeostasis. *Immunity*. 2018 Sep 18;49(3):413-426.e5.
- [83] Evavold CL, Ruan J, Tan Y, Xia S, Wu H, Kagan JC. The Pore-Forming Protein Gasdermin D Regulates Interleukin-1 Secretion from Living Macrophages. *Immunity*. 2018 Jan 16;48(1):35-44.e6.
- [84] Liu Z, Wang C, Yang J, Zhou B, Yang R, Ramachandran R, Abbott DW, Xiao TS. Crystal Structures of the Full-Length Murine and Human Gasdermin D Reveal Mechanisms of Autoinhibition, Lipid Binding, and Oligomerization. *Immunity*. 2019 Jul 16;51(1):43-49.e4.
- [85] Yan S, Shen H, Lian Q, Jin W, Zhang R, Lin X, Gu W, Sun X, Meng G, Tian Z, Chen ZW, Sun B. Correction: Deficiency of the AIM2-ASC Signal Uncovers the STING-

Driven Overreactive Response of Type I IFN and Reciprocal Depression of Protective IFN- γ Immunity in Mycobacterial Infection. *J Immunol.* 2020 Jan 15;204(2):472.

[86] Múzes G, Bohusné Barta B, Szabó O, Horgas V, Sipos F. Cell-Free DNA in the Pathogenesis and Therapy of Non-Infectious Inflammations and Tumors. *Biomedicines.* 2022 Nov 8;10(11):2853.

[87] O'Neill LA. The interleukin-1 receptor/Toll-like receptor superfamily: 10 years of progress. *Immunol Rev.* 2008 Dec;226:10-18.

[88] Fischer M, Ehlers M. Toll-like receptors in autoimmunity. *Ann N Y Acad Sci.* 2008 Nov;1143:21-34.

[89] Lee J, Mo JH, Katakura K, Alkalay I, Rucker AN, Liu YT, Lee HK, Shen C, Cojocaru G, Shenouda S, Kagnoff M, Eckmann L, Ben-Neriah Y, Raz E. Maintenance of colonic homeostasis by distinctive apical TLR9 signalling in intestinal epithelial cells. *Nat Cell Biol.* 2006 Dec;8(12):1327-1336.

[90] Leifer CA, Kennedy MN, Mazzoni A, Lee C, Kruhlak MJ, Segal DM. TLR9 is localized in the endoplasmic reticulum prior to stimulation. *J Immunol.* 2004 Jul 15;173(2):1179-83.

[91] Latz E, Visintin A, Espevik T, Golenbock DT. Mechanisms of TLR9 activation. *J Endotoxin Res.* 2004;10(6):406-412.

[92] Espevik T, Latz E, Lien E, Monks B, Golenbock DT. Cell distributions and functions of Toll-like receptor 4 studied by fluorescent gene constructs. *Scand J Infect Dis.* 2003;35(9):660-664.

[93] Akira S, Hemmi H. Recognition of pathogen-associated molecular patterns by TLR family. *Immunol Lett.* 2003 Jan 22;85(2):85-95.

[94] Kanzler H, Barrat FJ, Hessel EM, Coffman RL. Therapeutic targeting of innate immunity with Toll-like receptor agonists and antagonists. *Nat Med.* 2007 May;13(5):552-559.

[95] Pinto A, Morello S, Sorrentino R. Lung cancer and Toll-like receptors. *Cancer Immunol Immunother.* 2011 Sep;60(9):1211-1220.

- [96] Lamphier MS, Sirois CM, Verma A, Golenbock DT, Latz E. TLR9 and the recognition of self and non-self nucleic acids. *Ann N Y Acad Sci.* 2006 Oct;1082:31-43.
- [97] Häcker H, Mischak H, Miethke T, Liptay S, Schmid R, Sparwasser T, Heeg K, Lipford GB, Wagner H. CpG-DNA-specific activation of antigen-presenting cells requires stress kinase activity and is preceded by non-specific endocytosis and endosomal maturation. *EMBO J.* 1998 Nov 2;17(21):6230-6240.
- [98] Zhu J, Mohan C. Toll-like receptor signaling pathways--therapeutic opportunities. *Mediators Inflamm.* 2010;2010:781235.
- [99] Okude H, Ori D, Kawai T. Signaling Through Nucleic Acid Sensors and Their Roles in Inflammatory Diseases. *Front Immunol.* 2021 Jan 28;11:625833.
- [100] Krieg AM. Therapeutic potential of Toll-like receptor 9 activation. *Nat Rev Drug Discov.* 2006 Jun;5(6):471-484.
- [101] Klinman DM. Immunotherapeutic uses of CpG oligodeoxynucleotides. *Nat Rev Immunol.* 2004 Apr;4(4):249-258.
- [102] Liu Y, Luo X, Yang C, Yu S, Xu H. Three CpG oligodeoxynucleotide classes differentially enhance antigen-specific humoral and cellular immune responses in mice. *Vaccine.* 2011 Aug 5;29(34):5778-5784.
- [103] Vollmer J, Weeratna R, Payette P, Jurk M, Schetter C, Laucht M, Wader T, Tluk S, Liu M, Davis HL, Krieg AM. Characterization of three CpG oligodeoxynucleotide classes with distinct immunostimulatory activities. *Eur J Immunol.* 2004 Jan;34(1):251-262.
- [104] Krug A, Rothenfusser S, Hornung V, Jahrsdörfer B, Blackwell S, Ballas ZK, Endres S, Krieg AM, Hartmann G. Identification of CpG oligonucleotide sequences with high induction of IFN-alpha/beta in plasmacytoid dendritic cells. *Eur J Immunol.* 2001 Jul;31(7):2154-2163.
- [105] Brody JD, Ai WZ, Czerwinski DK, Torchia JA, Levy M, Advani RH, Kim YH, Hoppe RT, Knox SJ, Shin LK, Wapnir I, Tibshirani RJ, Levy R. In situ vaccination with a TLR9 agonist induces systemic lymphoma regression: a phase I/II study. *J Clin Oncol.* 2010 Oct 1;28(28):4324-4332.

- [106] Thompson JA, Kuzel T, Drucker BJ, Urba WJ, Bukowski RM. Safety and efficacy of PF-3512676 for the treatment of stage IV renal cell carcinoma: an open-label, multicenter phase I/II study. *Clin Genitourin Cancer*. 2009 Oct;7(3):E58-E65.
- [107] Hofmann MA, Kors C, Audring H, Walden P, Sterry W, Trefzer U. Phase I evaluation of intralesionally injected TLR9-agonist PF-3512676 in patients with basal cell carcinoma or metastatic melanoma. *J Immunother*. 2008 Jun;31(5):520-527.
- [108] Yamada K, Nakao M, Fukuyama C, Nokihara H, Yamamoto N, Sekine I, Kunitoh H, Ohe Y, Ohki E, Hashimoto J, Tamura T. Phase I study of TLR9 agonist PF-3512676 in combination with carboplatin and paclitaxel in patients with advanced non-small-cell lung cancer. *Cancer Sci*. 2010 Jan;101(1):188-195.
- [109]. Katsuda M, Iwahashi M, Matsuda K, Miyazawa M, Nakamori M, Nakamura M, Naka T, Ojima T, Iida T, Yamaue H. [Peptide vaccine therapy with TLR-9 agonist for patients with esophageal squamous cell carcinoma]. *Gan To Kagaku Ryoho*. 2011 Nov;38(12):1942-1944.
- [110] Tarhini AA, Leng S, Moschos SJ, Yin Y, Sander C, Lin Y, Gooding WE, Kirkwood JM. Safety and immunogenicity of vaccination with MART-1 (26-35, 27L), gp100 (209-217, 210M), and tyrosinase (368-376, 370D) in adjuvant with PF-3512676 and GM-CSF in metastatic melanoma. *J Immunother*. 2012 May;35(4):359-366.
- [111] Kim YH, Gratzinger D, Harrison C, Brody JD, Czerwinski DK, Ai WZ, Morales A, Abdulla F, Xing L, Navi D, Tibshirani RJ, Advani RH, Lingala B, Shah S, Hoppe RT, Levy R. In situ vaccination against mycosis fungoides by intratumoral injection of a TLR9 agonist combined with radiation: a phase 1/2 study. *Blood*. 2012 Jan 12;119(2):355-363.
- [112] Zent CS, Smith BJ, Ballas ZK, Wooldridge JE, Link BK, Call TG, Shanafelt TD, Bowen DA, Kay NE, Witzig TE, Weiner GJ. Phase I clinical trial of CpG oligonucleotide 7909 (PF-03512676) in patients with previously treated chronic lymphocytic leukemia. *Leuk Lymphoma*. 2012 Feb;53(2):211-217.
- [113] Manegold C, van Zandwijk N, Szczesna A, Zatloukal P, Au JSK, Blasinska-Morawiec M, Serwatowski P, Krzakowski M, Jassem J, Tan EH, Benner RJ, Ingrosso A, Meech SJ, Readett D, Thatcher N. A phase III randomized study of gemcitabine and

cisplatin with or without PF-3512676 (TLR9 agonist) as first-line treatment of advanced non-small-cell lung cancer. *Ann Oncol.* 2012 Jan;23(1):72-77.

[114] Rayburn ER, Wang W, Zhang Z, Li M, Zhang R, Wang H. Experimental therapy of prostate cancer with an immunomodulatory oligonucleotide: effects on tumor growth, apoptosis, proliferation, and potentiation of chemotherapy. *Prostate.* 2006 Nov 1;66(15):1653-1663.

[115] Krieg AM. CpG motifs: the active ingredient in bacterial extracts? *Nat Med.* 2003 Jul;9(7):831-835.

[116] Basith S, Manavalan B, Yoo TH, Kim SG, Choi S. Roles of toll-like receptors in cancer: a double-edged sword for defense and offense. *Arch Pharm Res.* 2012 Aug;35(8):1297-1316.

[117] Fűri I, Sipos F, Germann TM, Kalmár A, Tulassay Z, Molnár B, Műzes G. Epithelial toll-like receptor 9 signaling in colorectal inflammation and cancer: clinico-pathogenic aspects. *World J Gastroenterol.* 2013 Jul 14;19(26):4119-4126.

[118] Huang B, Zhao J, Li H, He KL, Chen Y, Chen SH, Mayer L, Unkeless JC, Xiong H. Toll-like receptors on tumor cells facilitate evasion of immune surveillance. *Cancer Res.* 2005 Jun 15;65(12):5009-5014.

[119] Fűri I, Sipos F, Spisák S, Kiszner G, Wichmann B, Schöller A, Tulassay Z, Műzes G, Molnár B. Association of self-DNA mediated TLR9-related gene, DNA methyltransferase, and cytokeratin protein expression alterations in HT29-cells to DNA fragment length and methylation status. *ScientificWorldJournal.* 2013 Dec 29;2013:293296.

[120] Pikarsky E, Porat RM, Stein I, Abramovitch R, Amit S, Kasem S, Gutkovich-Pyest E, Urieli-Shoval S, Galun E, Ben-Neriah Y. NF-kappaB functions as a tumour promoter in inflammation-associated cancer. *Nature.* 2004 Sep 23;431(7007):461-466.

[121] Pradere JP, Dapito DH, Schwabe RF. The Yin and Yang of Toll-like receptors in cancer. *Oncogene.* 2014 Jul 3;33(27):3485-3495.

[122] Grivennikov S, Karin E, Terzic J, Mucida D, Yu GY, Vallabhapurapu S, Scheller J, Rose-John S, Cheroutre H, Eckmann L, Karin M. IL-6 and Stat3 are required for survival

of intestinal epithelial cells and development of colitis-associated cancer. *Cancer Cell*. 2009 Feb 3;15(2):103-113.

[123] Popivanova BK, Kitamura K, Wu Y, Kondo T, Kagaya T, Kaneko S, Oshima M, Fujii C, Mukaida N. Blocking TNF-alpha in mice reduces colorectal carcinogenesis associated with chronic colitis. *J Clin Invest*. 2008 Feb;118(2):560-570.

[124] Dutta J, Fan Y, Gupta N, Fan G, Gélinas C. Current insights into the regulation of programmed cell death by NF-kappaB. *Oncogene*. 2006 Oct 30;25(51):6800-6816.

[125] Wang CY, Mayo MW, Korneluk RG, Goeddel DV, Baldwin AS Jr. NF-kappaB antiapoptosis: induction of TRAF1 and TRAF2 and c-IAP1 and c-IAP2 to suppress caspase-8 activation. *Science*. 1998 Sep 11;281(5383):1680-1683.

[126] Palucka K, Banchereau J. Cancer immunotherapy via dendritic cells. *Nat Rev Cancer*. 2012 Mar 22;12(4):265-277.

[127] Garaude J, Kent A, van Rooijen N, Blander JM. Simultaneous targeting of toll- and nod-like receptors induces effective tumor-specific immune responses. *Sci Transl Med*. 2012 Feb 8;4(120):120ra16.

[128] Drobits B, Holcman M, Amberg N, Swiecki M, Grundtner R, Hammer M, Colonna M, Sibilina M. Imiquimod clears tumors in mice independent of adaptive immunity by converting pDCs into tumor-killing effector cells. *J Clin Invest*. 2012 Feb;122(2):575-585.

[129] Cubillos-Ruiz JR, Engle X, Scarlett UK, Martinez D, Barber A, Elgueta R, Wang L, Nesbeth Y, Durant Y, Gewirtz AT, Sentman CL, Kedl R, Conejo-Garcia JR. Polyethylenimine-based siRNA nanocomplexes reprogram tumor-associated dendritic cells via TLR5 to elicit therapeutic antitumor immunity. *J Clin Invest*. 2009 Aug;119(8):2231-2244.

[130] Nierkens S, den Brok MH, Garcia Z, Togher S, Wagenaars J, Wassink M, Boon L, Ruers TJ, Figdor CG, Schoenberger SP, Adema GJ, Janssen EM. Immune adjuvant efficacy of CpG oligonucleotide in cancer treatment is founded specifically upon TLR9 function in plasmacytoid dendritic cells. *Cancer Res*. 2011 Oct 15;71(20):6428-6437.

[131] Sipos F, Múzes G, Fűri I, Spisák S, Wichmann B, Germann TM, Constantinovits M, Krenács T, Tulassay Z, Molnár B. Intravenous administration of a single-dose free-

circulating DNA of colitic origin improves severe murine DSS-colitis. *Pathol Oncol Res.* 2014 Oct;20(4):867-877.

[132] Krieg AM. Development of TLR9 agonists for cancer therapy. *J Clin Invest.* 2007 May;117(5):1184-1194.

[133] Kadowaki N, Antonenko S, Liu YJ. Distinct CpG DNA and polyinosinic-polycytidylic acid double-stranded RNA, respectively, stimulate CD11c- type 2 dendritic cell precursors and CD11c+ dendritic cells to produce type I IFN. *J Immunol.* 2001 Feb 15;166(4):2291-2295.

[134] Dongye Z, Li J, Wu Y. Toll-like receptor 9 agonists and combination therapies: strategies to modulate the tumour immune microenvironment for systemic anti-tumour immunity. *Br J Cancer.* 2022 Nov;127(9):1584-1594.

[135] Yang Z, Klionsky DJ. Eaten alive: a history of macroautophagy. *Nat Cell Biol.* 2010 Sep;12(9):814-822.

[136] Mizushima N, Levine B, Cuervo AM, Klionsky DJ. Autophagy fights disease through cellular self-digestion. *Nature.* 2008 Feb 28;451(7182):1069-1075.

[137]. Rabinowitz JD, White E. Autophagy and metabolism. *Science.* 2010 Dec 3;330(6009):1344-1348.

[138] Múzes G, Sipos F. Anti-tumor immunity, autophagy and chemotherapy. *World J Gastroenterol.* 2012 Dec 7;18(45):6537-6540.

[139] Behrends C, Sowa ME, Gygi SP, Harper JW. Network organization of the human autophagy system. *Nature.* 2010 Jul 1;466(7302):68-76.

[140] He C, Klionsky DJ. Regulation mechanisms and signaling pathways of autophagy. *Annu Rev Genet.* 2009;43:67-93.

[141] Mehrpour M, Esclatine A, Beau I, Codogno P. Autophagy in health and disease. 1. Regulation and significance of autophagy: an overview. *Am J Physiol Cell Physiol.* 2010 Apr;298(4):C776-C785.

[142] Sanjuan MA, Dillon CP, Tait SW, Moshiah S, Dorsey F, Connell S, Komatsu M, Tanaka K, Cleveland JL, Withoff S, Green DR. Toll-like receptor signalling in

macrophages links the autophagy pathway to phagocytosis. *Nature*. 2007 Dec 20;450(7173):1253-1257.

[143] Gordy C, He YW. The crosstalk between autophagy and apoptosis: where does this lead? *Protein Cell*. 2012 Jan;3(1):17-27.

[144] Peng C, Ouyang Y, Lu N, Li N. The NF- κ B Signaling Pathway, the Microbiota, and Gastrointestinal Tumorigenesis: Recent Advances. *Front Immunol*. 2020 Jun 30;11:1387.

[145] Levine B, Kroemer G. Autophagy in the pathogenesis of disease. *Cell*. 2008 Jan 11;132(1):27-42.

[146] Mathew R, Karantza-Wadsworth V, White E. Role of autophagy in cancer. *Nat Rev Cancer*. 2007 Dec;7(12):961-967.

[147] Cadwell K, Liu JY, Brown SL, Miyoshi H, Loh J, Lennerz JK, Kishi C, Kc W, Carrero JA, Hunt S, Stone CD, Brunt EM, Xavier RJ, Sleckman BP, Li E, Mizushima N, Stappenbeck TS, Virgin HW 4th. A key role for autophagy and the autophagy gene Atg16l1 in mouse and human intestinal Paneth cells. *Nature*. 2008 Nov 13;456(7219):259-263.

[148] Dalby KN, Tekedereli I, Lopez-Berestein G, Ozpolat B. Targeting the prodeath and prosurvival functions of autophagy as novel therapeutic strategies in cancer. *Autophagy*. 2010 Apr;6(3):322-329.

[149] Manzoor S, Muhammad JS, Maghazachi AA, Hamid Q. Autophagy: A Versatile Player in the Progression of Colorectal Cancer and Drug Resistance. *Front Oncol*. 2022 Jul 14;12:924290.

[150] Mehta P, Henault J, Kolbeck R, Sanjuan MA. Noncanonical autophagy: one small step for LC3, one giant leap for immunity. *Curr Opin Immunol*. 2014 Feb;26:69-75.

[151] Shin DM, Yuk JM, Lee HM, Lee SH, Son JW, Harding CV, Kim JM, Modlin RL, Jo EK. Mycobacterial lipoprotein activates autophagy via TLR2/1/CD14 and a functional vitamin D receptor signalling. *Cell Microbiol*. 2010 Nov;12(11):1648-1665.

[152] Deretic V, Saitoh T, Akira S. Autophagy in infection, inflammation and immunity. *Nat Rev Immunol*. 2013 Oct;13(10):722-737.

- [153] Delgado MA, Deretic V. Toll-like receptors in control of immunological autophagy. *Cell Death Differ.* 2009 Jul;16(7):976-983.
- [154] Lee HK, Lund JM, Ramanathan B, Mizushima N, Iwasaki A. Autophagy-dependent viral recognition by plasmacytoid dendritic cells. *Science.* 2007 Mar 9;315(5817):1398-1401.
- [155] Lee MS, Kim YJ. Signaling pathways downstream of pattern-recognition receptors and their cross talk. *Annu Rev Biochem.* 2007;76:447-480.
- [156] Shi CS, Kehrl JH. MyD88 and Trif target Beclin 1 to trigger autophagy in macrophages. *J Biol Chem.* 2008 Nov 28;283(48):33175-33182.
- [157] Shi CS, Kehrl JH. TRAF6 and A20 regulate lysine 63-linked ubiquitination of Beclin-1 to control TLR4-induced autophagy. *Sci Signal.* 2010 May 25;3(123):ra42.
- [158] Múzes G, Constantinovits M, Fúri I, Tulassay Z, Sipos F. Interaction of autophagy and Toll-like receptors: a regulatory cross-talk--even in cancer cells? *Curr Drug Targets.* 2014;15(8):743-752.
- [159] Into T, Inomata M, Takayama E, Takigawa T. Autophagy in regulation of Toll-like receptor signaling. *Cell Signal.* 2012 Jun;24(6):1150-1162.
- [160] Knaevelsrud H, Simonsen A. Fighting disease by selective autophagy of aggregate-prone proteins. *FEBS Lett.* 2010 Jun 18;584(12):2635-2645.
- [161] Inomata M, Niida S, Shibata K, Into T. Regulation of Toll-like receptor signaling by NDP52-mediated selective autophagy is normally inactivated by A20. *Cell Mol Life Sci.* 2012 Mar;69(6):963-979.
- [162] Saitoh T, Fujita N, Jang MH, Uematsu S, Yang BG, Satoh T, Omori H, Noda T, Yamamoto N, Komatsu M, Tanaka K, Kawai T, Tsujimura T, Takeuchi O, Yoshimori T, Akira S. Loss of the autophagy protein Atg16L1 enhances endotoxin-induced IL-1beta production. *Nature.* 2008 Nov 13;456(7219):264-268.
- [163] Schmid D, Münz C. Innate and adaptive immunity through autophagy. *Immunity.* 2007 Jul;27(1):11-21.

- [164] Zhan Z, Xie X, Cao H, Zhou X, Zhang XD, Fan H, Liu Z. Autophagy facilitates TLR4- and TLR3-triggered migration and invasion of lung cancer cells through the promotion of TRAF6 ubiquitination. *Autophagy*. 2014 Feb;10(2):257-268.
- [165] Chen GY, Chen CL, Tuan HY, Yuan PX, Li KC, Yang HJ, Hu YC. Graphene oxide triggers toll-like receptors/autophagy responses in vitro and inhibits tumor growth in vivo. *Adv Healthc Mater*. 2014 Sep;3(9):1486-1495.
- [166] Bertin S, Samson M, Pons C, Guignon JM, Gavelli A, Baqué P, Brossette N, Pagnotta S, Ricci JE, Pierrefite-Carle V. Comparative proteomics study reveals that bacterial CpG motifs induce tumor cell autophagy in vitro and in vivo. *Mol Cell Proteomics*. 2008 Dec;7(12):2311-2322.
- [167] Bertin S, Pierrefite-Carle V. Autophagy and toll-like receptors: a new link in cancer cells. *Autophagy*. 2008 Nov;4(8):1086-1089.
- [168] Schmid D, Pypaert M, Münz C. Antigen-loading compartments for major histocompatibility complex class II molecules continuously receive input from autophagosomes. *Immunity*. 2007 Jan;26(1):79-92.
- [169] Ulrich BC, Paweletz CP. Cell-Free DNA in Oncology: Gearing up for Clinic. *Ann Lab Med*. 2018 Jan;38(1):1-8.
- [170] Siravegna G, Mussolin B, Venesio T, Marsoni S, Seoane J, Dive C, Papadopoulos N, Kopetz S, Corcoran RB, Siu LL, Bardelli A. How liquid biopsies can change clinical practice in oncology. *Ann Oncol*. 2019 Oct 1;30(10):1580-1590.
- [171] Domínguez-Vigil IG, Moreno-Martínez AK, Wang JY, Roehrl MHA, Barrera-Saldaña HA. The dawn of the liquid biopsy in the fight against cancer. *Oncotarget*. 2017 Dec 8;9(2):2912-2922.
- [172] Guo Q, Wang J, Xiao J, Wang L, Hu X, Yu W, Song G, Lou J, Chen J. Heterogeneous mutation pattern in tumor tissue and circulating tumor DNA warrants parallel NGS panel testing. *Mol Cancer*. 2018 Aug 28;17(1):131.
- [173] Li J, Dittmar RL, Xia S, Zhang H, Du M, Huang CC, Druliner BR, Boardman L, Wang L. Cell-free DNA copy number variations in plasma from colorectal cancer patients. *Mol Oncol*. 2017 Aug;11(8):1099-1111.

- [174] Yu D, Liu Z, Su C, Han Y, Duan X, Zhang R, Liu X, Yang Y, Xu S. Copy number variation in plasma as a tool for lung cancer prediction using Extreme Gradient Boosting (XGBoost) classifier. *Thorac Cancer*. 2020 Jan;11(1):95-102.
- [175] Willis J, Lefterova MI, Artyomenko A, Kasi PM, Nakamura Y, Mody K, Catenacci DVT, Fakih M, Barbacioru C, Zhao J, Sikora M, Fairclough SR, Lee H, Kim KM, Kim ST, Kim J, Gavino D, Benavides M, Peled N, Nguyen T, Cusnir M, Eskander RN, Azzi G, Yoshino T, Banks KC, Raymond VM, Lanman RB, Chudova DI, Talasz A, Kopetz S, Lee J, Odegaard JI. Validation of Microsatellite Instability Detection Using a Comprehensive Plasma-Based Genotyping Panel. *Clin Cancer Res*. 2019 Dec 1;25(23):7035-7045.
- [176] Müller JN, Falk M, Talwar J, Neemann N, Mariotti E, Bertrand M, Zacherle T, Lakis S, Menon R, Gloeckner C, Tiemann M, Heukamp LC, Thomas RK, Griesinger F, Heuckmann JM. Concordance between Comprehensive Cancer Genome Profiling in Plasma and Tumor Specimens. *J Thorac Oncol*. 2017 Oct;12(10):1503-1511.
- [177] Park S, Olsen S, Ku BM, Lee MS, Jung HA, Sun JM, Lee SH, Ahn JS, Park K, Choi YL, Ahn MJ. High concordance of actionable genomic alterations identified between circulating tumor DNA-based and tissue-based next-generation sequencing testing in advanced non-small cell lung cancer: The Korean Lung Liquid Versus Invasive Biopsy Program. *Cancer*. 2021 Aug 15;127(16):3019-3028.
- [178] Schmiegel W, Scott RJ, Dooley S, Lewis W, Meldrum CJ, Pockney P, Draganic B, Smith S, Hewitt C, Philimore H, Lucas A, Shi E, Namdarian K, Chan T, Acosta D, Ping-Chang S, Tannapfel A, Reinacher-Schick A, Uhl W, Teschendorf C, Wolters H, Stern J, Viebahn R, Friess H, Janssen KP, Nitsche U, Slotta-Huspenina J, Pohl M, Vangala D, Baraniskin A, Dockhorn-Dworniczak B, Hegewisch-Becker S, Ronga P, Edelstein DL, Jones FS, Hahn S, Fox SB. Blood-based detection of RAS mutations to guide anti-EGFR therapy in colorectal cancer patients: concordance of results from circulating tumor DNA and tissue-based RAS testing. *Mol Oncol*. 2017 Feb;11(2):208-219.
- [179] Phallen J, Sausen M, Adleff V, Leal A, Hruban C, White J, Anagnostou V, Fiksel J, Cristiano S, Papp E, Speir S, Reinert T, Orntoft MW, Woodward BD, Murphy D, Parpart-Li S, Riley D, Nesselbush M, Sengamalay N, Georgiadis A, Li QK, Madsen MR, Mortensen FV, Huiskens J, Punt C, van Grieken N, Fijneman R, Meijer G, Husain H,

Scharpf RB, Diaz LA Jr, Jones S, Angiuoli S, Ørntoft T, Nielsen HJ, Andersen CL, Velculescu VE. Direct detection of early-stage cancers using circulating tumor DNA. *Sci Transl Med.* 2017 Aug 16;9(403):eaan2415.

[180] Nesic M, Bødker JS, Terp SK, Dybkær K. Optimization of Preanalytical Variables for cfDNA Processing and Detection of ctDNA in Archival Plasma Samples. *Biomed Res Int.* 2021 Jul 8;2021:5585148.

[181] Bredno J, Lipson J, Venn O, Aravanis AM, Jamshidi A. Clinical correlates of circulating cell-free DNA tumor fraction. *PLoS One.* 2021 Aug 25;16(8):e0256436.

[182] Cai Z, Chen G, Zeng Y, Dong X, Li Z, Huang Y, Xin F, Qiu L, Xu H, Zhang W, Su X, Liu X, Liu J. Comprehensive Liquid Profiling of Circulating Tumor DNA and Protein Biomarkers in Long-Term Follow-Up Patients with Hepatocellular Carcinoma. *Clin Cancer Res.* 2019 Sep 1;25(17):5284-5294.

[183] Isaksson S, George AM, Jönsson M, Cirenajwis H, Jönsson P, Bendahl PO, Brunnström H, Staaf J, Saal LH, Planck M. Pre-operative plasma cell-free circulating tumor DNA and serum protein tumor markers as predictors of lung adenocarcinoma recurrence. *Acta Oncol.* 2019 Aug;58(8):1079-1086.

[184] Chen Z, Liu L, Zhu F, Cai X, Zhao Y, Liang P, Ou L, Zhong R, Yu Z, Li C, Li J, Xiong S, Feng Y, Cheng B, Liang H, Xie Z, Liang W, He J. Dynamic monitoring serum tumor markers to predict molecular features of EGFR-mutated lung cancer during targeted therapy. *Cancer Med.* 2022 Aug;11(16):3115-3125.

[185] Tarazona N, Gimeno-Valiente F, Gambardella V, Zuñiga S, Rentero-Garrido P, Huerta M, Roselló S, Martínez-Ciarpaglini C, Carbonell-Asins JA, Carrasco F, Ferrer-Martínez A, Bruixola G, Fleitas T, Martín J, Tébar-Martínez R, Moro D, Castillo J, Espí A, Roda D, Cervantes A. Targeted next-generation sequencing of circulating-tumor DNA for tracking minimal residual disease in localized colon cancer. *Ann Oncol.* 2019 Nov 1;30(11):1804-1812.

[186] Parsons HA, Rhoades J, Reed SC, Gydush G, Ram P, Exman P, Xiong K, Lo CC, Li T, Fleharty M, Kirkner GJ, Rotem D, Cohen O, Yu F, Fitarelli-Kiehl M, Leong KW, Hughes ME, Rosenberg SM, Collins LC, Miller KD, Blumenstiel B, Trippa L, Cibulskis C, Neuberger DS, DeFelice M, Freeman SS, Lennon NJ, Wagle N, Ha G, Stover DG,

Choudhury AD, Getz G, Winer EP, Meyerson M, Lin NU, Krop I, Love JC, Makrigiorgos GM, Partridge AH, Mayer EL, Golub TR, Adalsteinsson VA. Sensitive Detection of Minimal Residual Disease in Patients Treated for Early-Stage Breast Cancer. *Clin Cancer Res.* 2020 Jun 1;26(11):2556-2564.

[187] Powles T, Assaf ZJ, Davarpanah N, Banchereau R, Szabados BE, Yuen KC, Grivas P, Hussain M, Oudard S, Gschwend JE, Albers P, Castellano D, Nishiyama H, Daneshmand S, Sharma S, Zimmermann BG, Sethi H, Aleshin A, Perdicchio M, Zhang J, Shames DS, Degaonkar V, Shen X, Carter C, Bais C, Bellmunt J, Mariathasan S. ctDNA guiding adjuvant immunotherapy in urothelial carcinoma. *Nature.* 2021 Jul;595(7867):432-437.

[188] Keller L, Belloum Y, Wikman H, Pantel K. Clinical relevance of blood-based ctDNA analysis: mutation detection and beyond. *Br J Cancer.* 2021 Jan;124(2):345-358.

[189] Colotta F, Allavena P, Sica A, Garlanda C, Mantovani A. Cancer-related inflammation, the seventh hallmark of cancer: links to genetic instability. *Carcinogenesis.* 2009 Jul;30(7):1073-1081.

[190] Hanahan D, Weinberg RA. The hallmarks of cancer. *Cell.* 2000 Jan 7;100(1):57-70.

[191] Hanahan D. Hallmarks of Cancer: New Dimensions. *Cancer Discov.* 2022 Jan;12(1):31-46.

[192] Niu Z, Tang W, Liu T, Xu P, Zhu D, Ji M, Huang W, Ren L, Wei Y, Xu J. Cell-free DNA derived from cancer cells facilitates tumor malignancy through Toll-like receptor 9 signaling-triggered interleukin-8 secretion in colorectal cancer. *Acta Biochim Biophys Sin (Shanghai).* 2018 Oct 1;50(10):1007-1017.

[193] Wang W, Kong P, Ma G, Li L, Zhu J, Xia T, Xie H, Zhou W, Wang S. Characterization of the release and biological significance of cell-free DNA from breast cancer cell lines. *Oncotarget.* 2017 Jun 27;8(26):43180-43191.

[194] Kang TH, Mao CP, Kim YS, Kim TW, Yang A, Lam B, Tseng SH, Farmer E, Park YM, Hung CF. TLR9 acts as a sensor for tumor-released DNA to modulate anti-tumor immunity after chemotherapy. *J Immunother Cancer.* 2019 Oct 16;7(1):260.

[195] Bayer AL, Alcaide P. MyD88: At the heart of inflammatory signaling and cardiovascular disease. *J Mol Cell Cardiol.* 2021 Dec;161:75-85.

- [196] Zierhut C, Yamaguchi N, Paredes M, Luo JD, Carroll T, Funabiki H. The Cytoplasmic DNA Sensor cGAS Promotes Mitotic Cell Death. *Cell*. 2019 Jul 11;178(2):302-315.e23.
- [197] An X, Zhu Y, Zheng T, Wang G, Zhang M, Li J, Ji H, Li S, Yang S, Xu D, Li Z, Wang T, He Y, Zhang L, Yang W, Zhao R, Hao D, Li X. An Analysis of the Expression and Association with Immune Cell Infiltration of the cGAS/STING Pathway in Pan-Cancer. *Mol Ther Nucleic Acids*. 2019 Mar 1;14:80-89.
- [198] Yang H, Wang H, Ren J, Chen Q, Chen ZJ. cGAS is essential for cellular senescence. *Proc Natl Acad Sci U S A*. 2017 Jun 6;114(23):E4612-E4620.
- [199] Sen T, Rodriguez BL, Chen L, Corte CMD, Morikawa N, Fujimoto J, Cristea S, Nguyen T, Diao L, Li L, Fan Y, Yang Y, Wang J, Glisson BS, Wistuba II, Sage J, Heymach JV, Gibbons DL, Byers LA. Targeting DNA Damage Response Promotes Antitumor Immunity through STING-Mediated T-cell Activation in Small Cell Lung Cancer. *Cancer Discov*. 2019 May;9(5):646-661.
- [200] Wang-Bishop L, Wehbe M, Shae D, James J, Hacker BC, Garland K, Chistov PP, Rafat M, Balko JM, Wilson JT. Potent STING activation stimulates immunogenic cell death to enhance antitumor immunity in neuroblastoma. *J Immunother Cancer*. 2020 Mar;8(1):e000282.
- [201] Ma F, Lei YY, Ding MG, Luo LH, Xie YC, Liu XL. LncRNA NEAT1 Interacted With DNMT1 to Regulate Malignant Phenotype of Cancer Cell and Cytotoxic T Cell Infiltration via Epigenetic Inhibition of p53, cGAS, and STING in Lung Cancer. *Front Genet*. 2020 Mar 31;11:250.
- [202] Man SM, Zhu Q, Zhu L, Liu Z, Karki R, Malik A, Sharma D, Li L, Malireddi RK, Gurung P, Neale G, Olsen SR, Carter RA, McGoldrick DJ, Wu G, Finkelstein D, Vogel P, Gilbertson RJ, Kanneganti TD. Critical Role for the DNA Sensor AIM2 in Stem Cell Proliferation and Cancer. *Cell*. 2015 Jul 2;162(1):45-58.
- [203] Schulmann K, Brasch FE, Kunstmann E, Engel C, Pagenstecher C, Vogelsang H, Krüger S, Vogel T, Knaebel HP, Rüschoff J, Hahn SA, Knebel-Doeberitz MV, Moeslein G, Meltzer SJ, Schackert HK, Tympner C, Mangold E, Schmiegel W; German HNPCC

Consortium. HNPCC-associated small bowel cancer: clinical and molecular characteristics. *Gastroenterology*. 2005 Mar;128(3):590-599.

[204] Farshchian M, Nissinen L, Siljamäki E, Riihilä P, Piipponen M, Kivisaari A, Kallajoki M, Grénman R, Peltonen J, Peltonen S, Quint KD, Bavinck JNB, Kähäri VM. Tumor cell-specific AIM2 regulates growth and invasion of cutaneous squamous cell carcinoma. *Oncotarget*. 2017 Jul 11;8(28):45825-45836.

[205] Qi M, Dai D, Liu J, Li Z, Liang P, Wang Y, Cheng L, Zhan Y, An Z, Song Y, Yang Y, Yan X, Xiao H, Shao H. AIM2 promotes the development of non-small cell lung cancer by modulating mitochondrial dynamics. *Oncogene*. 2020 Mar;39(13):2707-2723.

[206] Trotta AP, Chipuk JE. Mitochondrial dynamics as regulators of cancer biology. *Cell Mol Life Sci*. 2017 Jun;74(11):1999-2017.

[207] Kondo Y, Nagai K, Nakahata S, Saito Y, Ichikawa T, Suekane A, Taki T, Iwakawa R, Enari M, Taniwaki M, Yokota J, Sakoda S, Morishita K. Overexpression of the DNA sensor proteins, absent in melanoma 2 and interferon-inducible 16, contributes to tumorigenesis of oral squamous cell carcinoma with p53 inactivation. *Cancer Sci*. 2012 Apr;103(4):782-790.

[208] Ponomareva L, Liu H, Duan X, Dickerson E, Shen H, Panchanathan R, Choubey D. AIM2, an IFN-inducible cytosolic DNA sensor, in the development of benign prostate hyperplasia and prostate cancer. *Mol Cancer Res*. 2013 Oct;11(10):1193-1202.

[209] Martínez-Cardona C, Lozano-Ruiz B, Bachiller V, Peiró G, Algaba-Chueca F, Gómez-Hurtado I, Such J, Zapater P, Francés R, González-Navajas JM. AIM2 deficiency reduces the development of hepatocellular carcinoma in mice. *Int J Cancer*. 2018 Dec 1;143(11):2997-3007.

[210] Ma X, Guo P, Qiu Y, Mu K, Zhu L, Zhao W, Li T, Han L. Loss of AIM2 expression promotes hepatocarcinoma progression through activation of mTOR-S6K1 pathway. *Oncotarget*. 2016 Jun 14;7(24):36185-36197.

[211] García-Olmo D, García-Olmo DC, Ontañón J, Martínez E, Vallejo M. Tumor DNA circulating in the plasma might play a role in metastasis. The hypothesis of the genomestasis. *Histol Histopathol*. 1999 Oct;14(4):1159-1164.

- [212] García-Olmo DC, Domínguez C, García-Arranz M, Anker P, Stroun M, García-Verdugo JM, García-Olmo D. Cell-free nucleic acids circulating in the plasma of colorectal cancer patients induce the oncogenic transformation of susceptible cultured cells. *Cancer Res.* 2010 Jan 15;70(2):560-567.
- [213] Trejo-Becerril C, Pérez-Cárdenas E, Taja-Chayeb L, Anker P, Herrera-Goepfert R, Medina-Velázquez LA, Hidalgo-Miranda A, Pérez-Montiel D, Chávez-Blanco A, Cruz-Velázquez J, Díaz-Chávez J, Gaxiola M, Dueñas-González A. Cancer progression mediated by horizontal gene transfer in an in vivo model. *PLoS One.* 2012;7(12):e52754.
- [214] Bergsmedh A, Szeles A, Henriksson M, Bratt A, Folkman MJ, Spetz AL, Holmgren L. Horizontal transfer of oncogenes by uptake of apoptotic bodies. *Proc Natl Acad Sci U S A.* 2001 May 22;98(11):6407-6411.
- [215] Gaiffe E, Prétet JL, Launay S, Jacquin E, Saunier M, Hetzel G, Oudet P, Mougin C. Apoptotic HPV positive cancer cells exhibit transforming properties. *PLoS One.* 2012;7(5):e36766.
- [216] Beyer C, Pisetsky DS. The role of microparticles in the pathogenesis of rheumatic diseases. *Nat Rev Rheumatol.* 2010 Jan;6(1):21-29.
- [217] Lee TH, Chennakrishnaiah S, Audemard E, Montermini L, Meehan B, Rak J. Oncogenic ras-driven cancer cell vesiculation leads to emission of double-stranded DNA capable of interacting with target cells. *Biochem Biophys Res Commun.* 2014 Aug 22;451(2):295-301.
- [218] Abdouh M, Floris M, Gao ZH, Arena V, Arena M, Arena GO. Colorectal cancer-derived extracellular vesicles induce transformation of fibroblasts into colon carcinoma cells. *J Exp Clin Cancer Res.* 2019 Jun 14;38(1):257.
- [219] Wartha F, Henriques-Normark B. ETosis: a novel cell death pathway. *Sci Signal.* 2008 May 27;1(21):pe25.
- [220] Chen Q, Zhang L, Li X, Zhuo W. Neutrophil Extracellular Traps in Tumor Metastasis: Pathological Functions and Clinical Applications. *Cancers (Basel).* 2021 Jun 6;13(11):2832.
- [221] Alekseeva L, Mironova N. Role of Cell-Free DNA and Deoxyribonucleases in Tumor Progression. *Int J Mol Sci.* 2021 Nov 12;22(22):12246..

- [222] Arelaki S, Arampatzioglou A, Kambas K, Papagoras C, Miltiades P, Angelidou I, Mitsios A, Kotsianidis I, Skendros P, Sivridis E, Maroulakou I, Giatromanolaki A, Ritis K. Gradient Infiltration of Neutrophil Extracellular Traps in Colon Cancer and Evidence for Their Involvement in Tumour Growth. *PLoS One*. 2016 May 2;11(5):e0154484.
- [223] Schedel F, Mayer-Hain S, Pappelbaum KI, Metze D, Stock M, Goerge T, Loser K, Sunderkötter C, Luger TA, Weishaupt C. Evidence and impact of neutrophil extracellular traps in malignant melanoma. *Pigment Cell Melanoma Res*. 2020 Jan;33(1):63-73.
- [224] Breitbach CJ, De Silva NS, Falls TJ, Aladl U, Evgin L, Paterson J, Sun YY, Roy DG, Rintoul JL, Daneshmand M, Parato K, Stanford MM, Lichty BD, Fenster A, Kirn D, Atkins H, Bell JC. Targeting tumor vasculature with an oncolytic virus. *Mol Ther*. 2011 May;19(5):886-894.
- [225] Park KC, Richardson DR. The c-MET oncoprotein: Function, mechanisms of degradation and its targeting by novel anti-cancer agents. *Biochim Biophys Acta Gen Subj*. 2020 Oct;1864(10):129650.
- [226] Trusolino L, Bertotti A, Comoglio PM. MET signalling: principles and functions in development, organ regeneration and cancer. *Nat Rev Mol Cell Biol*. 2010 Dec;11(12):834-848.
- [227] Papaccio F, Della Corte CM, Viscardi G, Di Liello R, Esposito G, Sparano F, Ciardiello F, Morgillo F. HGF/MET and the Immune System: Relevance for Cancer Immunotherapy. *Int J Mol Sci*. 2018 Nov 14;19(11):3595.
- [228] García-Vilas JA, Medina MÁ. Updates on the hepatocyte growth factor/c-Met axis in hepatocellular carcinoma and its therapeutic implications. *World J Gastroenterol*. 2018 Sep 7;24(33):3695-3708.
- [229] Samamé Pérez-Vargas JC, Biondani P, Maggi C, Gariboldi M, Gloghini A, Inno A, Volpi CC, Gualeni AV, di Bartolomeo M, de Braud F, Castano A, Bossi I, Pietrantonio F. Role of cMET in the development and progression of colorectal cancer. *Int J Mol Sci*. 2013 Sep 3;14(9):18056-18077.
- [230] Jia Y, Dai G, Wang J, Gao X, Zhao Z, Duan Z, Gu B, Yang W, Wu J, Ju Y, Wang M, Li Z. c-MET inhibition enhances the response of the colorectal cancer cells to irradiation *in vitro* and *in vivo*. *Oncol Lett*. 2016 Apr;11(4):2879-2885.

- [231] Comoglio PM, Trusolino L, Boccaccio C. Known and novel roles of the MET oncogene in cancer: a coherent approach to targeted therapy. *Nat Rev Cancer*. 2018 Jun;18(6):341-358.
- [232] Organ SL, Tsao MS. An overview of the c-MET signaling pathway. *Ther Adv Med Oncol*. 2011 Nov;3(1 Suppl):S7-S19.
- [233] Liu X, Sun R, Chen J, Liu L, Cui X, Shen S, Cui G, Ren Z, Yu Z. Crosstalk Mechanisms Between HGF/c-Met Axis and ncRNAs in Malignancy. *Front Cell Dev Biol*. 2020 Jan 31;8:23.
- [234] Garajová I, Giovannetti E, Biasco G, Peters GJ. c-Met as a Target for Personalized Therapy. *Transl Oncogenomics*. 2015 Nov 23;7(Suppl 1):13-31.
- [235] Parikh RA, Wang P, Beumer JH, Chu E, Appleman LJ. The potential roles of hepatocyte growth factor (HGF)-MET pathway inhibitors in cancer treatment. *Onco Targets Ther*. 2014 Jun 11;7:969-983.
- [236] Joosten SPJ, Zeilstra J, van Andel H, Mijns RC, Zaunbrecher J, Duivenvoorden AAM, van de Wetering M, Clevers H, Spaargaren M, Pals ST. MET Signaling Mediates Intestinal Crypt-Villus Development, Regeneration, and Adenoma Formation and Is Promoted by Stem Cell CD44 Isoforms. *Gastroenterology*. 2017 Oct;153(4):1040-1053.e4.
- [237] Raghav K, Morris V, Tang C, Morelli P, Amin HM, Chen K, Manyam GC, Broom B, Overman MJ, Shaw K, Meric-Bernstam F, Maru D, Menter D, Ellis LM, Eng C, Hong D, Kopetz S. MET amplification in metastatic colorectal cancer: an acquired response to EGFR inhibition, not a de novo phenomenon. *Oncotarget*. 2016 Aug 23;7(34):54627-54631.
- [238] White E. The role for autophagy in cancer. *J Clin Invest*. 2015 Jan;125(1):42-46.
- [239] Dutta D, Chakraborty B, Sarkar A, Chowdhury C, Das P. A potent betulinic acid analogue ascertains an antagonistic mechanism between autophagy and proteasomal degradation pathway in HT-29 cells. *BMC Cancer*. 2016 Jan 16;16:23.
- [240] Lin X, Peng Z, Wang X, Zou J, Chen D, Chen Z, Li Z, Dong B, Gao J, Shen L. Targeting autophagy potentiates antitumor activity of Met-TKIs against Met-amplified gastric cancer. *Cell Death Dis*. 2019 Feb 13;10(2):139.

- [241] Huang X, Gan G, Wang X, Xu T, Xie W. The HGF-MET axis coordinates liver cancer metabolism and autophagy for chemotherapeutic resistance. *Autophagy*. 2019 Jul;15(7):1258-1279.
- [242] Liu Y, Liu JH, Chai K, Tashiro S, Onodera S, Ikejima T. Inhibition of c-Met promoted apoptosis, autophagy and loss of the mitochondrial transmembrane potential in oridonin-induced A549 lung cancer cells. *J Pharm Pharmacol*. 2013 Nov;65(11):1622-1642.
- [243] Liu Y, Yu XF, Zou J, Luo ZH. Prognostic value of c-Met in colorectal cancer: a meta-analysis. *World J Gastroenterol*. 2015 Mar 28;21(12):3706-3710.
- [244] Ciuculete DM, Voisin S, Kular L, Welihinda N, Jonsson J, Jagodic M, Mwinyi J, Schiöth HB. Longitudinal DNA methylation changes at MET may alter HGF/c-MET signalling in adolescents at risk for depression. *Epigenetics*. 2020 Jun-Jul;15(6-7):646-663.
- [245] Ueki R, Uchida S, Kanda N, Yamada N, Ueki A, Akiyama M, Toh K, Cabral H, Sando S. A chemically unmodified agonistic DNA with growth factor functionality for in vivo therapeutic application. *Sci Adv*. 2020 Apr 1;6(14):eaay2801.
- [246] Dutta D, Chakraborty A, Mukherjee B, Gupta S. Aptamer-Conjugated Apigenin Nanoparticles To Target Colorectal Carcinoma: A Promising Safe Alternative of Colorectal Cancer Chemotherapy. *ACS Appl Bio Mater*. 2018 Nov 19;1(5):1538-1556.
- [247] Saito T, Tomida M. Generation of inhibitory DNA aptamers against human hepatocyte growth factor. *DNA Cell Biol*. 2005 Oct;24(10):624-633.
- [248] Bohusné Barta B, Simon Á, Nagy L, Dankó T, Raffay RE, Petővári G, Zsiros V, Sebestyén A, Sipos F, Múzes G. Survival of HT29 cancer cells is influenced by hepatocyte growth factor receptor inhibition through modulation of self-DNA-triggered TLR9-dependent autophagy response. *PLoS One*. 2022 May 12;17(5):e0268217.
- [249] Girnita L, Worrall C, Takahashi S, Seregard S, Girnita A. Something old, something new and something borrowed: emerging paradigm of insulin-like growth factor type 1 receptor (IGF-1R) signaling regulation. *Cell Mol Life Sci*. 2014 Jul;71(13):2403-27.

- [250] Chen PC, Kuo YC, Chuong CM, Huang YH. Niche Modulation of IGF-1R Signaling: Its Role in Stem Cell Pluripotency, Cancer Reprogramming, and Therapeutic Applications. *Front Cell Dev Biol.* 2021 Jan 12;8:625943.
- [251] Wit JM, Walenkamp MJ. Role of insulin-like growth factors in growth, development and feeding. *World Rev Nutr Diet.* 2013;106:60-65.
- [252] Sell C, Rubini M, Rubin R, Liu JP, Efstratiadis A, Baserga R. Simian virus 40 large tumor antigen is unable to transform mouse embryonic fibroblasts lacking type 1 insulin-like growth factor receptor. *Proc Natl Acad Sci U S A.* 1993 Dec 1;90(23):11217-11221.
- [253] Sell C, Dumenil G, Deveaud C, Miura M, Coppola D, DeAngelis T, Rubin R, Efstratiadis A, Baserga R. Effect of a null mutation of the insulin-like growth factor I receptor gene on growth and transformation of mouse embryo fibroblasts. *Mol Cell Biol.* 1994 Jun;14(6):3604-3612.
- [254] Weber MM, Fottner C, Liu SB, Jung MC, Engelhardt D, Baretton GB. Overexpression of the insulin-like growth factor I receptor in human colon carcinomas. *Cancer.* 2002 Nov 15;95(10):2086-2095.
- [255] Hakam A, Yeatman TJ, Lu L, Mora L, Marcet G, Nicosia SV, Karl RC, Coppola D. Expression of insulin-like growth factor-1 receptor in human colorectal cancer. *Hum Pathol.* 1999 Oct;30(10):1128-1133.
- [256] Mitsiades CS, Mitsiades NS, McMullan CJ, Poulaki V, Shringarpure R, Akiyama M, Hideshima T, Chauhan D, Joseph M, Libermann TA, García-Echeverría C, Pearson MA, Hofmann F, Anderson KC, Kung AL. Inhibition of the insulin-like growth factor receptor-1 tyrosine kinase activity as a therapeutic strategy for multiple myeloma, other hematologic malignancies, and solid tumors. *Cancer Cell.* 2004 Mar;5(3):221-230.
- [257] Ge RT, Mo LH, Wu R, Liu JQ, Zhang HP, Liu Z, Liu Z, Yang PC. Insulin-like growth factor-1 endues monocytes with immune suppressive ability to inhibit inflammation in the intestine. *Sci Rep.* 2015 Jan 15;5:7735.
- [258] Hofmann C, Dunger N, Doser K, Lippert E, Siller S, Edinger M, Falk W, Obermeier F. Physiologic TLR9-CpG-DNA interaction is essential for the homeostasis of the intestinal immune system. *Inflamm Bowel Dis.* 2014 Jan;20(1):136-43.

- [259] Sipos F, Galamb O, Herszényi L, Molnár B, Solymosi N, Zágoni T, Berczi L, Tulassay Z. Elevated insulin-like growth factor 1 receptor, hepatocyte growth factor receptor and telomerase protein expression in mild ulcerative colitis. *Scand J Gastroenterol.* 2008 Mar;43(3):289-298.
- [260] Kawanishi S, Ohnishi S, Ma N, Hiraku Y, Murata M. Crosstalk between DNA Damage and Inflammation in the Multiple Steps of Carcinogenesis. *Int J Mol Sci.* 2017 Aug 19;18(8):1808.
- [261] Hagiwara A, Nishiyama M, Ishizaki S. Branched-chain amino acids prevent insulin-induced hepatic tumor cell proliferation by inducing apoptosis through mTORC1 and mTORC2-dependent mechanisms. *J Cell Physiol.* 2012 May;227(5):2097-2105.
- [262] Durai R, Yang W, Gupta S, Seifalian AM, Winslet MC. The role of the insulin-like growth factor system in colorectal cancer: review of current knowledge. *Int J Colorectal Dis.* 2005 May;20(3):203-220.
- [263] Sipos F, Székely H, Kis ID, Tulassay Z, Múzes G. Relation of the IGF/IGF1R system to autophagy in colitis and colorectal cancer. *World J Gastroenterol.* 2017 Dec 14;23(46):8109-8119.
- [264] Wu Q, Tian AL, Kroemer G, Kepp O. Autophagy induction by IGF1R inhibition with picropodophyllin and linsitinib. *Autophagy.* 2021 Aug;17(8):2046-2047.
- [265] Wu Q, Tian AL, Li B, Leduc M, Forveille S, Hamley P, Galloway W, Xie W, Liu P, Zhao L, Zhang S, Hui P, Madeo F, Tu Y, Kepp O, Kroemer G. IGF1 receptor inhibition amplifies the effects of cancer drugs by autophagy and immune-dependent mechanisms. *J Immunother Cancer.* 2021 Jun;9(6):e002722.
- [266] Renna M, Bento CF, Fleming A, Menzies FM, Siddiqi FH, Ravikumar B, Puri C, Garcia-Arencibia M, Sadiq O, Corrochano S, Carter S, Brown SD, Acevedo-Arozena A, Rubinsztein DC. IGF-1 receptor antagonism inhibits autophagy. *Hum Mol Genet.* 2013 Nov 15;22(22):4528-4544.
- [267] Wu W, Ma J, Shao N, Shi Y, Liu R, Li W, Lin Y, Wang S. Co-Targeting IGF-1R and Autophagy Enhances the Effects of Cell Growth Suppression and Apoptosis Induced by the IGF-1R Inhibitor NVP-AEW541 in Triple-Negative Breast Cancer Cells. *PLoS One.* 2017 Jan 3;12(1):e0169229.

- [268] Rubinsztein DC, Codogno P, Levine B. Autophagy modulation as a potential therapeutic target for diverse diseases. *Nat Rev Drug Discov*. 2012 Sep;11(9):709-730.
- [269] Wang RC, Wei Y, An Z, Zou Z, Xiao G, Bhagat G, White M, Reichelt J, Levine B. Akt-mediated regulation of autophagy and tumorigenesis through Beclin 1 phosphorylation. *Science*. 2012 Nov 16;338(6109):956-959.
- [270] Choi AM, Ryter SW, Levine B. Autophagy in human health and disease. *N Engl J Med*. 2013 Feb 14;368(7):651-662.
- [271] Eskelinen EL, Prescott AR, Cooper J, Brachmann SM, Wang L, Tang X, Backer JM, Lucocq JM. Inhibition of autophagy in mitotic animal cells. *Traffic*. 2002 Dec;3(12):878-893.
- [272] Liu JJ, Nilsson A, Oredsson S, Badmaev V, Zhao WZ, Duan RD. Boswellic acids trigger apoptosis via a pathway dependent on caspase-8 activation but independent on Fas/Fas ligand interaction in colon cancer HT-29 cells. *Carcinogenesis*. 2002 Dec;23(12):2087-2093.
- [273] Liu JJ, Huang B, Hooi SC. Acetyl-keto-beta-boswellic acid inhibits cellular proliferation through a p21-dependent pathway in colon cancer cells. *Br J Pharmacol*. 2006 Aug;148(8):1099-1107.
- [274] Takahashi M, Sung B, Shen Y, Hur K, Link A, Boland CR, Aggarwal BB, Goel A. Boswellic acid exerts antitumor effects in colorectal cancer cells by modulating expression of the let-7 and miR-200 microRNA family. *Carcinogenesis*. 2012 Dec;33(12):2441-2449.
- [275] Pathania AS, Guru SK, Kumar S, Kumar A, Ahmad M, Bhushan S, Sharma PR, Mahajan P, Shah BA, Sharma S, Nargotra A, Vishwakarma R, Korkaya H, Malik F. Interplay between cell cycle and autophagy induced by boswellic acid analog. *Sci Rep*. 2016 Sep 29;6:33146.
- [276] Sipos F, Bohusné Barta B, Simon Á, Nagy L, Dankó T, Raffay RE, Petővári G, Zsiros V, Wichmann B, Sebestyén A, Múzes G. Survival of HT29 Cancer Cells Is Affected by IGF1R Inhibition *via* Modulation of Self-DNA-Triggered TLR9 Signaling and the Autophagy Response. *Pathol Oncol Res*. 2022 May 16;28:1610322.

- [277] Wang C, Ji L, Yuan X, Jin Y, Cardona CJ, Xing Z. Differential Regulation of TLR Signaling on the Induction of Antiviral Interferons in Human Intestinal Epithelial Cells Infected with Enterovirus 71. *PLoS One*. 2016 Mar 23;11(3):e0152177.
- [278] Takeuchi H, Bilchik A, Saha S, Turner R, Wiese D, Tanaka M, Kuo C, Wang HJ, Hoon DS. c-MET expression level in primary colon cancer: a predictor of tumor invasion and lymph node metastases. *Clin Cancer Res*. 2003 Apr;9(4):1480-1488.
- [279] Bell ES, Coelho PP, Ratcliffe CDH, Rajadurai CV, Peschard P, Vaillancourt R, Zuo D, Park M. LC3C-Mediated Autophagy Selectively Regulates the Met RTK and HGF-Stimulated Migration and Invasion. *Cell Rep*. 2019 Dec 17;29(12):4053-4068.e6.
- [280] Lampada A, O'Prey J, Szabadkai G, Ryan KM, Hochhauser D, Salomoni P. mTORC1-independent autophagy regulates receptor tyrosine kinase phosphorylation in colorectal cancer cells via an mTORC2-mediated mechanism. *Cell Death Differ*. 2017 Jun;24(6):1045-1062.
- [281] Li Y, Lu K, Zhao B, Zeng X, Xu S, Ma X, Zhi Y. Depletion of insulin-like growth factor 1 receptor increases radiosensitivity in colorectal cancer. *J Gastrointest Oncol*. 2020 Dec;11(6):1135-1145.
- [282] Buck E, Gokhale PC, Koujak S, Brown E, Eyzaguirre A, Tao N, Rosenfeld-Franklin M, Lerner L, Chiu MI, Wild R, Epstein D, Pachter JA, Miglarese MR. Compensatory insulin receptor (IR) activation on inhibition of insulin-like growth factor-1 receptor (IGF-1R): rationale for cotargeting IGF-1R and IR in cancer. *Mol Cancer Ther*. 2010 Oct;9(10):2652-2664.
- [283] Nowakowska M, Pospiech K, Lewandowska U, Piastowska-Ciesielska AW, Bednarek AK. Diverse effect of WWOX overexpression in HT29 and SW480 colon cancer cell lines. *Tumour Biol*. 2014 Sep;35(9):9291-9301.
- [284] Ogoshi K, Hashimoto S, Nakatani Y, Qu W, Oshima K, Tokunaga K, Sugano S, Hattori M, Morishita S, Matsushima K. Genome-wide profiling of DNA methylation in human cancer cells. *Genomics*. 2011 Oct;98(4):280-287.
- [285] Rampersad SN. Multiple applications of Alamar Blue as an indicator of metabolic function and cellular health in cell viability bioassays. *Sensors (Basel)*. 2012;12(9):12347-12360.

- [286] R: A language and environment for statistical computing. R Foundation for Statistical Computing, Vienna, Austria. Available from: <https://www.R-project.org/>
- [287] Mansour H. Cell-free nucleic acids as noninvasive biomarkers for colorectal cancer detection. *Front Genet.* 2014 Aug 27;5:182.
- [288] Kubiritova Z, Radvanszky J, Gardlik R. Cell-Free Nucleic Acids and their Emerging Role in the Pathogenesis and Clinical Management of Inflammatory Bowel Disease. *Int J Mol Sci.* 2019 Jul 26;20(15):3662.
- [289] Butt AN, Swaminathan R. Overview of circulating nucleic acids in plasma/serum. *Ann N Y Acad Sci.* 2008 Aug;1137:236-242.
- [290] Gormally E, Caboux E, Vineis P, Hainaut P. Circulating free DNA in plasma or serum as biomarker of carcinogenesis: practical aspects and biological significance. *Mutat Res.* 2007 May-Jun;635(2-3):105-117.
- [291] Rauh P, Rickes S, Fleischhacker M. Microsatellite alterations in free-circulating serum DNA in patients with ulcerative colitis. *Dig Dis.* 2003;21(4):363-366.
- [292] Gosu V, Basith S, Kwon OP, Choi S. Therapeutic applications of nucleic acids and their analogues in Toll-like receptor signaling. *Molecules.* 2012 Nov 14;17(11):13503-13529.
- [293] Sipos F, Kiss AL, Constantinovits M, Tulassay Z, Múzes G. Modified Genomic Self-DNA Influences In Vitro Survival of HT29 Tumor Cells via TLR9- and Autophagy Signaling. *Pathol Oncol Res.* 2019 Oct;25(4):1505-1517.
- [294] Akhtar M, Watson JL, Nazli A, McKay DM. Bacterial DNA evokes epithelial IL-8 production by a MAPK-dependent, NF-kappaB-independent pathway. *FASEB J.* 2003 Jul;17(10):1319-1321.
- [295] Colell A, Ricci JE, Tait S, Milasta S, Maurer U, Bouchier-Hayes L, Fitzgerald P, Guio-Carrion A, Waterhouse NJ, Li CW, Mari B, Barbry P, Newmeyer DD, Beere HM, Green DR. GAPDH and autophagy preserve survival after apoptotic cytochrome c release in the absence of caspase activation. *Cell.* 2007 Jun 1;129(5):983-997.

- [296] Djavaheri-Mergny M, Amelotti M, Mathieu J, Besançon F, Bauvy C, Souquère S, Pierron G, Codogno P. NF-kappaB activation represses tumor necrosis factor-alpha-induced autophagy. *J Biol Chem*. 2006 Oct 13;281(41):30373-30382.
- [297] Lemasters JJ. Selective mitochondrial autophagy, or mitophagy, as a targeted defense against oxidative stress, mitochondrial dysfunction, and aging. *Rejuvenation Res*. 2005 Spring;8(1):3-5.
- [298] Shahriari S, Rezaeifard S, Moghimi HR, Khorramizadeh MR, Faghieh Z. Cell membrane and intracellular expression of toll-like receptor 9 (TLR9) in colorectal cancer and breast cancer cell-lines. *Cancer Biomark*. 2017;18(4):375-380.
- [299] Sun H, Li X, Fan L, Wu G, Li M, Fang J. TRAF6 is upregulated in colon cancer and promotes proliferation of colon cancer cells. *Int J Biochem Cell Biol*. 2014 Aug;53:195-201.
- [300] Marcuello M, Mayol X, Felipe-Fumero E, Costa J, López-Hierro L, Salvans S, Alonso S, Pascual M, Grande L, Pera M. Modulation of the colon cancer cell phenotype by pro-inflammatory macrophages: A preclinical model of surgery-associated inflammation and tumor recurrence. *PLoS One*. 2018 Feb 20;13(2):e0192958.
- [301] Ning Y, Manegold PC, Hong YK, Zhang W, Pohl A, Lurje G, Winder T, Yang D, LaBonte MJ, Wilson PM, Ladner RD, Lenz HJ. Interleukin-8 is associated with proliferation, migration, angiogenesis and chemosensitivity in vitro and in vivo in colon cancer cell line models. *Int J Cancer*. 2011 May 1;128(9):2038-2049.
- [302] Liu H, Li G, Zhang B, Sun D, Wu J, Chen F, Kong F, Luan Y, Jiang W, Wang R, Xue X. Suppression of the NF-κB signaling pathway in colon cancer cells by the natural compound Riccardin D from *Dumortierahirsute*. *Mol Med Rep*. 2018 Apr;17(4):5837-5843.
- [303] Yang F, Gao JY, Chen H, Du ZH, Zhang XQ, Gao W. Targeted inhibition of the phosphoinositide 3-kinase impairs cell proliferation, survival, and invasion in colon cancer. *Onco Targets Ther*. 2017 Sep 11;10:4413-4422.
- [304] Fritsche-Guenther R, Zasada C, Mastrobuoni G, Royle N, Rainer R, Roßner F, Pietzke M, Klipp E, Sers C, Kempa S. Alterations of mTOR signaling impact metabolic

stress resistance in colorectal carcinomas with BRAF and KRAS mutations. *Sci Rep*. 2018 Jun 15;8(1):9204.

[305] Koehler BC, Scherr AL, Lorenz S, Urbanik T, Kautz N, Elssner C, Welte S, Bermejo JL, Jäger D, Schulze-Bergkamen H. Beyond cell death - antiapoptotic Bcl-2 proteins regulate migration and invasion of colorectal cancer cells in vitro. *PLoS One*. 2013 Oct 3;8(10):e76446.

[306] Yang SY, Miah A, Sales KM, Fuller B, Seifalian AM, Winslet M. Inhibition of the p38 MAPK pathway sensitises human colon cancer cells to 5-fluorouracil treatment. *Int J Oncol*. 2011 Jun;38(6):1695-1702.

[307] Kim HJ, Kim SK, Kim BS, Lee SH, Park YS, Park BK, Kim SJ, Kim J, Choi C, Kim JS, Cho SD, Jung JW, Roh KH, Kang KS, Jung JY. Apoptotic effect of quercetin on HT-29 colon cancer cells via the AMPK signaling pathway. *J Agric Food Chem*. 2010 Aug 11;58(15):8643-8650.

[308] Kim L, Butcher BA, Lee CW, Uematsu S, Akira S, Denkers EY. *Toxoplasma gondii* genotype determines MyD88-dependent signaling in infected macrophages. *J Immunol*. 2006 Aug 15;177(4):2584-2591.

[309] Kfoury A, Le Corf K, El Sabeih R, Journeaux A, Badran B, Hussein N, Lebecque S, Manié S, Renno T, Coste I. MyD88 in DNA repair and cancer cell resistance to genotoxic drugs. *J Natl Cancer Inst*. 2013 Jul 3;105(13):937-46. doi: 10.1093/jnci/djt120. Epub 2013 Jun 13.

[310] Ryoo HD, Bergmann A. The role of apoptosis-induced proliferation for regeneration and cancer. *Cold Spring Harb Perspect Biol*. 2012 Aug 1;4(8):a008797.

[311] Parachoniak CA, Park M. Dynamics of receptor trafficking in tumorigenicity. *Trends Cell Biol*. 2012 May;22(5):231-240.

[312] Feng Y, He D, Yao Z, Klionsky DJ. The machinery of macroautophagy. *Cell Res*. 2014 Jan;24(1):24-41.

[313] Lampada A, Hochhauser D, Salomoni P. Autophagy and receptor tyrosine kinase signalling: A mTORC2 matter. *Cell Cycle*. 2017 Oct 18;16(20):1855-1856.

- [314] Barrow-McGee R, Kishi N, Joffre C, Ménard L, Hervieu A, Bakhouché BA, Noval AJ, Mai A, Guzmán C, Robbez-Masson L, Iturrioz X, Hult J, Brennan CH, Hart IR, Parker PJ, Ivaska J, Kermorgant S. Beta 1-integrin-c-Met cooperation reveals an inside-in survival signalling on autophagy-related endomembranes. *Nat Commun*. 2016 Jun 23;7:11942.
- [315] Corvinus FM, Orth C, Moriggl R, Tsareva SA, Wagner S, Pfitzner EB, Baus D, Kaufmann R, Huber LA, Zatloukal K, Beug H, Ohlschläger P, Schütz A, Halbhuber KJ, Friedrich K. Persistent STAT3 activation in colon cancer is associated with enhanced cell proliferation and tumor growth. *Neoplasia*. 2005 Jun;7(6):545-555.
- [316] Zhao S, Gao N, Qi H, Chi H, Liu B, He B, Wang J, Jin Z, He X, Zheng H, Wang Z, Wang X, Jin G. Suppressive effects of sunitinib on a TLR activation-induced cytokine storm. *Eur J Pharmacol*. 2019 Jul 5;854:347-353.
- [317] Suman S, Das TP, Reddy R, Nyakeriga AM, Luevano JE, Konwar D, Pahari P, Damodaran C. The pro-apoptotic role of autophagy in breast cancer. *Br J Cancer*. 2014 Jul 15;111(2):309-317.
- [318] Yu F, Ma R, Liu C, Zhang L, Feng K, Wang M, Yin D. SQSTM1/p62 Promotes Cell Growth and Triggers Autophagy in Papillary Thyroid Cancer by Regulating the AKT/AMPK/mTOR Signaling Pathway. *Front Oncol*. 2021 Apr 15;11:638701.
- [319] Niklaus M, Adams O, Berezowska S, Zlobec I, Graber F, Slotta-Huspenina J, Nitsche U, Rosenberg R, Tschan MP, Langer R. Expression analysis of LC3B and p62 indicates intact activated autophagy is associated with an unfavorable prognosis in colon cancer. *Oncotarget*. 2017 May 2;8(33):54604-54615.
- [320] Chen X, Clark J, Wunderlich M, Fan C, Davis A, Chen S, Guan JL, Mulloy JC, Kumar A, Zheng Y. Autophagy is dispensable for Kmt2a/Mll-Mllt3/Af9 AML maintenance and anti-leukemic effect of chloroquine. *Autophagy*. 2017 May 4;13(5):955-966.
- [321] Zheng XY, Li LJ, Li W, Jiang PF, Shen HQ, Chen YH, Chen X. Low concentrations of chloroquine and 3-methyladenine suppress the viability of retinoblastoma cells synergistically with vincristine independent of autophagy inhibition. *Graefes Arch Clin Exp Ophthalmol*. 2015 Dec;253(12):2309-2315.

- [322] Stamenkovic M, Janjetovic K, Paunovic V, Ciric D, Kravic-Stevovic T, Trajkovic V. Comparative analysis of cell death mechanisms induced by lysosomal autophagy inhibitors. *Eur J Pharmacol*. 2019 Sep 15;859:172540.
- [323] Humbert M, Medová M, Aebersold DM, Blaukat A, Bladt F, Fey MF, Zimmer Y, Tschan MP. Protective autophagy is involved in resistance towards MET inhibitors in human gastric adenocarcinoma cells. *Biochem Biophys Res Commun*. 2013 Feb 8;431(2):264-269.
- [324] Qu X, Yu J, Bhagat G, Furuya N, Hibshoosh H, Troxel A, Rosen J, Eskelinen EL, Mizushima N, Ohsumi Y, Cattoretti G, Levine B. Promotion of tumorigenesis by heterozygous disruption of the beclin 1 autophagy gene. *J Clin Invest*. 2003 Dec;112(12):1809-1820.
- [325] Fimia GM, Stoykova A, Romagnoli A, Giunta L, Di Bartolomeo S, Nardacci R, Corazzari M, Fuoco C, Ucar A, Schwartz P, Gruss P, Piacentini M, Chowdhury K, Cecconi F. Ambra1 regulates autophagy and development of the nervous system. *Nature*. 2007 Jun 28;447(7148):1121-1125.
- [326] Wang RC, Levine B. Autophagy in cellular growth control. *FEBS Lett*. 2010 Apr 2;584(7):1417-1426.
- [327] Trumpi K, Steller EJ, de Leng WW, Raats DA, Nijman IJ, Morsink FH, Borel Rinkes IH, Kranenburg O. Mice lacking functional CD95-ligand display reduced proliferation of the intestinal epithelium without gross homeostatic alterations. *Med Mol Morphol*. 2016 Jun;49(2):110-118.
- [328] Luppi F, Longo AM, de Boer WI, Rabe KF, Hiemstra PS. Interleukin-8 stimulates cell proliferation in non-small cell lung cancer through epidermal growth factor receptor transactivation. *Lung Cancer*. 2007 Apr;56(1):25-33.
- [329] Valcz G, Buzás EI, Kittel Á, Krenács T, Visnovitz T, Spisák S, Török G, Homolya L, Zsigrai S, Kiszler G, Antalffy G, Pálóczi K, Szállási Z, Szabó V, Sebestyén A, Solymosi N, Kalmár A, Dede K, Lőrincz P, Tulassay Z, Igaz P, Molnár B. *En bloc* release of MVB-like small extracellular vesicle clusters by colorectal carcinoma cells. *J Extracell Vesicles*. 2019 Apr 8;8(1):1596668.

- [330] Fader CM, Colombo MI. Autophagy and multivesicular bodies: two closely related partners. *Cell Death Differ.* 2009 Jan;16(1):70-78.
- [331] Berg TO, Fengsrud M, Strømhaug PE, Berg T, Seglen PO. Isolation and characterization of rat liver amphisomes. Evidence for fusion of autophagosomes with both early and late endosomes. *J Biol Chem.* 1998 Aug 21;273(34):21883-21892.
- [332] Eskelinen EL. Maturation of autophagic vacuoles in Mammalian cells. *Autophagy.* 2005 Apr;1(1):1-10.
- [333] Xu J, Camfield R, Gorski SM. The interplay between exosomes and autophagy - partners in crime. *J Cell Sci.* 2018 Aug 3;131(15):jcs215210.
- [334] Souza AG, Bastos VAF, Fujimura PT, Ferreira ICC, Leal LF, da Silva LS, Laus AC, Reis RM, Martins MM, Santos PS, Corrêa NCR, Marangoni K, Thomé CH, Colli LM, Goulart LR, Goulart VA. Cell-free DNA promotes malignant transformation in non-tumor cells. *Sci Rep.* 2020 Dec 10;10(1):21674.
- [335] Zhou J, Rossi J. Aptamers as targeted therapeutics: current potential and challenges. *Nat Rev Drug Discov.* 2017 Mar;16(3):181-202.
- [336] Li X, Jiang S, Tapping RI. Toll-like receptor signaling in cell proliferation and survival. *Cytokine.* 2010 Jan;49(1):1-9.
- [337] Chand HS, Harris JF, Mebratu Y, Chen Y, Wright PS, Randell SH, Tesfaigzi Y. Intracellular insulin-like growth factor-1 induces Bcl-2 expression in airway epithelial cells. *J Immunol.* 2012 May 1;188(9):4581-4589.
- [338] Veleparambil M, Poddar D, Abdulkhalek S, Kessler PM, Yamashita M, Chattopadhyay S, Sen GC. Constitutively Bound EGFR-Mediated Tyrosine Phosphorylation of TLR9 Is Required for Its Ability To Signal. *J Immunol.* 2018 Apr 15;200(8):2809-2818.
- [339] Zhao ZQ, Yu ZY, Li J, Ouyang XN. Gefitinib induces lung cancer cell autophagy and apoptosis via blockade of the PI3K/AKT/mTOR pathway. *Oncol Lett.* 2016 Jul;12(1):63-68.

- [340] Wang H, Liu Y, Wang D, Xu Y, Dong R, Yang Y, Lv Q, Chen X, Zhang Z. The Upstream Pathway of mTOR-Mediated Autophagy in Liver Diseases. *Cells*. 2019 Dec 9;8(12):1597.
- [341] Le Roith D, Zick Y. Recent advances in our understanding of insulin action and insulin resistance. *Diabetes Care*. 2001 Mar;24(3):588-597.
- [342] Cheng Z, Tseng Y, White MF. Insulin signaling meets mitochondria in metabolism. *Trends Endocrinol Metab*. 2010 Oct;21(10):589-598.
- [343] Ning J, Xi G, Clemmons DR. Suppression of AMPK activation via S485 phosphorylation by IGF-I during hyperglycemia is mediated by AKT activation in vascular smooth muscle cells. *Endocrinology*. 2011 Aug;152(8):3143-3154.
- [344] De Leo MG, Staiano L, Vicinanza M, Luciani A, Carissimo A, Mutarelli M, Di Campli A, Polishchuk E, Di Tullio G, Morra V, Levchenko E, Oltrabella F, Starborg T, Santoro M, Di Bernardo D, Devuyst O, Lowe M, Medina DL, Ballabio A, De Matteis MA. Autophagosome-lysosome fusion triggers a lysosomal response mediated by TLR9 and controlled by OCRL. *Nat Cell Biol*. 2016 Aug;18(8):839-850.
- [345] Liu L, Han C, Yu H, Zhu W, Cui H, Zheng L, Zhang C, Yue L. Chloroquine inhibits cell growth in human A549 lung cancer cells by blocking autophagy and inducing mitochondrial-mediated apoptosis. *Oncol Rep*. 2018 Jun;39(6):2807-2816.
- [346] Ngo MT, Jeng HY, Kuo YC, Diony Nanda J, Brahmadi A, Ling TY, Chang TS, Huang YH. The Role of IGF/IGF-1R Signaling in Hepatocellular Carcinomas: Stemness-Related Properties and Drug Resistance. *Int J Mol Sci*. 2021 Feb 16;22(4):1931.
- [347] Wang XH, Wu HY, Gao J, Wang XH, Gao TH, Zhang SF. IGF1R facilitates epithelial-mesenchymal transition and cancer stem cell properties in neuroblastoma via the STAT3/AKT axis. *Cancer Manag Res*. 2019 Jun 12;11:5459-5472.
- [348] Singh RK, Dhadve A, Sakpal A, De A, Ray P. An active IGF-1R-AKT signaling imparts functional heterogeneity in ovarian CSC population. *Sci Rep*. 2016 Nov 7;6:36612.
- [349] Xue F, Hu L, Ge R, Yang L, Liu K, Li Y, Sun Y, Wang K. Autophagy-deficiency in hepatic progenitor cells leads to the defects of stemness and enhances susceptibility to neoplastic transformation. *Cancer Lett*. 2016 Feb 1;371(1):38-47.

- [350] Kantara C, O'Connell M, Sarkar S, Moya S, Ullrich R, Singh P. Curcumin promotes autophagic survival of a subset of colon cancer stem cells, which are ablated by DCLK1-siRNA. *Cancer Res.* 2014 May 1;74(9):2487-2498.
- [351] Nazio F, Bordi M, Cianfanelli V, Locatelli F, Cecconi F. Autophagy and cancer stem cells: molecular mechanisms and therapeutic applications. *Cell Death Differ.* 2019 Mar;26(4):690-702.
- [352] Wollert T, Hurley JH. Molecular mechanism of multivesicular body biogenesis by ESCRT complexes. *Nature.* 2010 Apr 8;464(7290):864-869.
- [353] DeRita RM, Zerlanko B, Singh A, Lu H, Iozzo RV, Benovic JL, Languino LR. c-Src, Insulin-Like Growth Factor I Receptor, G-Protein-Coupled Receptor Kinases and Focal Adhesion Kinase are Enriched Into Prostate Cancer Cell Exosomes. *J Cell Biochem.* 2017 Jan;118(1):66-73.
- [354] Crudden C, Song D, Cismas S, Trocmé E, Pasca S, Calin GA, Girnita A, Girnita L. Below the Surface: IGF-1R Therapeutic Targeting and Its Endocytic Journey. *Cells.* 2019 Oct 9;8(10):1223.

9. BIBLIOGRAPHY OF THE CANDIDATE'S PUBLICATIONS

Cumulative IF: 16.5

Publications / abstracts related to PhD dissertation (subtotal IF: 11.2)

1. **Bohusné Barta Bettina**, Simon Ágnes, Nagy Lőrinc, Dankó Titanilla, Raffay Regina Eszter, Petővári Gábor, Zsiros Viktória, Sebestyén Anna, Sipos Ferenc, Múzes Györgyi. Survival of HT29 cancer cells is influenced by hepatocyte growth factor receptor inhibition through modulation of self-DNA-triggered TLR9-dependent autophagy response. PLOS ONE 2022; 17(5): e0268217. IF: 3.7 (Q1)

2. Sipos Ferenc / **Bohusné Barta Bettina**, Simon Ágnes, Nagy Lőrinc, Dankó Titanilla, Raffay Regina Eszter, Petővári Gábor, Zsiros Viktória, Wichmann Barnabás, Sebestyén Anna, Múzes Györgyi. Survival of HT29 cancer cells is affected by IGF1R inhibition via modulation of self-DNA-triggered TLR9 signaling and the autophagy response. PATHOLOGY AND ONCOLOGY RESEARCH 2022; 28: 1610322. IF: 2.8 (Q2)

3. Múzes Györgyi, **Bohusné Barta Bettina**, Szabó Orsolya, Horgas Vanessza, Sipos Ferenc. Cell-Free DNA in the Pathogenesis and Therapy of Non-Infectious Inflammations and Tumors. BIOMEDICINES 2022; 10(11): 2853. IF: 4.7 (Q1)

4. Sipos Ferenc, **Bohusné Barta Bettina**, Dankó Titanilla, Sebestyén Anna, Zsiros Viktória, Múzes Györgyi. Relation of IGF1R inhibition to TLR9- and autophagy signaling in HT29 cancer cells. ALLERGY: EUROPEAN JOURNAL OF ALLERGY AND CLINICAL IMMUNOLOGY 2023; 78(S111): 281.

5. Sipos Ferenc, Nagy Lőrinc, **Barta Bettina**, Simon Ágnes, Dankó Titanilla, Sebestyén Anna, L. Kiss Anna, Múzes Györgyi. Modulation of TLR9-dependent autophagy response via inhibition of c-Met signaling influences the survival of HT29 cancer cells. ANNALS OF ONCOLOGY 2019; 30(Suppl.5): 807.

6. Nagy Lőrinc, **Barta Bettina**, Simon Ágnes, Sebestyén Anna, Dankó Titanilla, Raffay Regina, Múzes Györgyi, Sipos Ferenc. Structurally modified forms of genomic self-DNA influence appreciably in vitro HT29 cancer cell survival through TLR9-signaling and modulation of autophagic response. In: 9th Lower Saxony International Summer Academy (LISA) in Immunology - Abstract Book 2019; p. e58.

Additional papers / abstracts not related to the PhD thesis (subtotal IF: 5.3)

1. Múzes Györgyi, **Bohusné Barta Bettina**, Sipos Ferenc. Colitis and Colorectal Carcinogenesis: The Focus on Isolated Lymphoid Follicles. BIOMEDICINES 2022; 10(2): 226. IF: 4.7 (Q1)

2. **Bohusné Barta Bettina**; Sipos Ferenc, Múzes Györgyi. Az intestinalis bojtos sejtek sajátosságai és szerepük a gyulladásos bélbetegség és a colorectalis carcinoma patomechanizmusában. ORVOSI HETILAP 2023; 164(44): 1727-1735. IF: 0.6 (Q4)

10. ACKNOWLEDGEMENTS

I would like to thank everyone for their help and support in my research work.

I owe my gratitude and thanks to my supervisor, Ferenc Sipos, MD, PhD, Senior Lecturer, who coordinated the research work, the writing of the articles, and the dissertation with infinite patience and without sparing any time or expertise.

I would like to express my sincere respect and gratitude to my professional consultant, Györgyi Múzes, MD, CSc, med. habil., Associate Professor, for her many professional contributions, precious guidance, and proofreading of my dissertation.

I would also like to thank the staff of the Department of Pathology and Experimental Cancer Research of Semmelweis University, especially Anna Sebestyén, DSc, Research Professor and the members of the Tumor Biology Working Group - Titanilla Dankó, PhD, Gábor Petővári PhD, Regina Raffay, and Dániel Sztankovics - for their professional and technical support, and for their time spent on my development.

In addition, I thank the staff of the Cell and Molecular Biology Laboratory of the Institute of Anatomy, Tissue and Developmental Biology, especially Anna L. Kiss, DSc and Viktória Zsiros, PhD, for their help with the electron microscopy. I thank Gabriella Farkasné Kónya, for her help with the immunocytochemical analyses and Barnabás Wichmann, PhD, for his assistance with the statistical analyses.

I owe my eternal gratitude to my friends, colleagues and family, especially to my mother, Erika Rohály, who has always kept me going as an eternal optimist and to my wonderful husband, Zoltán Bohus, who has supported me throughout the most difficult times to make my dreams come true.

Last but not least, I would like to thank András Matolcsy, MD, DSc, Head of the Institute, for the opportunity to conduct my research at the Institute of Pathology and Experimental Cancer Research, Semmelweis University.

11. SUPPLEMENTS

SUPPLEMENTARY TABLE 1 | Assayed genes with probe NSIDs in NanoString experiments.

TLR9-signaling and NF- κ B activation: *TLR9* (Toll-like receptor 9; NM_017442.2:985), *MyD88* (Myeloid differentiation factor 88; NM_002468.3:2145), *IRAK2* (Interleukin 1 receptor associated kinase 2; NM_001570.3:1285), *TRAF6* (Tumor necrosis factor receptor associated factor 6; NM_145803.2:745), IL1- β (Interleukin 1 β ; NM_000576.2:840), IL-8 (Interleukin 8; NM_000584.2:25), *NF- κ B* (Nuclear factor- κ B; NM_003998.2:1675).

Extrinsic and intrinsic apoptosis-related genes: *CD95* (Fas; NM_152876.1:1740), *CD95L* (Fas-ligand; NM_000639.1:625), *Cytochrom-c* (NM_001916.4:344), *Caspase-3* (NM_004346.3:2156), *Caspase-8* (NM_033355), *Caspase-9* (NM_032996).

Anti-apoptotic and autophagy suppressor genes: *PI3KCA* (Phosphoinositide 3-kinase; NM_006218.2:2445), *Akt* (Ak strain transforming; NM_001014432.1:1275), *mTOR* (Mechanistic/mammalian target of rapamycin; NM_004958.3:1865), *Bcl-2* (B-cell lymphoma 2; NM_000657.2:5).

Pro-apoptotic and autophagy activator genes: *MAPK* (Mitogen-activated protein kinase; NM_002755.2:970), *AMPK* (AMP-activated protein kinase; NM_006251.5:366), *Bax* (BCL2 associated X; NM_138761.3:342).

Autophagy genes: *Beclin-1* (NM_003766.2:810), *ATG16L1* (Autophagy related 16 like 1; NM_017974.3:2405), *MAP1LC3B* (Microtubule-associated proteins 1A/1B light chain 3B; NM_022818.4:1685), *ULK1* (Unc-51 like autophagy activating kinase; NM_003565.1:465), *Ambra-1* (activating molecule in Beclin-1-regulated autophagy; NM_017749).

c-Met/HGFR and c-Met canonical and non-canonical signaling pathways: *HGFR* (NM_001127500.1:1925), *PI3KCA* (see above), *STAT3* (Signal transducer and activator of transcription 3; NM_003150.3:2060), *CD95* (see above).

IGF1R signaling pathway: *IGF1R* (Insulin-like growth factor 1 receptor; NM_000875); *MAPK* (Mitogen-activated protein kinase; NM_002755.2:970); *PI3K* (Phosphoinositide 3-kinase; NM_006218.2:2445); *Akt* (Ak strain transforming; NM_001014432.1:1275).

HT29 cancer cell stemness-related gene: *CD133* (NM_006017).

Housekeeping genes: *Clorf43* (NM_015449.2:477), *CHMP2A* (NM_014453.3:241), *PSMB2* (NM_002794.3:639), *RAB7A* (NM_004637.5:277), *REEP5* (NM_005669.4:280), *SNRPD3* (NM_004175.3:309), *VCP* (NM_007126.2:615), *VPS29* (NM_016226.4:565).

SUPPLEMENTARY TABLE 2 | Standard deviation results of the Taqman fold changes in HGFR studies [248]

The table displays the related standard deviation results (SD) ($p < 0.05$; $n = 3$).

g/f/m: genomic/fragmented/hypermethylated DNA; K: control; O: ODN2088 CpG oligonucleotide; D: DISU; C: chloroquine

SD values	<i>TLR9</i>	<i>mTOR</i>	<i>ATG16L1</i>	<i>LC3B</i>	<i>BECN1</i>	<i>HGFR</i>	<i>PI3KCA</i>	<i>STAT3</i>	<i>CD95</i>
K	0.12	0.23	0.18	0.24	0.29	0.16	0.13	0.22	0.28
Kg	0.13	0.22	0.19	0.34	0.19	0.24	0.19	0.18	0.17
Kf	0.22	0.22	0.25	0.19	0.31	0.21	0.24	0.18	0.25
Km	0.21	0.27	0.28	0.29	0.32	0.28	0.21	0.27	0.28
gO	0.27	0.29	0.29	0.21	0.27	0.21	0.27	0.32	0.29
gD	0.18	0.21	0.24	0.19	0.31	0.19	0.18	0.21	0.24
gC	0.32	0.29	0.32	0.24	0.25	0.22	0.32	0.29	0.32
gOD	0.12	0.23	0.18	0.37	0.29	0.16	0.12	0.23	0.18
gOC	0.19	0.21	0.19	0.34	0.19	0.24	0.29	0.19	0.19
gDC	0.22	0.15	0.25	0.19	0.31	0.21	0.22	0.32	0.23
fO	0.21	0.27	0.28	0.29	0.22	0.28	0.21	0.27	0.28
fD	0.27	0.29	0.29	0.21	0.27	0.21	0.27	0.29	0.29
fC	0.18	0.21	0.24	0.19	0.31	0.19	0.18	0.21	0.24
fOD	0.32	0.29	0.32	0.34	0.25	0.22	0.32	0.29	0.32
fOC	0.12	0.23	0.18	0.24	0.39	0.16	0.12	0.23	0.18
fDC	0.19	0.19	0.19	0.34	0.19	0.24	0.19	0.19	0.19
mO	0.22	0.22	0.25	0.19	0.31	0.21	0.23	0.22	0.25
mD	0.21	0.27	0.28	0.36	0.32	0.28	0.21	0.27	0.28
mC	0.27	0.29	0.29	0.21	0.37	0.29	0.27	0.29	0.19
mOD	0.28	0.31	0.24	0.19	0.31	0.19	0.18	0.24	0.24
mOC	0.32	0.29	0.32	0.24	0.25	0.22	0.32	0.29	0.32
mDC	0.12	0.25	0.18	0.24	0.29	0.16	0.14	0.23	0.18

SUPPLEMENTARY TABLE 3 | Standard deviation results of the Taqman fold changes in IGF1R studies [276]

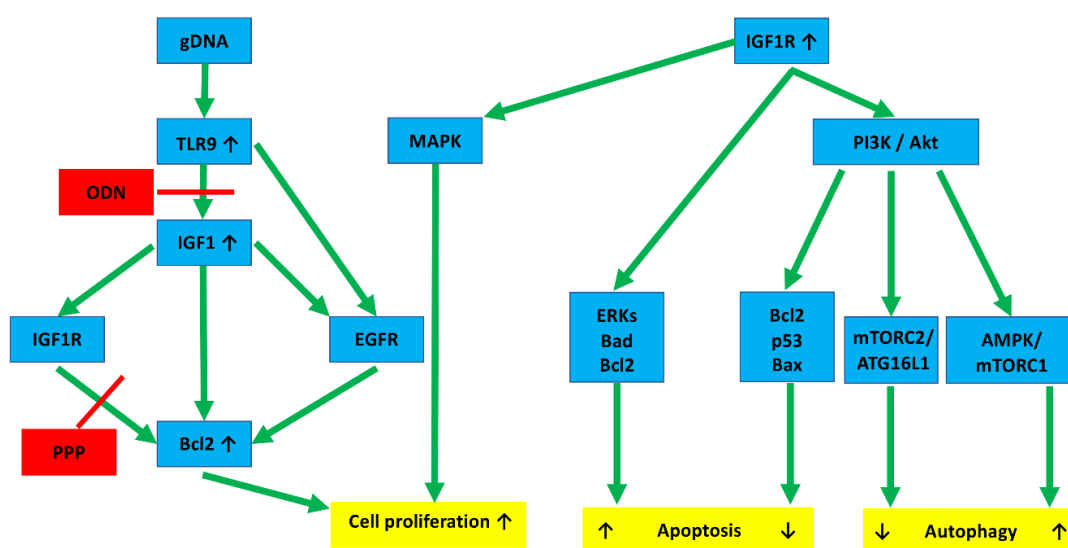
The table indicates the SD values in each case ($p < 0.05$; $n=3$).

g: genomic DNA; K: control; O: ODN2088 CpG oligonucleotide; P: picropodophyllin; C: chloroquine

SD values	<i>mTOR</i>	<i>ATG16L1</i>	<i>LC3B</i>	<i>BECN1</i>	<i>IGF1R</i>	<i>TLR9</i>
K	0.12	0.23	0.18	0.24	0.29	0.16
gOP	0.19	0.19	0.19	0.34	0.19	0.24
gP	0.22	0.22	0.25	0.19	0.31	0.21
Kg	0.21	0.27	0.28	0.29	0.32	0.28
gC	0.27	0.29	0.29	0.21	0.27	0.21
gO	0.18	0.21	0.24	0.19	0.31	0.19
gPC	0.32	0.29	0.32	0.24	0.25	0.22

p adj		p adj		p adj		p adj		p adj		p adj		p adj	
Kg- K 0.0001596	Kg- K 0.0000002	Kg- K 0.0000738	Kg- K 0.0000000	Kg- K 0.7711846	Kg- K 0.9994039	Kg- K 1.0000000	Kg- K 0.9994039	Kg- K 0.0000000	Kg- K 0.0000000	Kg- K 0.0000000	Kg- K 0.0000000	Kg- K 0.0000000	Kg- K 0.0000000
gO- K 0.0000000	gO- K 0.0000000	gO- K 0.0000000	gO- K 0.0000000	gO- K 0.0000000	gO- K 0.0000000	gO- K 0.0000000	gO- K 0.0000000	gO- K 0.0000000	gO- K 0.0000000	gO- K 0.0000000	gO- K 0.0000000	gO- K 0.0000000	gO- K 0.0000000
gP- K 0.0000000	gP- K 0.0000000	gP- K 0.0001267	gP- K 0.0000000	gP- K 0.0000112	gP- K 0.0000000	gP- K 0.0000000	gP- K 0.0000000	gP- K 0.0000000	gP- K 0.0000000	gP- K 0.0000000	gP- K 0.0000000	gP- K 0.0000000	gP- K 0.0000000
gC- K 0.8191770	gC- K 0.0000000	gC- K 0.1011046	gC- K 0.1636749	gC- K 0.0000112	gC- K 0.0000000	gC- K 0.0000000	gC- K 0.0000000	gC- K 0.0000000	gC- K 0.0000000	gC- K 0.0000000	gC- K 0.0000000	gC- K 0.0000000	gC- K 0.0000000
gPC- K 0.8191770	gPC- K 0.7165617	gPC- K 0.1131291	gPC- K 0.0000000	gPC- K 0.9792494	gPC- K 1.0000000	gPC- K 1.0000000	gPC- K 0.9998943	gPC- K 0.0000000	gPC- K 0.0000000	gPC- K 0.0000000	gPC- K 0.0000000	gPC- K 0.0000000	gPC- K 0.0000000
gOP- K 0.0000000	gOP- K 0.0000000	gOP- K 0.0000000	gOP- K 0.0000000	gOP- K 0.0000000	gOP- K 0.0000000	gOP- K 0.0000000	gOP- K 0.0000000	gOP- K 0.0000000	gOP- K 0.0000000	gOP- K 0.0000000	gOP- K 0.0000000	gOP- K 0.0000000	gOP- K 0.0000000
gO- Kg 0.0000000	gO- Kg 0.0000000	gO- Kg 0.0000000	gO- Kg 0.0000000	gO- Kg 0.0000000	gO- Kg 0.0000000	gO- Kg 0.0000000	gO- Kg 0.0000000	gO- Kg 0.0000000	gO- Kg 0.0000000	gO- Kg 0.0000000	gO- Kg 0.0000000	gO- Kg 0.0000000	gO- Kg 0.0000000
gP- Kg 0.9999776	gP- Kg 0.9997711	gP- Kg 0.9999990	gP- Kg 0.9999367	gP- Kg 0.0020509	gP- Kg 0.0020509	gP- Kg 0.0000000	gP- Kg 0.1801721	gP- Kg 0.0000000	gP- Kg 0.1801721	gP- Kg 0.0000000	gP- Kg 0.0000000	gP- Kg 0.0000000	gP- Kg 0.0000000
gC- Kg 0.0000000	gC- Kg 0.0000000	gC- Kg 0.2537020	gC- Kg 0.0000000	gC- Kg 0.0020509	gC- Kg 0.0020509	gC- Kg 0.0000000	gC- Kg 0.0425945	gC- Kg 0.0000000	gC- Kg 0.0425945	gC- Kg 0.0000000	gC- Kg 0.0000000	gC- Kg 0.0000000	gC- Kg 0.0000000
gPC- Kg 0.0000000	gPC- Kg 0.0000000	gPC- Kg 0.2314966	gPC- Kg 0.6493183	gPC- Kg 0.9963031	gPC- Kg 0.9997239	gPC- Kg 0.9999617	gPC- Kg 0.9999617	gPC- Kg 0.0000000	gPC- Kg 0.9999617	gPC- Kg 0.0000000	gPC- Kg 0.9997239	gPC- Kg 0.0000000	gPC- Kg 0.0000000
gOP- Kg 0.0000000	gOP- Kg 0.0000000	gOP- Kg 0.0000000	gOP- Kg 0.0000000	gOP- Kg 0.0000000	gOP- Kg 0.0000000	gOP- Kg 0.0000000	gOP- Kg 0.0000000	gOP- Kg 0.0000000	gOP- Kg 0.0000000	gOP- Kg 0.0000000	gOP- Kg 0.0000000	gOP- Kg 0.0000000	gOP- Kg 0.0000000
gO- gO 0.0000000	gO- gO 0.0000000	gO- gO 0.0000000	gO- gO 0.0000000	gO- gO 0.0002527	gO- gO 0.0002527	gO- gO 0.0016792	gO- gO 0.0000000	gO- gO 0.0000000	gO- gO 0.0002527	gO- gO 0.0000000	gO- gO 0.0016792	gO- gO 0.0000000	gO- gO 0.0000000
gP- gO 0.7705728	gP- gO 0.8073773	gP- gO 0.0000000	gP- gO 0.0000000	gP- gO 0.0002527	gP- gO 0.0002527	gP- gO 0.0024147	gP- gO 0.0000000	gP- gO 0.0000000	gP- gO 0.0002527	gP- gO 0.0000000	gP- gO 0.0024147	gP- gO 0.0000000	gP- gO 0.0000000
gC- gO 0.0000000	gC- gO 0.0000000	gC- gO 0.0000000	gC- gO 0.0000000	gC- gO 0.0000000	gC- gO 0.0000000	gC- gO 0.0000000	gC- gO 0.0000000	gC- gO 0.0000000	gC- gO 0.0000000	gC- gO 0.0000000	gC- gO 0.0000000	gC- gO 0.0000000	gC- gO 0.0000000
gPC- gO 0.8812464	gPC- gO 0.7787057	gPC- gO 0.0001809	gPC- gO 0.0000000	gPC- gO 0.7162045	gPC- gO 0.4027717	gPC- gO 0.9996134	gPC- gO 0.9996134	gPC- gO 0.0000000	gPC- gO 0.4027717	gPC- gO 0.9996134	gPC- gO 0.4027717	gPC- gO 0.0000000	gPC- gO 0.0000000
gOP- gO 0.0000000	gOP- gO 0.0000000	gOP- gO 0.3282589	gOP- gO 0.0000194	gOP- gO 1.0000000	gOP- gO 1.0000000	gOP- gO 0.9999998	gOP- gO 0.9999998	gOP- gO 0.0000000	gOP- gO 0.9999998	gOP- gO 0.9999998	gOP- gO 0.9999998	gOP- gO 0.0000000	gOP- gO 0.0000000
gO- gP 0.0000004	gO- gP 0.0000000	gO- gP 0.3021208	gO- gP 0.3853722	gO- gP 0.0000007	gO- gP 0.0000007	gO- gP 0.3074993	gO- gP 0.3074993	gO- gP 0.0000000	gO- gP 0.0000007	gO- gP 0.3074993	gO- gP 0.3074993	gO- gP 0.0000000	gO- gP 0.0000000
gP- gP 0.0000000	gP- gP 0.0000000	gP- gP 0.0000000	gP- gP 0.0000000	gP- gP 0.0000000	gP- gP 0.0000000	gP- gP 0.0000000	gP- gP 0.0000000	gP- gP 0.0000000	gP- gP 0.0000000	gP- gP 0.0000000	gP- gP 0.0000000	gP- gP 0.0000000	gP- gP 0.0000000
gC- gP 0.0000000	gC- gP 0.0000000	gC- gP 1.0000000	gC- gP 0.0000000	gC- gP 0.0000000	gC- gP 0.0000000	gC- gP 0.0000000	gC- gP 0.0000000	gC- gP 0.0000000	gC- gP 0.0000000	gC- gP 0.0000000	gC- gP 0.0000000	gC- gP 0.0000000	gC- gP 0.0000000
gPC- gP 0.0000000	gPC- gP 0.0000000	gPC- gP 0.0000000	gPC- gP 0.0000000	gPC- gP 0.0000000	gPC- gP 0.0000000	gPC- gP 0.0000000	gPC- gP 0.0000000	gPC- gP 0.0000000	gPC- gP 0.0000000	gPC- gP 0.0000000	gPC- gP 0.0000000	gPC- gP 0.0000000	gPC- gP 0.0000000
gOP- gC 0.0000000	gOP- gC 0.0000000	gOP- gC 0.0000000	gOP- gC 0.0000000	gOP- gC 0.0000000	gOP- gC 0.0000000	gOP- gC 0.0000000	gOP- gC 0.0000000	gOP- gC 0.0000000	gOP- gC 0.0000000	gOP- gC 0.0000000	gOP- gC 0.0000000	gOP- gC 0.0000000	gOP- gC 0.0000000
gO- gC 0.1205394	gO- gC 0.0864032	gO- gC 0.0000000	gO- gC 0.0000000	gO- gC 0.0000000	gO- gC 0.0000000	gO- gC 0.0000014	gO- gC 0.0000000	gO- gC 0.0000000	gO- gC 0.0000014	gO- gC 0.0000000	gO- gC 0.0000014	gO- gC 0.0000000	gO- gC 0.0000000
gPC- gC 0.0000000	gPC- gC 0.0000000	gPC- gC 0.0000000	gPC- gC 0.0000000	gPC- gC 0.0000000	gPC- gC 0.0000000	gPC- gC 0.0000000	gPC- gC 0.0000000	gPC- gC 0.0000000	gPC- gC 0.0000000	gPC- gC 0.0000000	gPC- gC 0.0000000	gPC- gC 0.0000000	gPC- gC 0.0000000
gOP- gOP 0.0000000	gOP- gOP 0.0000000	gOP- gOP 0.0000000	gOP- gOP 0.0000000	gOP- gOP 0.0000000	gOP- gOP 0.0000000	gOP- gOP 0.0000000	gOP- gOP 0.0000000	gOP- gOP 0.0000000	gOP- gOP 0.0000000	gOP- gOP 0.0000000	gOP- gOP 0.0000000	gOP- gOP 0.0000000	gOP- gOP 0.0000000

SUPPLEMENTARY FIGURE 1 | Regarding immunocytochemistries, the results of the Tukey HSD test and the adjusted p-values of the comparisons of each treatment group can be seen ($p < 0.05$ represents statistical significance) [276]



SUPPLEMENTARY FIGURE 2 | Hypothesized molecular links connecting IGF1R and TLR9 signaling to autophagy and cell proliferation in HT29 cancer cells [276]

TLR9 binding of gDNA through IGF1 and IGF1R activation promotes cell division by enhancing Bcl2. ODN and PPP may inhibit this, but the inhibitory effect can be counteracted by EGFR cross-activation. IGF1R activation via the PI3K/Akt pathway affects autophagy. If it is through the AMPK/mTORC1 pathway, it is a stimulant. If it is through the mTORC2/ATG16L1 pathway, it is primarily inhibitory. Similarly, IGF1R inhibits apoptosis via the Akt-Bcl2-p53-Bax proteins, whereas the Erk-Bad-Bcl2 pathway tends to stimulate it. The final effects are always context-dependent.

Red lines: inhibitory effect; gDNA: genomic self-DNA; TLR9: Toll-like receptor 9; ODN: oligodeoxynucleic acid 2088; IGF1: insulin-like growth factor 1; IGF1R: insulin-like growth factor 1 receptor; EGFR: epidermal growth factor receptor; PPP: picropodophyllin; Bcl2: B-cell lymphoma 2; MAPK: mitogen-activated protein kinase; PI3K: phosphoinositide 3-kinase; Akt: Ak strain transforming; Bax: BCL2 associated X; AMPK: AMP-activated protein kinase; mTOR: mammalian target of rapamycin; mTORC1/2: mTOR complex 1/2; ERKs: extracellular signal-regulated kinases; ATG16L1: Autophagy Related 16 Like 1; Bad: BCL2-associated agonist of cell death